Université Mohamed Khider de Biskra
Faculté : Science exactes et sciences de la nature et de vie
Département : Sciences de matière

MÉMOIRE DE MASTER

Science de matière
Filière : Chimie
Spécialité : Chimie pharmaceutique

Réf. :   /

Présenté et soutenu par :
Azri Soumia et Azri Meriem
Le: 27/09/ 2020

Etude théorique de la réactivité des ligands Salicylidèneaniline substituées et la stabilité de leurs complexes de métaux de transition

---

Jury :

Yousef Oum Hani	Présidente	MCB
Sellami Mohammed	Promoteur	MAA
Djouamaa.A	Examinatrice	MCB

Année universitaire : 2019/2020

بسم الله الرحمن الرحيم

Acknowledgement

First, we need to express our deep gratitude to Almighty Allah who gifted us his blessings, and aided us to accomplish our studies for the Master's degree. Thanks to Allah for granting us more than what we deserve, and for Allah's continuous care and generosity.

This work would not have been possible without the help and support of so many people.

A special thanks to our supervisor, **Dr. SELLAMI MOHAMMED**, for his persistent and professional advice throughout our graduate studies at Mohammed Khaider University.

We wish to thank our committee members who were more than generous with their expertise and precious time. Thank you **Dr. YOUSEF OUM HANI, Dr. DJOUAMAA ,** for agreeing to serve on our committee.

Thanks to our best friends for their encouragement and understanding. Finally, our biggest thanks go beyond all doubt to our parents and families for their countless support and love!

Azri Soumia & Meriem

Dedication

I dedicate my dissertation work to my family and my friends.

A special feeling of gratitude to my loving parents **Ahmed** & **Fatma** whose words of encouragement and push for tenacity ring in my ears.

To my sister **Hadjer** and anuty **Kenza** whose have never left my side and to my brothers **Mossaab** and **Kasem**, and to my sweet cousin sisters.

To my friends whose have supported me throughout the process. I will always appreciate all they have done, especially to my special friends **Sumaya Begum** and **Tasneem Eghabria** for their moral support and prayers when things looked bleak to me.

AZRI SOUMIA

Dedication

To my:

Mother & Father,

Brother & Sisters

AZRI MERIEM

Table of contents

Table of contents

List of tables

List of figures

List of abbreviations

CHAPTER III

Study on the reactivity of Salicylideneaniline ligands

CHAPTER VI

Study of substituted SA complexes of Platinum & Copper divalents

List of tables

List of tables

List of figures

List of abbreviation

List of abbreviations

DFT: Density-Functional Theory

QM: Quantum Mechanics

HF: Hartree-Fock

CI: Configuration Interaction

MP: Møller–Plesset perturbation theory

CC: Coupled-cluster method

LDA: The local-density approximation

GGA: The Generalized Gradient Approximation

EXC: The exact exchange-correlation functional

B3LYP: Becke 3 term Lee, Yang, Parr exchange

TZP: Triple Zeta polarized

HSA: Salicylidenenaniline

ZORA: Zeroth Order Regular Approximation

MM: Molecular Modeling

Sub: Substituent

HOMO: Highest Occupied Molecular Orbital

LUMO: Lowest Unoccupied Molecular Orbital

FO: Frontier Orbital

AO: Atomic Orbital

MO: Molecular Orbital

ΔE: HOMO-LUMO energy gap

General Introduction

General introduction

The pollution is caused by a variety of pollutants in water, air, and soil. Hazardous metals that occur naturally in the earth's crust are one of the most concerned globally distributed pollutants of the living environment. It enter and continuously circulate in the environment as a result of human activities such as mining, smelting, electroplating, energy and fuel production, power transmission, intensive agriculture, sludge dumping, etc.. and their distribution in the environment depend on their properties and the influences of environmental factors **[1,2]**.

The contamination chain of heavy metals almost always follows a cyclic order: Industry →Atmosphere → Soil → Water → Foods → Humans. So the concern about exposures, intakes, and absorption of heavy metals by humans is increasing day by day in the developing world **[1].**

In industrial effluents, we can find so many metal ions such as Cd, Cr, Cu, Pb, Mg, and Fe, etc. The extraction of these metals have done by several methods such as chemical precipitation, flocculation, filtration, chemical coagulation, reverse osmosis, ion exchange, solvent extraction, adsorption, and membrane technologies, and so on **[3]**.

Among recent techniques, solvent extraction is the most versatile procedure that is used for the separation and removal of the metals. The development of selective extractants has expanded the use of solvent extraction for metal recovery and purification, from those extractants oximes, and Schiff bases are used widely in solvent extraction because of their chelating property that gives extra stability to the metal complexes **[3,4]**.

From Schiff bases, N-Salicylideneaniline is one of the best extractants for metal ions, including transition metal. These compounds are well known as ligands that can be synthesized easily and characterized by their structural rigidity, catalytic activity in hydrogenation of olefins, transfer of an amino group, and their complexing ability towards toxic metals **[4]**.

The development of quantum chemistry calculation methods will allow an exact description of metal-ligand bonds.

A good understanding of the geometric and electronic structures of the ligands will determine their reactivity towards metals and the stability of their complexes.

General introduction

Our work represents a theoretical contribution to the extraction process of divalent transition metals and our main objective from this work is to determine the main characteristics for each of Salicylideneaniline (of $C_{13}H_{11}ON$ formula) and its substituted derivatives to study their reactivity and selectivity with respect to metallic ions, and their transition metal complexes.

The ADF program (Amsterdam Density Functional) is used for this, which is well suited to the treatment of large organometallic systems.

This thesis is divided into 4 principal chapters:

Two bibliographical chapters

✓ First chapter on quantum chemical methods with a glance about DFT strength and weakness.

✓ Second chapter on general overview of the transition metals and Schiff bases with its complexes and the liquid-liquid extraction process.

✓ While 3rd chapter is devoted to the detailed study on the geometrical and chemical descriptors and structures of reactivity of Salicylideneaniline and its ligands for the objective of the study of the reactivity of the studied systems.

✓ Finally the 4th chapter is on the complexes resulting from the coordination of Salicylideneaniline and its ligands with the divalent transition metals (case of platinum and copper) with representing of a qualitative estimate of the extraction efficiency of metal ions for the purpose of knowing the stability of each of those complexes.

And at the end, a general conclusion brings together the main results obtained from the calculations made during this thesis.

General introduction

References

[1] V. Sharma, P. Singh. Heavy metals pollution and its effect on environment and human health. International Journal of Recent Scientific Research. **2015**, 6. 7752-7755.

[2] K. A. Ghazaryan, H.S. Movsesyan, N.P. Ghazaryan, Sh.V. Shalunts. Assessment of heavy metal contamination of soils around agarak(RA) copper-molybdenum mine complex. Chemistry and biology. **2016**, № 1, 34–42.

[3] B. Dede, F. Karipcin, and M. Cengiz. Synthesis, characterization and extraction studies of N, N″- bis[1-biphenyl-2-hydroxyimino-2-(4-acetylanilino)-1-ethylidene]-diamines and their homo-and heteronuclear copper(II) complexes. J. Chem. Sci. **2009**, 121, 163–171.

[4] A. Sana, A. Fatima & B. Djamel. Synergistic Extraction of Nickel(II) from Sulfate Medium by a Mixture of N -(2-hydroxybenzylidene)aniline and Methyl-Isobutyl Ketone, Inorganic and Nano-Metal Chemistry, **2017**, DOI: 10.1080/24701556.2017.1357612.

Chapter I

Quantum chemistry methods

1.   Introduction

Computational quantum chemistry is a branch of theoretical chemistry whose major aim is to make efficient mathematical approximations and computer programs for calculating the properties of the molecules such as their total energy, vibrational frequencies, dipole and quadrupole moments, potential energy (free energy) surfaces, excitation energies, and some other diverse spectroscopic quantities, reactivity behavior, the involved reaction mechanism, and reaction dynamics. The term is sometimes useful in covering the areas of overlap between computer science and chemistry [1].

Quantum Chemistry is a very nice tool for studying properties and reactions of molecules. Recently years the quantum chemistry development particularly that of density functional theory (DFT) methods, have made calculations of quantum chemistry more accurate and matching to those of experimental calculations for molecules of moderate sizes. The quick advancement of computer technology has enormously urged chemists to utilize quantum science for understanding the model and predicting properties and reactions of the molecules, nanometer materials properties, as well the techniques which be used in the biological systems.

Mostly these methods include various empirical parameters those are optimized by reproducing properties of some reference molecules and that parameters usually be accurate for the systems that are parameterized for. For many properties e.g. the relative energies of different conformations of a big molecule, the binding energy, and the hydrogen-bonded system structure. The results from semi-empirical calculations are not trustable, so this limits their applications to large systems, particularly those where hydrogen bonds are significant. In recent years, many quantum chemistry methods introduced specifically for studying large molecular systems [2].

2.   Quantum chemistry definition

Quantum chemistry is a branch of chemistry that uses quantum mechanics principals to address some aspects of phenomena associated with chemical systems and reactions from a theoretical point of view. Theoretical quantum chemistry that is called as well by computational chemistry uses computer algorithms for solving the Schrödinger equation of a given chemical system for predicting its behavior, structure, or properties **[3]**.

3.   Quantum mechanics

Quantum mechanics (QM) is the correct mathematical description of the behavior of the electrons and thus of chemistry. Theoretically, by QM it's possible to predict any property of an individual atom or molecule precisely. Practically, its equations are solved only for one-electron systems. A myriad collection of methods has been developed for approximating the solution for multiple electron systems so these approximations can be very helpful and valuable, but this needs some sophistication by a scientific researcher to know when each approximation is valid and how accurate the results are going to be.

Two equivalent formulations of QM were devised by Schrödinger and Heisenberg. Here, we will present only the Schrödinger form since it is the basis for nearly all computational chemistry methods **[4]**, The Schrödinger equation is:

$$\hat{H}\Psi = E\Psi \tag{I.1}$$

Where Ĥ represents the Hamiltonian of the system, accounting for the potential and kinetic energy of the system, while Ψ represents the wave function which contains all the information of the system. In a compact form H is given **[5]**:

$$H = T_n + T_e + V_{ne} + V_{ee} + V_{nn} \tag{I.2}$$

Where:

- $\triangleright$ T_n and T_e are the kinetic energy operators for the nuclei and electrons,
- $\triangleright$ V_{ne}, V_{ee}, and V_{nn} are the potential energy operators for the nucleus-electron, electron-electron, and nucleus-nucleus interactions, respectively.

In atomic units H becomes:

$$H = -\frac{1}{2}\sum_{A}^{nuclei}\frac{1}{(M_A/m_e)}\nabla_A^2 - \frac{1}{2}\sum_{a}^{electrons}\nabla_a^2 - \sum_{A}^{nuclei}\sum_{a}^{electrons}\frac{Z_A}{r_{Aa}}$$
$$+ \sum_{A>B}^{nuclei}\sum_{B}^{nuclei}\frac{Z_AZ_B}{R_{AB}} + \sum_{a>b}^{electrons}\sum_{b}^{electrons}\frac{1}{r_{ab}}$$

(I.3)

Where the Hamiltonian will include **[6]**:

- ➢ **A**: kinetic energy terms for the nuclei.
- ➢ **a**: Electrons.
- ➢ **r$_{Aa}$**: distance of separation(electron-nucleus potential).
- ➢ **R$_{AB}$**: distance of separation (nuclear-nuclear potential).
- ➢ **r$_{ab}$**: distance of separation (electron-electron repulsion).

Maybe it looks simple. But analytically, this equation is so hard to solve and impossible for more than two particles, and the problem is in the description of the correlated motion of many particles. So to reach a solution, we must use a series of approximations. The first commonly used and one of the most conceptually important ones is the Born-Oppenheimer approximation **[7]**.

4. Born-Oppenheimer approximation

An approximation that can be made to realize that the motion of the nuclei is sluggish compared to the motion of the electrons due to the large differences in mass. So because of the big difference in motion between the nuclei and the electrons, the electrons are capable of immediately adjusting to any change in the position of the nuclei. So, the electron motion is determined for a fixed position of the nuclei making the distances. R$_{AB}$ in Eq.(I.3) now a constant. This approximation is called the Born-Oppenheimer approximation.

The Born-Oppenheimer approximation removes the kinetic energy operators for the nuclear motion in Eq.(I.3)

$$\hat{H} = -\frac{1}{2}\sum_{a}^{electrons}\nabla_a^2 - \sum_{A}^{nuclei}\sum_{a}^{electrons}\frac{Z_A}{r_{Aa}} + \sum_{A>B}^{nuclei}\sum_{B}^{nuclei}\frac{Z_AZ_B}{R_{AB}} + \sum_{a>b}^{electrons}\sum_{b}^{electrons}\frac{1}{r_{ab}}$$

(I.4)

The Schrödinger equation that is solved for then just becomes the electronic Schrödinger equation for the molecule plus a constant term for the nuclear repulsion.

$$\hat{H}^{electronic}\,\psi^{\,electronic} = \left(E^{electronic} + E^{nuclear}\right)\psi^{\,electronic} \tag{I.5}$$

The Schrödinger equation is solved for the electrons in a fixed static electric potential emerging from the nuclei in that particular arrangement. Different arrangements of the nuclei may then be adopted and the calculation is repeated. The set of solutions obtained can then be used to construct a molecular potential energy curve for a diatomic molecule or a potential energy surface for a polyatomic molecule. The lowest point of the potential energy curve or surface is then determined to identify the equilibrium geometry of the molecule. The wave functions that result in the computation are called molecular orbitals (MO).

5.   Ab initio essentials

The term "ab initio" comes from Latin meaning "from the beginning". The implication is that the computations are exact with no approximations. This is certainly not the case, as the Schrödinger equation for more than a two body system cannot be solved without approximations and using approximation techniques. What "ab initio" does mean here that the integrals involved in the Schrödinger equation for the system are explicitly solved without the use of empirical parameters.

The first supposition that is made is the Born-Oppenheimer approximation. As described in section 4, this reduces the Schrödinger equation for a molecular system to only the electronic motion for a particular nuclear configuration. As mentioned in section 3, an optimized nuclear configuration as a starting point for an ab initio computation can be obtained by using a molecular mechanics method. This reduces the number of computational cycles needed to find the equilibrium geometry and hence the energy of the molecule **[6]**.

The majority of ab initio calculations solve only the electronic part of the molecular wave function, so it cannot account for systems where the electronic states are strongly coupled to nuclear vibrations **[8]**.

Ab initio methods for molecular calculations must satisfy a set of stringent criteria **[9]**:

1. Solutions must be well defined and specified by both the structure and the electronic states of the molecule.

2. The potential energy of the molecule must differ smoothly and continuously with respecting the atomic nuclei displacement.

3. The model must not have bias, for example, assuming a chemical bond exists between two atoms.

4. The model must be 'size-consistent'- which means that solutions and their associated errors must scale in proportion to the size of the molecule.

5. The model must be 'variational'- which means that solutions must provide an upper bound to the 'true' energy of the system. Therefore, the approximate solution having the lowest energy represents the closest fit to the true wavefunction, within the constraints of the method.

6.   Quantum chemistry methods

6.1.   Wave function based methods

The variational principle, which can be viewed as another form of the many-body Schrödinger equation, states that any state vector of the electrons for which the average energy, defined as:

$$E_e[\Phi] \equiv \frac{\langle \Phi | \hat{H}_e | \Phi \rangle}{\langle \Phi | \Phi \rangle} \tag{I.6}$$

is stationary corresponds to an eigenvector of $\hat{H}_e$, with eigenvalue E_e. Furthermore, for any state of the system, the corresponding average energy satisfies:

$$E_e[\Phi] \geqslant E_0 \tag{I.7}$$

Where E_0 is the ground-state energy of the electronic system. The essence of the wave function-based methods involves obtaining the stationary solutions of Eq. (I.6) within a trial-function space. The accuracy of the method is naturally determined by the choice of this trial-function space.

By taking more sophisticated approximations for the trial many-body wave function of these electrons, the accuracy can be systematically improved.

Unfortunately, at the same time its computational cost can be expensive. In this section, we will introduce some of these approximations in order of increasing complexity **[10]**.

6.1.1. Hartree-Fock

Hartree–Fock calculation is the simplest kind and the common type of ab initio calculation. Modern molecular HF calculations grew out of calculations first performed on atoms by Hartree1 in 1928.

HF calculation in which the primary approximation is the central field approximation, this means that the Coulombicelectron±electron repulsion is taken into account by integrating the repulsion term. This gives the average effect of the repulsion, but not the explicit repulsion interaction. This is a variational calculation, meaning that the approximate energies calculated are all equal to or greater than the exact energy.

The calculated energies are in units called Hartrees (1 Hartree = 27.2116 ev). Due to the central field approximation, the energies from HF calculations are always bigger than the exact energy and tend to a limiting value called the HF limit as the basis set is improved.

This method has many advantages, and one of its advantages is that it ruptures the many-electron Schrödinger equation into many simpler one-electron equations. Each one electron equation is solved to obtain a single-electron wave function, called an orbital, and energy, called orbital energy. The orbital describes the behavior of an electron in the net field of all the other electrons **[4]**.

Slater determinants

Electrons are fermions and obey the Pauli exclusion principle, so it requires that the wave function of electrons should be antisymmetric with respect of the interchange of the coordinates x of any two electrons **[11]**:

$$\Phi\left(x_1, \dots, x_i, \dots, x_j, \dots, x_N\right) = -\Phi\left(x_1, \dots, x_j, \dots, x_i, \dots, x_N\right) \qquad \text{(I.8)}$$

Slater determinants nicely satisfy this anti-symmetric condition through an appropriate linear combination of Hartree products, which are the non-interacting electron wave functions e.g. a two-electron case in which we occupy the spin orbitals χ_i and χ_j.

If we put electron one in χ_i and electron two in χ_j, we will have:

$$\Phi_{12}(x_1, x_2) = \chi_i(x_1)\chi_j(x_2) \tag{I.9}$$

Reversely, if we put the electron one in χ_j and electron two in χ_i, we will have:

$$\Phi_{21}(x_1, x_2) = \chi_i(x_2)\chi_j(x_1) \tag{I.10}$$

By taking a linear combination of these two products, we will obtain:

$$\Phi(x_1, x_2) = 2^{-1/2}(\chi_i(x_1)\chi_j(x_2) - \chi_i(x_2)\chi_j(x_1)) \tag{I.11}$$

Where the factor $2^{-1/2}$ is a normalization factor. It can be seen the antisymmetry is guaranteed during an interchange of the coordinates of electron one and electron two:

$$\Phi(x_1, x_2) = -\Phi(x_2, x_1) \tag{I.12}$$

The antisymmetric wave function of Eq. (I.11) can be rewritten as a determinant:

$$\Phi(x_1, x_2) = 2^{-1/2} \begin{vmatrix} \chi_i(x_1) & \chi_j(x_1) \\ \chi_i(x_2) & \chi_j(x_2) \end{vmatrix} \tag{I.13}$$

And this is called a Slater determinant. For an N-electron system, the Slater determinant becomes:

$$\Phi(x_1, x_2, \dots, x_N) = (N!)^{-1/2} \begin{vmatrix} \chi_i(x_1) & \chi_j(x_1) & \cdots & \chi_K(x_1) \\ \chi_i(x_2) & \chi_j(x_2) & \cdots & \chi_K(x_2) \\ \vdots & \vdots & & \vdots \\ \chi_i(x_N) & \chi_j(x_N) & \cdots & \chi_K(x_N) \end{vmatrix} \tag{I.14}$$

Note that:

- The rows of the N-electron Slater determinant are labeled by electrons:

   First row (x_1), second row (x_2), final row (x_N).

- The columns are labeled by spin orbitals:

   First column (χ_i), second (χ_j), final column (χ_k).

Interchanging the coordinates of two electrons equals to the interchange of two rows of the Slater determinant which will change its sign. Thus the Slater determinant meets the requirement of anti-symmetry.

For having two electrons occupying the same spin orbital corresponds to having two columns of the determinant identical which leads to the determinant being zero.

It is convenient to use a short-hand notation for a Slater determinant which only shows the diagonal elements:

$$\Phi(x_1, x_2, ..., x_N) = |\chi_i(x_1)\chi_j(x_2) ... \chi_K(x_N)\rangle \qquad (I.15)$$

Furthermore, if the order of electrons is always to be $x_1, x_2, \cdots, x_N$, then:

$$\Phi(x_1, x_2, ..., x_N) = |\chi_i\chi_j ... \chi_K\rangle \qquad (I.16)$$

6.1.2. Post-Hartree-Fock Methods

The main problem in the Hartree-Fock method is that it completely neglects correlations between electrons with the same spin (beyond exchange). Following Löwdin, in quantum chemistry, it is common to define the energy associated with the missing electron correlation energy as:

$$E_{corr} = E_{exact} - E_{HF} \qquad (I.17)$$

Where E_{exact} is the exact energy of the system and E_{corr} is thus the missing energy associated with correlations in the exact many-body ground state wave function.

E_{corr} is negative because E_{HF} is always the upper bound of the E_{exact}. The missing correlation energy is typically a very small fraction of the total energy. However it can be a very important contribution to many systems of physical and chemical interest. For example, the restricted HF method can't describe the dissociation of H_2 into two open-shell H atoms. Or, at least one-quarter of the strength of hydrogen bonds between water molecules comes from correlations beyond HF **[11]**.

Among the post HF methods, the configuration interaction (CI) method, the Møller–Plesset (MP) perturbation theory, and the coupled-cluster (CC) method, in recent years this all methods achieved a great success. As a general disadvantage of all these methods, their application is limited only on atoms and small molecules, because of the expensive computational costs with the system size **[10]**.

6.1.2.1. Configuration interaction (CI) method

Configuration interaction calculations are classified by the excitations number that is used for making each determinant.

The first calculation is called configuration interaction single-excitation (CIS) calculation, in which only one electron moved for each determinant.

CIS calculations give an approximation to the excited states of the molecule but, it doesn't change the ground-state energy. The second calculation is Single-and double excitation (CISD) calculations which give ground-state energy that has been corrected for correlation. Triple-excitation (CISDT) and quadruple-excitation (CISDTQ) calculations are done only when very-high-accuracy results are desired.

There is also another type of configuration interaction calculation called full CI, which be with all possible excitation, and it's using to an infinitely large basis set will give an exact quantum mechanical result. However, these full CI calculations are very rarely to do because of the immense amount of computer power required **[4]**.

6.1.2.2. Møller–Plesset (MP) perturbation theory

Perturbational approaches for the description of electron correlation are based on the separation of the electronic Hamiltonian into an unperturbed $\hat{H}_0$ and a perturbed $\hat{H}_0$ part:

$$\hat{H} = \hat{H}_0 + \lambda \hat{H}'$$

(I.18)

The energy E and the wavefunction Ψ are expanded in a Taylor series, where λ is the perturbation parameter. After insertion of the expansions into the Schrodinger equation the resulting terms are sorted by the order of the parameter λ.

Projection into the eigenfunctions of the unperturbed system leads to n-th order energy expressions. MP perturbation theory defines the unperturbed Hamiltonian as a sum of Fock operators:

$$\hat{H}_0 = \sum_j \hat{F}(j)$$

(I.19)

The perturbed part of the Hamiltonian which describes electron correlation is obtained from the difference between the true molecular electronic Hamiltonian and $\hat{H}_0$:

$$\hat{H}' = \hat{H} - \hat{H}_0 = \sum_{i<j} \frac{1}{r_{ij}} \sum_j \hat{F}(j)$$

(I.20)

This results in the following expressions for the second order energy:

$$E^{(2)} = \frac{1}{4} \sum_{ijab} \frac{|\langle ij \| ab \rangle|^2}{\epsilon_i - \epsilon_j - \epsilon_a - \epsilon_b} \tag{I.21}$$

As is the usual convention, i, j, k… denote occupied and a, b, c ... virtual orbitals. Within the framework of the MP and the HF energy is represented by the sum of zeroth and first order energy. Electron correlation is recovered by second (MP2) and higher-order perturbation theory **[12]**.

6.1.2.3. Coupled-cluster (CC) method

The coupled-cluster is a method that has been used to find expansion of wave function in terms of slater determinants that could preserve size consistency) In this method, the wave function for the electronic ground state is obtained as a result of the operation of the wave operator $\exp(\hat{T})$ on the HF function (this ensures size consistency).

The wave operator $\exp(\hat{T})$ contains the cluster operator $\hat{T}$ (defined as the sum of operators for the l-tuple excitations), $\hat{T}_l$ up to a certain maximum $l = l_{max}$. Each $\hat{T}_l$ operator is the sum of the operators each responsible for a particular l-tuple excitation multiplied by its amplitude t. CC method aims to find the t values because it determine the wave function and energy.

The method also generates non-linear (concerning unknown t amplitudes) equations. Usually, this CC method offers very good results **[13]**.

6.2. Semi empirical methods

Semi-empirical methods increase the computational speed by using ab initio approximations techniques (for example, by limiting choices of Molecular orbitals or considering only valence electrons), which fit experimental data (recently, structures and formation energies of organic molecules).

Until now, the size of many energetic molecules placed them beyond the scope of ab initio calculations, so preliminary theoretical studies introduced using semi-empirical methods. However, semi-empirical methods have been calibrated to typical organic or biological systems and tend to be inaccurate for problems that involve hydrogen-bonding, chemical transitions, or nitrated compounds.

Many of semi-empirical methods are available and appear in commercially available computational chemistry software packages like both HyperChem and Chem3D, more common semi-empirical methods can be grouped according to their treatment of electron-electron interactions.

6.2.1. The extended Hückel method

Extended Hückel calculations neglect all electron-electron interactions, making them fast computationally but not so accurate. The model provides a qualitative estimate of the shapes and relative energies of molecular orbitals and approximates the spatial distribution of electron density. Extended Hückel models are better for chemical visualization and can be applied to 'frontier orbital' treatments of chemical reactivity.

6.2.2. Neglect of differential overlap (NDO)

NDO models neglect few but not all the interactions of electron-electron. The HF Self-Consistent Field (HF-SCF) is a method used for solving the Schrödinger equation with different approximations:

- Complete NDO abbreviated (CNDO): the product of two atomic orbitals on different atoms and set equal to zero everywhere. So the repulsion between electrons in different orbitals depends only on the nature of the atoms involved, not on the particular orbitals.

Due to neglecting most of all descriptions of electron exchange properties by CNDO, it doesn't differ between states that have the same electronic configuration, but different values of electron spin.

- Intermediate NDO (INDO): differential overlap between orbitals on the same atom is taken into account in the description of electron-electron repulsion, but differential overlap between orbitals on different atoms is neglected.
- Modified INDO, version 3 (MINDO/3): it is a reparameterised version of INDO developed to predict good enthalpies of formation and reasonable molecular geometries for a range of chemical systems, especially for compounds that contain sulfur, for carbocations, and polynitro organic compounds.

- Zerner's INDO methods (ZINDO/1 and ZINDO/S) - Michael Zernerís (University of Florida) both of these methods are versions of INDO developed for the use with molecular systems that contain transition metals. ZINDO/1 optimized for predicting molecular geometries, while ZINDO/S optimized for predicting UV spectra.

6.2.3. Neglect of diatomic differential overlap (NDDO)

NDDO methods are based on INDO model by including the overlap density between two orbitals on one atom interacting with the overlap density between two orbitals on the same or another atom.

- Modified NDO (MNDO) – It's a method introduced to correct some of the problems which are related to MINDO/3. MNDO method does not work well for sterically crowded molecules, four-membered rings, and hydrogen bonding, hypervalent compounds, nitro groups, and peroxides. Generally, MNDO overestimates activation barriers to chemical reactions.

- Austin Method, version 1 abbreviated (AM1) - it is a reparameterised version of MNDO which includes changes in nuclear repulsion terms. Even though it's more accurate than MNDO method, it doesn't handle phosphorus-oxygen bonds, nitro compounds, or even peroxide bonds.

- Parameterisation Model, version 3 abbreviated (PM3): it's the second reparameterization of the MNDO method, similar to AM1 functionally, but with some significant improvements.

PM3 is yet a new semi-empirical method that recently developed, so it may contain some defects that are till now undiscovered **[9]**.

6.3. Density-Functional Theory

DFT is a quantum mechanical modeling method used in physics and chemistry as well, this method used for studying the electronic structure (principally of ground state) of many-body systems, in particular atoms, molecules, and the condensed phases. With this theory, we can determine the properties of a many-electron system by using functionals, which means functions of another function, which in this case is the spatially dependent electron density. So density functional theory name comes from the use of functionals of the electron density.

DFT is one of the most popular and versatile methods that are available in computational chemistry, condensed-matter physics and computational physics.

Since the 1970s, DFT was very popular for calculations in solid-state physics. But, it wasn't considered accurate enough for calculations in quantum chemistry until the 1990s, when the approximations used in DFT theory it was nicely optimized for better modeling of the exchange and correlation interactions.

Mostly the results of DFT calculations for solid-state systems agree quite satisfactorily with experimental data. Compared to traditional methods, computational costs are relatively low **[14]**.

Acronyms	Name	Type
Xα	*X alpha*	Exchange only
HFS	Hartree-Fock Slater	HF with LDA exchange
VWN	Vosko,Wilks,andNusair	LDA
BLYP	Becke correlation functional with Lee ,Yang, Parr exchange	Gradient-corrected
B3LYP, Becke3LYP	Becke 3 term with Lee, Yang, Parr exchange	Hybrid
PW91	Perdue and Wang 1991	Gradient-corrected
G96	*Gill 1996*	Exchange
P86	Perdew 1986	Gradient-corrected
B96	Becke 1996	Gradient-corrected
B3P86	Becke exchange, Perdew correlation	Hybrid
B3PW91	Becke exchange, Perdew and Wang correlation	Hybrid

Table I.1: Density functionals **[4]**.

6.3.1. Thomas–Fermi Theory

The history of using the electron density rather than the wave function begins with the early work of Thomas and Fermi. Firstly, let us start by defining the electron density:

$$\rho(r) = N \int \cdots \int |\Psi(X_1, X_2, \cdots, X_N)|^2 \, ds_1 X_2 \cdots X_N \qquad (I.22)$$

Where ρ(r) determines the probability of finding any of the N electrons within the volume r but with arbitrary spin while the other N − 1 electrons have arbitrary positions and spin in the state represented by Ψ. This is a nonnegative simple function of three variables, x, y, and z, integrating to the total number of electrons.

$$\int \rho(r)\, dr = N \tag{I.23}$$

In Thomas-Fermi theory, the kinetic energy of electrons are derived from the quantum statistical theory based on the uniform electron gas, but the interaction between electron-nucleus and electron-electron are treated classically. Within this model, the kinetic energy of the electrons is defined as:

$$T[\rho] = C_F \int \rho^{5/3}(r)\, dr \tag{I.24}$$

With

$$C_F = \frac{3}{10}(3\pi^2)^{2/3} = 2.871 \tag{I.25}$$

From the above equation, the approximation is made that the kinetic energy only of the electron depends exclusively on the electron density. By adding the interaction between electron-nucleus and electron-electron into Eq. (3), a total energy in terms of electron density is obtained:

$$E[\rho] = C_F \int \rho^{5/3}(r)\, dr - Z \int \frac{\rho(r)}{r}\, dx + \frac{1}{2} \iint \frac{\rho(r_1)\rho(r_2)}{|r_1 - r_2|}\, dr_1 dr_2 \tag{I.26}$$

The second and third terms are the electron-nucleus and electron-electron interactions, respectively.

The importance of this simple Thomas-Fermi model is not how well it performs in computing the ground state energy and density but more as an illustration that the energy can be determined purely using the electron density **[11]**.

6.3.2. Hohenberg–Kohn theorems

The first Hohenberg–Kohn theorem states that 'the ground state of any interacting many particle system with a given fixed inter-particle interaction is a unique functional of the electron density n(r)'. This implies that Eq.(I.27) can be inverted to write the ground state wave function as a unique functional of the ground state electron density, i.e. $\Psi_0 = \Psi[n_0]$.

This will enable one to write the ground state energy E as a functional of the ground state density as shown in Eq.(I.27).

$$E\big[\Psi[n_0]\big] = \langle \Psi[n_0]|\hat{T} + \hat{V} + \hat{U}|\Psi[n_0]\rangle \tag{I.27}$$

Even though the first Hohenberg–Kohn theorem precisely proves that a functional of the electron density E [n0] exists, it doesn't say anything about the actual form of the functional.

While the second Hohenberg–Kohn theorem defines an important property of the functional and it states that 'the electron density that minimizes the energy of the overall functional is the true electron density corresponding to the full solutions of the Schrödinger equation'. So if we know the true functional form we can try to minimize the energy by varying the electron density to find the ground-state electron density. Once the ground-state electron density is known, we can calculate all the properties **[15]**.

6.3.3. Kohn-Sham equations

From the Hohenberg-Kohn theorem, we can get the ground-state energy by minimizing the energy functional:

$$E[\rho] = \int \rho(r)v(r)dr + F_{HK}\left(\rho(r)\right) \tag{I.28}$$

To use the Kohn-Sham equations we should recognize the exchange-correlation energy functional form. However, the specific form of Exc isn't known and may never be known (in some simple closed form).

So since the DFT birth, some sorts of approximations for Exc have been used. Till now, there is an unlimited list of approximations with varying levels of complexity.
Recently, Perdew proposed "Jacob's ladder" which is a useful way for categorizing the varied and many Exc functionals that exist.

In this scheme, functionals are grouped according to their complexity ascendingly that leads from the Hartree approximation on earth to the exact exchange-correlation functional in heaven. We will discuss so briefly about the first few rungs of this ladder for introducing some of the most common types of exchange-correlation functionals in widespread use:

(a) The local-density approximation (**LDA**): This is simplest approximation, and can be written as:

$$E^{xc-LDA}[\rho(r)] = \int \rho(r)\varepsilon^{xc-unif}\left(\rho(r)\right)d(r) \tag{I.29}$$

Where $\varepsilon^{xc-unif}$ is the exchange-correlation energy per particle of the homogeneous electron gas of density ($\rho(r)$), which means that the exchange-correlation energy density is taken to be that of a uniform electron gas of the same density.

The exchange energy is exactly known and the correlation energy is obtained by fitting to the many-body studies of Gell-Mann and Brueckner and Ceperly and Alder.

Modern LDA functional tend to be exceedingly similar, differing only in how their correlation contributions have been fitted to the many-body free electron gas data. The most common LDA functional are Perdew-Zunger (PZ), Perdew-Wang (PW), and Vosko-Wilk-Nusair (VWN). Strictly, the LDA is valid only for slowly varying densities. Experience with calculations of atoms, molecules, and solids shows that **Eq.(I.29)** generally can also be applied to these systems. Indeed LDA works surprisingly well, and much current understanding of metal or semiconductor (Si or GaAs) surfaces comes from LDA simulations. A partial rationalization of the success of LDA is provided by the observation that it satisfies a number of so-called sum rules.

(b) The generalised gradient approximation **(GGA)**: These are the second generation functionals (sitting on the second rung of Jacob's ladder) in which the gradient of the density, $\nabla\rho(r)$, at each coordinate is taken into account as well as the density itself:

$$E^{xc-GGA}[\rho(r)] = \int \rho(r)\varepsilon^{xc-unif}\left(\rho(r)\right)\nabla\rho(r)d(r) \qquad (I.30)$$

So GGAs are "semi-local" functionals, comprising corrections to the LDA while (again) ensuring consistency with known sum rules. For many properties such as geometries and ground-state energies of molecules, GGAs can offer better results than the LDAs.

Although for the properties of metals and their surfaces, GGA results are not necessarily superior to LDA results. The most common functionals of GGAs that are used in surface physics are the PW91 functional, and its close relative PBE. PBE actually has several off-spring; revPBE, RPBE, PBE-WC, and PBEsol. From those, RPBE is the most popular of the off-spring, even though the latest addition to the PBE family, PBE-WC and PBEsol, offers promise for the simulation of solids and their surfaces. There is also the special designed functional, AM05 that is dedicated to including the surface effect which has been shown a much improved performance for bulk properties like lattice constant and bulk modulous, and jellium surface energy than PBE and PW91.

(c) The **meta-GGAs**: These are the third generation functionals (third rung of Jacob's ladder) and use the second derivative of the density, $\nabla^2\rho(r)$, and or kinetic energy densities, $\tau_\sigma(\rho(r)) = 1/2\sum_i |\nabla_{\emptyset_i}|^2$, as additional degree of freedom.

In gas phase studies of molecular properties meta-GGAs such as the TPSS functional have been shown to offer improved performance over LDAs and GGAs. However, aside from some benchmark studies of bulk materials and jellium surfaces, these functionals have not yet been exploited to any great extend in the solid state.

(d) The **hybrid functionals**: These fourth-generation functionals add "exact exchange" from the HF theory to some conventional treatment of DFT exchange and correlation. B3LYP is the most widely used functional in the quantum chemistry community, and it employs three parameters, a_{1-3} (determined according to fitting to experiment) to control the mixing of the HF exchange and density functional exchange and correlation.

It takes the following form:

$$E^{xc} = E^{x-LDA} + a_1(E^{x-HF} - E^{x-LDA}) + a_2\Delta E^{x-GGA} + a_3\Delta E^{c-GGA} \tag{I.31}$$

Reformulating this to eliminate two parameters leads to an equation of the form:

$$E^{xc} = E^{xc-GGA} + a(E^{x-HF} - E^{x-GGA}) \tag{I.32}$$

Note that: $a=\frac{1}{4}$(based on the grounds of perturbation theory) leads to a class of functionals with only as many parameters as their underlying GGAs. If PBE is the GGA used in Eq. (I.32) we arrive at the hybrid PBE0 functional.

Another popular hybrid functional worth mentioning here is BH&HLYP, which has 50% HF exchange. Such functionals have been shown to offer noticeably improved performance over LDA and GGA functionals for the calculation of gas phase properties of molecules and band gaps in solids.

Else than these few mentioned rungs of Jacob's ladder, other more complicated EXC functionals are there. However, adding complexity by climbing higher on Jacob's ladder or by obeying more and more constraints does not necessarily lead to bring improved performance in total energies **[11]**.

6.3.4. Strengths and Weaknesses of DFT

6.3.4.1. Strengths

DFT includes electron correlation in its theoretical basis, in contrast to wavefunction methods, which must take correlation into account by add-ons (MP perturbation, CI, CC) to ab initio HF theory, or by parameterization in semi-empirical methods.

Due to DFT has correlation fundamentally built-in, it can calculate geometries and relative energies with an accuracy comparable to MP2 calculations, in roughly the same time as needed for HF calculations. DFT calculations tend to be basis-set saturated easier than are ab initio: limiting results are (sometimes) approached with smaller basis sets than for ab initio calculations.

So, Post-HF calculations accuracy can thus be done on bigger molecules than what ab initio methods can make. So the DFT method is supposed to be the best method for geometry and energy calculations on transition metal compounds, for which conventional ab initio calculations often give poor results.

DFT works with electron density, which can be measured and is easily intuitively grasped, rather than a wavefunction, a mathematical entity whose physical meaning is still controversial **[16]**.

6.3.4.2. Weaknesses

From the DFT terms, the exact exchange-correlation functional EXC [r0] is the term which its expression for the energy be unknown, and no one knows how to fully systematically improve our approximations to it.

While for ab initio energies, it can be systematically lowered by using bigger basis sets and by expanding the correlation method: MP2, MP3, or more determinants in the CI approach.

Maybe for some aims 6-311G* doesn't be better than 6-31G*, and MP3 is surely not necessarily better than MP2 but, as much basis sets are bigger and correlation levels are higher, that will eventually approach an exact solution of the Schrodinger equation.

The DFT accuracy is gradually being improved by modifying functionals, not according to some grand theoretical prescription, but rather with the assistance of the experience and predictions, and comparing calculations to experiment. So this makes DFT philosophically somewhat semi-empirical.

Some functionals of DFT contain parameters which must be fitting to experiment; these methods are even more distinctly empirical. Since the functionals are not based purely on fundamental theory, so we should be careful about applying DFT to very novel molecules. The semiempirical character of current DFT is surely not a fundamental feature of the basic method but arises only from our ignorance of the exact exchange-correlation functional. Because our functionals are only approximative, DFT is used today is not variational (that the calculated energy could be lower than the actual energy).

DFT is not accurate as of the highest-level ab initio methods, e.g. QCISD (T) and CCSD (T) (but it can handle much bigger molecules than those methods can do). Even gradient-corrected functional clearly shows it is not able to handle van der Waals interactions, although it gives better structures and energies for hydrogen-bonded species, but recent progress in treating van der Waals and other weak interactions is being encouraged. Although the development of DFT ways that are applying to excited states, DFT is mainly a ground-state theory **[16]**.

7. Synopsis of Molecular modeling methods

To summarize, this table below attempts to capture specifies of each of recent mentioned methods **[9]**:

Method	Advantages	Disadvantages	Best for
Ab initio ✓ Uses quantum physics.	✓ Useful for a broad range of systems ✓ Does not depend on experimental data. ✓ Calculations transition states and excited states.	✓ Computationally expensive.	✓ Small systems (tens of atoms). ✓ Electronic transitions. ✓ Systems without experimental data. ✓ Systems requiring high accuracy.
Semi-empirical ✓ Uses quantum physics. ✓ Uses experimental parameters. ✓ Uses extensive approximations.	✓ Less demanding computationally than ab initio methods. ✓ Calculates transition states and excited states.	✓ Requires ab initio or experimental data for parameters. ✓ Less rigorous than ab initio methods.	✓ Medium-sized systems (hundreds of atoms). ✓ Electronic transitions.

Table I.2: Synopsis of molecular modeling techniques.

References

[1]   R. Ursula. Introduction to Electronic Structure Methods. EPFL, Lausanne, **2017**.

[2]   Y. Tua, A. Laaksonen. Advances in quantum chemistry Chapter 1 - Implementing Quantum Mechanics into Molecular Mechanics—Combined QM/MM Modeling Methods. **2010**, 59, 1-15.

[3]   C. Lillian. Quantum chemistry, University of Pittsburgh, **2009**.

[4]   David C. Young. Computational Chemistry: A Practical Guide for Applying Techniques to Real-World Problems, **2001**, 10-44.

[5]   M. Izquierdo, A. Maria. Large Scale Modelling of Photo-Excitation Processes in Materials with Application in Organic Photovoltaics. [Groningen]: University of Groningen, **2019**.

[6]   M.A. Michael. Molecular Spectroscopy and Modern Electronic Structure Computations, Rose-Hullman Institute of Technology Terre Haute, Indiana. **2001**, 222-235.

[7]   G. D. Mickael. Extending the Reach of Accurate Wavefunction Methods. Digital Comprehensive Summaries of Uppsala Dissertations from the Faculty of Science and Technology 1228. Uppsala: ActaUniversitatisUpsaliensis, **2014**.

[8]   Oliver Baum. Doctoral thesis, HSOH: An elusive species with many different traits, **2008**.

[9]   H. Dorsett and A. White, Overview of Molecular Modelling and Ab initio Molecular Orbital Methods Suitable for Use with Energetic Materials, Salisbury South Australia 5108, Australia, **2000**.

[10] L. Xin-Zheng, W. En-Ge. Computer simulations of molecules and condensed matter: from electronic structures to molecular dynamics. Singapore ; Hackensack, NJ : World Scientific. **2017**, 3, 17-22.

[11] M. Sc, Bo Li. Doctoral thesis, Density-Functional Theory and Quantum Chemistry Studies on "dry" and "wet" NaCl(001) vorgelegt .Doctoral dissertation,Universität Berlin, **2009**.

[12] H. Michael. Doctoral dissertation, Large-Scale Coupled-Cluster calculations, Doctoral dissertation. Universität in Mainz, **2008**.

[13] P. Lucjan. Ideas of Quantum Chemistry, Amsterdam; Boston, 1st ed., Elsevier, **2007**.

[14] N. Mihail, N.D. young. New Generation of Europium and Terbium Activated Phosphors from syntheses to applications, Singapore, Pan Stanford, **2011**.

[15]   C. C. M. Rindt, S. V. Gaastra-Nedea. Modeling thermochemical reactions in thermal energy storage systems. Advances in Thermal Energy Storage Systems. Eindhoven University of Technology, the Netherlands. Elsevier Ltd, **2015**, 392-393.

[16]   Errol G. Lewars. Computational Chemistry: Introduction to the Theory and Applications of Molecular and Quantum Mechanics, London New York,2nd ed, Springer Netherlands , **2011**, 509-510.

Chapter II
Schiff bases & Liquid-Liquid extraction of metals

1.   Transition metals

In 1921, Charles Bury was the first English chemist that used "transition" word regarding elements, and due to the inner layer changing of the electrons he adverted to a transition series of elements. Today this series calls d-block. Till now transition metal or element definition differs between authors and publications **[1]**.

1.1. Definition

The most common definition of transition metals is the one accepted by the IUPAC which defines it as "An element whose atom has an incomplete d sub-shell, or which can give rise to cations with a complete d sub-shell" **[2]**.

Others deal that transition metals are any of the elements of block d in the periodic table, this means that the transition metals are from group 3 to 12, while from f-block lanthanide and actinide series are called "Internal transition metals" **[3]**:

Figure II.1: The position of transition metals.

Note that the metals Hg, Cd, and Zn are not viewed as transition metals due to their electronic configurations, which is **(n-1) d^{10} ns^2**. These metals have totally filled *d* orbitals in their ground states and even in a portion of their oxidation states. One such model is the +2 oxidation state of mercury, which relates to an electronic configuration of **(n-1) d^1**.

1.2. Characteristics of transition metals

The most common transition metals characteristics are **[4,5]**:

1. **Variable oxidation states**

   Transition metals show variable oxidation because of the tendency of (n-1) d just as ns electrons to partake in bond formation.

2. **Metallic character**

   All transition metals are naturally metallic, i.e they have solid metallic bonds due to the existence of unpaired electrons. This offers to ascend to properties such as high density, high atomization enthalpies, and high boiling and melting points.

3. **Magnetic property**

   The substances that have paired electrons numbers are termed as diamagnetic substances, while those are containing unpaired electrons are supposed to be paramagnetic, except for ions of d^0(Sc^{+3}, Ti^{+4}) or d^{10}(Cu^+, Zn^{+2}) configurations. All other simple ions of transition metals contain unpaired electrons in their (n-1) d subshell so they are paramagnetic.

4. **Formation of complexes**

   Complexes can be formed by transition metals because of the presence of empty *d*-orbitals of reasonable energy, smaller size, and higher charge on cations.

5. **Ionisation enthalpy and electrode potential**

   The first ionization enthalpy of *d*-block elements is higher than those of *s*-block elements and lesser than those of *p*-square elements. IE increases with the atomic number increasing (i.e., size deceases). Except for Zn, although it is large in size, it has a higher IE due to its saturated orbitals.

6. **Ionic radii**

   With the increment in oxidation state, the ionic radii decrease from left to right. Usually for a similar oxidation state the ionic radii also decrease with increment in nuclear charge.

7. **Catalytic property**

   The majority of transition metals are utilized as a catalyst as a result of the empty *d*-orbitals, large surface zone, variable oxidation state, complexes formation ability, e.g., Fe, Ni, V2O3, Pt, MO, CO, and utilized as catalyst.

8. **Colored ions**

   The majority of the transition metals ions are coloured in solution just as in solid states that is because of the fractional absorption of visible light. The absorbed light moves the electron starting with one orbital then onto the next orbital of a similar d subshell. Since the electronic transition happens inside the d-orbitals of transition metal ions, they are called d–d transitions.

9. **Interstitial compounds**

   Due to the interstitials voids that are presented in transition metals, fitting of the atoms C, H, N, B, etc.., can produce interstitial compounds that are asymmetric, for example: for steel, it is more difficult, less malleable and ductile.

10. **Alloy formation**

    The majority of the transition structure can be in the form of alloys, as a result of similar ionic size, and in their crystal lattice it can commonly substitute their situations with each other easily, for example brass, bronze, steel, etc...

11. **Reactivity**

    Although the transition metals are electropositive enough, yet they are not reactive due to their sublimation heats and their high ionization energies.

1.3. Heavy metals

Heavy metals are defined as metallic elements that have a relatively high density compared to water. With the assumption that heaviness and toxicity are inter-related, heavy metals also include metalloids, such as arsenic, that are able to induce toxicity at low level of exposure [6].

1.4. Heavy metals toxicity

Heavy metals are harmful natural toxins, their toxicity causes many problems for the environment, humankind, alimentation, and ecological adjusts.

Generally we can find heavy metals in sewerages, e.g., Cd, As, Pb, Cr, Cu, Zn, and Ni as well these metals play a dangerous role for human wellbeing and the ecological balance, by the environmental natural factors or through the human's activity.

The sources of heavy metals can be the erosion of soil, natural weathering of the earth's crust, modern effluents, mining, urban runoff, sewage discharge, insect or disease control agents, which are applied to crops [7].

More so, the industrial products such as paints, cosmetics, pesticides, and herbicides also serve as sources of heavy metals [8].

According to the U.S geological survey 1133, 1995 heavy metals were classified into various categories like nontoxic, low toxic moderate and highly toxic. As shown in (Table II.2) below [9]:

Nontoxic	Low toxic	Moderately toxic	Highly toxic
Aluminum	Tin	Antimony	Uranium
Bismuth	Scandium	Beryllium	Vanadium
Calcium	Barium	Boron	Zinc
Iron	Germanium	Actinium	Zirconium
Magnesium	Gold	Cadmium	Tungsten
Manganese	Erbium	Chromium	Radium
Lithium	Gallium	Hafnium	Ruthenium
Sodium	Holmium	Copper	Thorium
Rubidium	Neodymium	Indium	Thallium
Strontium	Terbium	Lead	Titanium
Potassium	Thulium	Mercury	Silver
Molybdenum	Ytterbium	Nickel	Polonium
	Samarium	Platinum	
		Palladium	

Table II.1: Heavy metals classification based on toxicity.

2.   Overview of Schiff bases and its complexes

2.1.   Schiff's bases definition

Schiff bases is a neutral molecule with an electron pair and contains a carbon-nitrogen double bond with the nitrogen atom connected to an aryl or alkyl group, not hydrogen [10,11].

Schiff bases are discovered by Hugo Schiff in 1864 and it has several names such as ANILIS, IMINES and AZOMETHINE. Among of ligands it has a significant role and multiple uses in many domains. **[10,12]** .

The general formula for these compounds is presented in (Fig II.2).
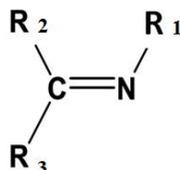
R_1, R_2 and / or R_3=alkyl or aryl

Figure II.2: General structure of a Schiff base.

Structurally, a Schiff base is a nitrogen analogue of an aldehyde or ketone in which the C=O has been replaced by an imines or azomethines group (C=N-R) **[11]**.

2.2. Synthesis of Schiff base

Schiff base be synthesized by condensation of a primary amine with an aldehyde or ketone as shown in scheme below (Sheme1):
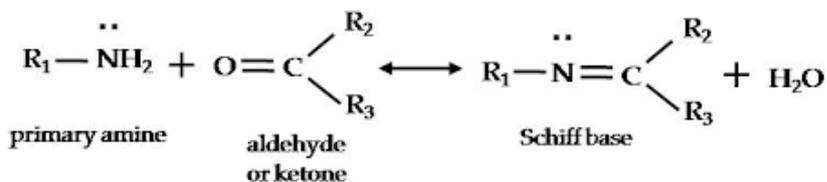
Scheme II.1: Formation of Shiff's bases.

Schiff's bases that contain aryl substituents are substantially more stable and more readily synthesized, while those which contain alkyl substituents are relatively unstable.

Schiff's bases of aliphatic aldehydes are relatively unstable and readily polymerizable while those of aromatic aldehydes having effective conjugation are more stable **[13]**.

2.3. Classes of Schiff base ligands

If Schiff bases carry a functional group they can act as coordinating ligands, when the hydroxyl is near enough to the condensation site while reacting with a metal ion that will leads to the formation of a five or six-member ring. Schiff bases are classified into 4 classes: bidentate, tridentate, tetradentate, or polydentate and those ligands have the ability of very stable complexes formation with the transition metals **[14]**.

(Fig I.3) Presents some classes of Schiff bases **[15]**:
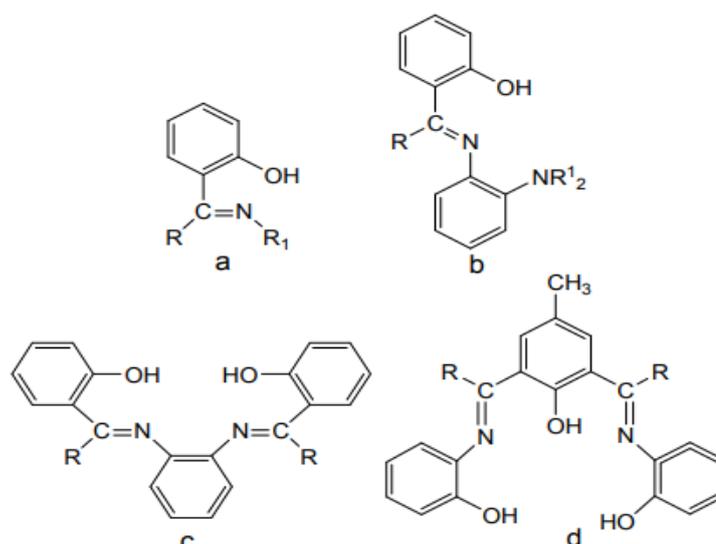
Figure II.3: Some classes of Schiff base ligands: a) bidentate; b) tridentate;
c) tetradentate; d) pentadentate

2.4. Schiff bases applications

Among the organic compounds, the Schiff bases are very important compounds due to their multiple uses in several fields such as biological, analytical, and inorganic chemistry. Among the biological activities that made it occupy great importance in the medical and pharmaceutical fields, are used as analgesics, anti-inflammatory, and antimicrobials, , anti-oxidants, anti-cancer, anti-convulsants, anthelmintics, and anti-tuberculous, etc.. **[16]**.

A few of Schiff bases which Salicylaldehyde is their based molecule or its derivatives are utilized in extraction in the analytical domain, and spectrophotometric determination of metal ions **[17]**.

2.5. Schiff Bases Metal Complexes

Schiff base metal complexes played an important role in the coordination chemistry development. This is because of the way that Schiff bases increase chances of substrate chirality's stimulation, tuning the metal centered electronic factor, also it improves the stabilization and solubilization of homogeneous or heterogeneous catalysts.

Schiff base complexes are known to facilitate synthetic procedures, and it's useful also in biology field as natural models or bioactive compounds. Most of them are focused on the catalytic activities in countless homogeneous and heterogeneous reactions **[15]**.

2.6. Formation of Schiff base-metal complexes

Schiff bases Metal complexes are commonly produced by treating metal salts with Schiff base ligands under favorable experimental conditions. Transition metal complexes of Schiff bases have been known for 130 years.

Mechanism of the formation and structure of these complexes and stereochemistry of four coordinate chelate complexes that are formed from Schiff bases and their analogs have been discussed in several reviews. The chelate group configuration of the four coordinate complexes might be square-planar, tetrahedral, distorted tetrahedral, or distorted trigonal pyramidal with the metal atom at the pinnacle. The configuration relies principally upon the nature of the metal atom furthermore on the symmetry of the ligand field. A diversity of physiochemical investigations on these complexes facilitates understanding of stereochemical and as well as electronic properties **[15]**.

The Schiff bases which are derived from Salicylaldehydes are remarkable as polydentate ligands coordinating in neutral forms. The interaction between these donors' ligands and metallic ions gives complexes of various geometries that complexes are possibly bioactive. Countless Schiff bases and their complexes are studied for their important and interesting properties, for example, their ability to bind oxygen reversibly, catalytic activity in hydrogenation of olefins, and transfer of an amino group, photochromic properties and the complexation ability towards certain toxic metals. The high affinity for the chelation of the Schiff bases towards some metallic ions is used in producing of their solid complexes **[18]**.

2.7. Applications of Schiff bases complexes

Numerous Schiff base metal complexes indicated in divers reactions an excellent catalytic activity at high temperature (>100°C) with moisture presence. In the recent few years, many reports reported on their applications in both homogeneous and heterogeneous catalysis.

In the previous two decades, Schiff base complexes structure, synthesis, and their properties have occupied a lot of attention for their notable contributions in single molecule-based magnetism, material science, catalysis of many reactions like carbonylation, hydroformylation, reduction, oxidation, epoxidation, and hydrolysis and so on.

A lot of work has been reported on the synthesis, structural investigations, various crystallographic features, mesogenic characteristics, structure-redox relationships, and catalytic properties of various types of Schiff bases and their complexes transition and non-transition elements. The most interest is being given to the study of Schiff bases that are containing Salicylaldehyde and their metal complexes. In past years Salicyladehyde derivatives have occupied an impressive interest because of their notable activities such as antifungal, antibacterial, antitumor, and anticancer **[18]**.

3.   **Liquid- Liquid Extraction of Metal ions**

Metal ion extraction is a hot topic and is important economically and environmentally. Metals are obtained from ores or scraps through metallurgical processes and then manufactured into final products used by humans, either directly or indirectly. The processing of raw materials into final products produces waste containing metal ions. These products are utilized and later discarded as waste. Metal ion extraction is an effort to recover the metal ions both from ores and from waste due to their limited availability in nature. In addition, metal ion extraction from metal-containing waste can reduce the level of environmental pollution. Therefore, an effective, efficient, economic and environmentally friendly method for the recovery of metal ions from ores and waste is an absolute necessity **[19]**.

A number of processes have been explored for metal ion recovery, such as precipitation, reverse osmosis, adsorption, ion exchange and solvent extraction using organic solvents. Solvent extraction (liquid-liquid extraction) is the most commonly used method for the separation of metal ions **[19]**.

3.1. **Definitions**

Liquid–liquid extraction (solvent extraction): is one of the most widely used techniques for the separation and purification of metal ion mixtures. A liquid–liquid extraction system generally consists of two immiscible phases: an organic phase (less polar, LP) containing the extractant(s), diluent(s) and possibly a modifier, and an aqueous phase (more polar, MP) containing the metals to be separated.

The less polar phase has been the objective of extensive studies for improving metal separations in many approaches, including developing new extractants, using mixtures of extractants, changing diluents, adding modifiers, and so on [20].

As well it's a suitable method to prevent and protect environment from pollution. Complexes of some metal ions with Schiff's bases have a big importance in organic synthesis and catalysis because of their variety of applications in biological, clinical, analytical, physiological, and pharmacological activities. The Schiff's bases ligands act as a good extracting agents for the transition of metal ions [21].

Solvent: In hydrometallurgical solvent-extraction systems, the term "solvent" is typically used to designate the organic phase.

Extractant: The active organic components of the solvent primarily responsible for the extraction off a metal; sometimes the term has been used to designate the total organic phase.

Diluent: The organic liquid in which an extractant and modifier are dissolved to form a solvent, some literature- has used the term "carrier".

Raffinate: The aqueous phase from which the metal solute has been removed by extraction.

Aqueous feed: The aqueous feed solution to the extraction stage that contains the metal or metals to be extracted [22].

3.2. Extraction parameters

a. Partition Coefficient

Firstly, we will assume a partition by a simple difference of solubility between two solvents (for example water and an organic solvent) according to [23]:

$$M \rightleftarrows \overline{M}$$
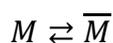
The partition is governed by the law of mass action and this equilibrium is characterized by the thermodynamic equilibrium constant K.

$$K = \frac{a_{\overline{M}}}{a_M} \qquad (1)$$

With a_M: M activity in the aqueous phase.

        $a_{\overline{M}}$: M activity in the organic phase.

Chemical activity "a" is linked to the concentration [M] by the Nernst law (in the molar scale):

The expression of the activity of M then becomes:

$$a = \frac{M\gamma_M}{C_0} \qquad (2)$$

With γ_M: Activity coefficient of the species M.

       [M]: Molar concentration of species M.

       C_0: Reference concentration, which by convention is equal to 1 mol.L^{-1}.

The expression (1) then becomes:

$$K = \frac{[\overline{M}]\gamma_{\overline{M}}}{[M]\gamma_M}$$

Depending on the concentration of the aqueous milieu, three cases can arise **[23]**:

1) The solutions are much diluted; concentrations are much lower than 1 mol.L^{-1}, we can then assume that the activities are equal to the concentrations. Indeed, the activity coefficients then tend towards the value 1.

$$\lim_{C \to 0} \frac{a_{org}}{a_{aqu}} = \frac{C_{org}}{C_{aqu}}$$

The expression of the equilibrium constant then becomes:

$$K = \frac{[\overline{M}]}{[M]}$$

2) The ionic force of the solution does not vary or little, the activity coefficients are then considered to be constant. The expression of the equilibrium constant becomes:

$$K = \frac{[\overline{M}]}{[M]}.cte$$

We define in this case an apparent constant K' (without unit) which is written:

$$K' = \frac{[\overline{M}]}{[M]}$$

3) The ionic force cannot be considered constant in this case; the equilibrium constant is expressed according to expression (2).

To evaluate the degree of extraction, we use the distribution coefficient D, which only takes into account the overall concentration of the element M in each phase.

If the metallic species M is not in the same chemical form in both phases, a new parameter D is then defined as the coefficient of distribution, its expression is as follows:

$$D = \frac{[\overline{M}]}{[M]}$$

$[\overline{M}]$: The total concentration of the species in the organic phase.

$[M]$: The total concentration of the species in the aqueous phase.

A so-called weak extraction, if the distribution coefficient is less than 1 (D <1).

Strong extraction, if the distribution coefficient is greater than 1 (D >> 1).

b. Efficiency of an extraction

The efficiency in liquid extraction - liquid can be expressed by the following expression [23]:

$$E\% = 100 \times \frac{C_{org}V_{org}}{C_{org}V_{org} + C_{aqu}V_{aqu}} = 100 \times \frac{D}{D + (V_{aqu}/V_{aqu})}$$

The efficiency E highlights the ratio of organic and aqueous phases.

When the volumes of the two phases are equal $V_{aqu} = V_{org}$ E% becomes:

$$E\% = 100 \frac{D}{D + 1}$$

c. Separation factor

The separation factor, also called the selectivity coefficient α_{MN} of two elements M and N is defined as the ratio of their distribution coefficient respective D_M and D_N established under the same conditions [23]:

$$\alpha_{MN} = \frac{D_M}{D_N}$$

D_M: Distribution coefficient of the species M.

D_N: Distribution coefficient of species N.

3.3. Classification of liquid-liquid extraction systems

Classification is based on the nature of interactions between extracted metal species and extractants. There are mainly four types of extraction [23]:

✓ Extraction by solvation.

✓ Cation exchange extraction.

✓ Chelation extraction.

✓ Anion exchange extraction.

3.3.1. Solvation extraction

An extracting organic compound is said to be solvatant if it has an atom (oxygen, sulfur, nitrogen, or phosphorus) likely to engage an electronic doublet in a coordination bond with some metallic atoms.

Such a compound generally has extractive properties that are related to neutral metallic salts.

If we note by E the extractant organic compound, M^{m+} metallic cation that extracted and X^- the anion associated with it in the aqueous phase, the extraction equilibrium is written as follows:
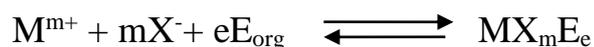
$$M^{m+} + mX^- + eE_{org} \rightleftharpoons MX_mE_e$$

Whose extraction constant is:

$$K_{ex} = \frac{[MX_mE_e]_{org}}{[M^{m+}][X^-]^m[E_{org}]^e}$$

The distribution coefficient of the metal written:

$$D_M = \frac{[MX_mE_e]_{org}}{M^{m+}} = K_{ex}[X^-]^m[E_{org}]^e$$

So: $$\log D_M = \log K_{ex} + m \log[X^-] + e \log[E_{org}]$$

The experimental use of this relation makes it possible to determine the stoihiometric coefficients of the equilibrium by varying a single parameter.

The extraction will be more forts if the concentration of extractant E is higher.

3.3.2. Extraction by exchange of cations

The extractant is an organic acid HL, with sufficient acidity. It can thus exchange the metallic cations with its protons according to the following equilibrium reaction:
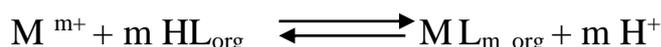
$$M^{m+} + m\ HL_{org} \rightleftharpoons ML_{m\ org} + m\ H^+$$

Extract equilibrium constant:

$$K_{ex} = \frac{[MLm]_{org}[H^+]^m}{[M^{m+}][HL]^m_{org}}$$

And distribution coefficient:

$$D_M = \frac{[ML_m]_{org}}{[M^{m+}]}$$

Hence the relation becomes:

$$\log D_M = \log K_{ex} + mpH + \log HL_{org}$$

The Study of the curves $\log D = f\ (pH)$ and $\log D = f\ (\log [HL]_{org})$ inform us of the number of exchanged protons, and therefore on the nature of the extracted complex.

3.3.3. Chelation extraction

In this case, the extractant molecule functions as a cation exchanger and as a solvent. It is a compound comprising a functional acid group in one hand and an electron donor atom in the other hand. Acid hydrogen is exchanged with the metallic cation, which neutralizes its charges. The donor group solvates the cation and saturates its coordination sites. The formation of the complex thus creates a cycle that will be all the more stable that has five to six bonds. As an example of extractants here, there are organophosphorus acids and hydroxy bases of Schiff.

3.3.4. Extraction by anion exchange

Some aqueous milieu complex metallic cations by forming anionic species, this type of extraction is governed by the following equilibrium reaction:

$$M^{m+} + nA^- \rightleftharpoons MAn^{(n-m)-} \quad with : n > m$$

The formed anionic species can't be extracted in the presence of an extractant having an anion which can be exchanged with the metal anion. The equilibrium extraction is as follows:

$$MA_n^{(n-m)-} + (n-m)(B^+, X^-)_{org} \rightleftarrows (MA_n^- \ B^+)_{(n-m)org} + (n-m)X^-$$
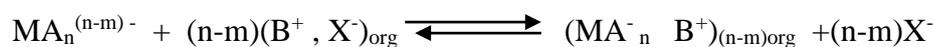
3.4. Solvent Selection

The molecular formula of the solute may suggest the type of solvent which may be selective for its extraction, based on probable affinities between related functional groups. Thus, to extract organic acids or alcohols from water, an ester, ether, or ketone (of sufficient molecular weight to have very limited solubility in the aqueous phase) might be chosen as the solvent **[24]**:

Specific factors taken into consideration in the selection of a solvent include:

1. Selectivity-the ability to remove and concentrate the solute from the other components likely present in the feed liquor.

2. Availability-the inventory of solvent in the extraction system can represent a significant capital investment.

3. Immiscibility with the feed-otherwise there will need to be recovery of the solvent from the Raffinate, or a continual and costly replacement of solvent as make up.

4. Density differential-too low a density difference between the phases will result in separation problems, lower capacity, and larger equipment. Too large a density difference may make it difficult to obtain the drop sizes desired for best extraction.

5. Reasonable physical properties-too viscous a solvent will impede both mass transfer and capacity. Too low an interfacial tension may lead to emulsion problems. The boiling point should be sufficiently different from that of the solute if recovery of the latter is to be by distillation.

6. Toxicity-must be considered for health considerations of the plant employees and for purity of the product.

7. Corrosiveness-may require use of more expensive materials of construction for the extraction process equipment.

8. Ease of recover- transfer of the solute from the feed still entails the further separation of solute from the solvent, solvent recovery will need to be as complete and pure as possible to permit recycle to the extractor as well as minimizing losses and potential pollution problems.

Solvent	Dielectric constant	Dipole moment (D)	Boiling point (C°)	Density (g/ml)	Solubility in water (% weight)	Solubiility of water in solvent (%weight)
Hexane	1.89	0	68.7	0.66	0.01	–
Benzene	2.28	0	80.1	0.88	0.08	0.06
Cyclohexane	2.02	0	80.72	0.78	–	0.01
Toluene	2.33	0.31	110.62	0.87	0.05	0.06
M-Xylene	2.4	0.4	139	0.86	0.01	0.04
Chloroform	4.81	1.04	61.15	1.49	0.81	0.97
Carbon tetrachloride	2.2	0	77	1.58	0.08	0.01
Chlorobenzene	5.5	1.6	132	1.11	0.05	0.05
Diethyl ether	4.4	1.2	35	0.71	6.9	1.26
Diisopropyl ether	3.9	1.2	68	0.72	0.9	0.6
Dibutyl ether	3.1	1.2	142	0.77	0.3	0.19
Diamyl ether	3.1	–	187	0.78	–	–
Ethyl acetate	6.4	1.8	77	0.9	7.94	3.01
Methyl isobutyl Ketone	13.1	–	116	0.8	1.7	1.9
Cyclohexanone	18.2	2.8	157	0.95	2.3	8

Table II.2: Physical properties of some common solvents used in Liquid-Liquid extraction **[25]**.

The most commonly used solvents are generally the aliphatic hydrocarbons, aromatics, and chlorinated solvents.

Solvents can be classified according to the specific interactions with the solute. we can classify Solvents into **[23]**:

- ✓ **Protic Solvents** (mobile hydrogen): water, acids, ammonia, alcohols, phenols, unsubstituted amides.
- ✓ **Dipolar aprotic Solvents** (it can't donate protons but are strongly polar): ketones, nitriles, sulfones.
- ✓ **Apolar aprotic Solvents: are** particularly hydrocarbons and, their halogenated derivatives.

3.5. Diluent Selection

The following characteristics are necessary for the choice of diluents **[26]**:

- ✓ Insolubility with water.
- ✓ Low viscosity.
- ✓ A density different from that of the aqueous phase (at least 120 Kg m^{-3}).

✓ An interfacial tension with water (less than 10N m^{-1}).

✓ Chemical stability and absence of toxicity.

✓ A boiling temperature above 170 °C in the case of a removal of water by distillation.

3.6. Effect of ionic force

It is known in the literature that the concentration of anions constituting the aqueous milieu has a significant effect on the extraction of metal ions. As this concentration is linked to the ionic force of the aqueous milieu by the relation below [23]:

$$\mu = \frac{1}{2}\sum C_i Z_i^{2}$$

μ: Being the ionic force of the aqueous milieu.

Z_i: Charge number of the species i.

C_i: Molar concentration the species i.

3.7. Factors influencing metals extraction

The most important factors that are influencing metals extraction are [27]:

✓ Influence of the nature of the chelator.

✓ Influence of the concentration of the chelator.

✓ Influence of the pH.

✓ Influence of the nature of the metal.

✓ Influence of the solvent.

3.8. Applications of Liquid-Liquid extraction

Industry	Phetochemical	Chemical	Pharceutical & alimentary	Metalurgical	Nuclear	Environmental
Applications	-Aromatics production. -Petrol purification. -Alkylation.	-Synthesis of polymers, Fibres, Pesticides, and Herbicides	-Antibiotics and vitamins recuperation. - Purification of genetic products.	-Recuperation and purification of metals.	-Treatment of wastes.	-Treatment of polluted waters. -Recovery and recycling of by-products.

Table II.3: Application of liquid-liquid extraction in industrial fields [26].

3.9. Advantages and disadvantages of Liquid-Liquid extraction

3.9.1 Advantages

✓ LLE offers significant advantages in toxicological analysis such as preconcentration of toxic substances, Simplicity, low cost, compatibility with analytical systems, high throughput, and ease of automatic operation, high purification, enrichment, separation and analyses of various compounds in mixtures **[28]**.

✓ Solvent extraction can be implemented in a continuous mode and is suitable for the processing of high metal feed concentrations **[29]**.

✓ Very large capacities are possible with a minimum of energy consumption**.**

✓ Heat sensitive products are processed at ambient or moderate temperatures (example: vitamin production) **[30]**.

3.9.2. Disadvantages

✓ Uses a large amount of organic solvent, such as Kerosence, toluence, dichloromethane or diethyl ether, which are often toxic and/or flammable and therefore environmentally unfriendly .Not only are their volatility and flammability an issue, but these organic also have a negative impact on human health if their vapors are emitted into the air **[19]**.

✓ Consumption of large volumes of expensive and toxic solvents, emulsion formation at the interface of the two phases and difficult phase separations **[31]**.

✓ Time/Labor intensive.

✓ May require an evaporation step prior to analysis to remove excess solvent.

✓ Contamination issues **[30]**.

References

[1]   J. Hicks. Preparation, Characterisation and Reactivity of Low Oxidation State d-Block Metal Complexes Stabilised by Extremely Bulky Amide Ligands. Springer theses, Monash University, Clayton, VIC, Australia, **2017**.

[2]   R. Gopalan, Inorganic chemistry for undergraduates. Universities Press (india), 1st ed, Hyderabad, **2009**.

[3]   A. Helmenstine, Transition Metals Definition, List and Properties, **2019**.

[4]   https://school.eckovation.com/short-notes-d-f-block/

[5]   https://mycbseguide.com/blog/the-d-and-f-block-elements-class-12-notes-chemistry/

[6]   P. B. Tchounwou , C. G. Yedjou, A. K. Patlolla, D. J. Sutton. Heavy metal toxicity and the environment. Molecular, Clinical and Environmental Toxicology, **2012**, 101,133-164

[7]   S.A. Bhat, T. Hassan, S. Majid, Heavy metal toxicity and their harmful effects on living organisms- a review. (IJMSDR). **2019**, 3, 106-122.

[8]   G.A Engwa, P.U. Ferdinand, F.N Nwalo, N.U. Marian. Mechanism and Health Effects of Heavy Metals Toxicity in Humans, **2019**.

[9]   P. Bhargava , N. Gupta, S. Vats, R. Goel. Health Issues and Heavy Metals. Austin J Environ Toxicol. **2017**, 3, 1.

[10] N.S Niyaz, R.S, K. Saud, G.R, S. Pandey, S.T Chavhan, RP Chavan. Synthesis, Characterization of some Schiff's bases derived from phenylhydrazine. International Journal of Chemical Studies. **2016**, 4, 109-111.

[11] K. Joginder, R. Amit, R.A. Vinit. Comprehensive Review on the Pharmacological Activity of Shiff base Containing Derivatives. Organic & Medicinal chem IJ. **2017**; 1 (3):555564.

[12] A. Mohammed Yimer. Review on preparation and description of some first series divalent transition metal complexes with novel Schiff's bases ligands. Review of Catalysts. **2015**, 2, 14-25.

[13] Z. Hussain, M.K., H. Adil, D.Z., F. Hassan, S.M., and E.Yousif. Metal Complexes of Schiff's Bases Containing Sulfonamides Nucleus: A Review. RJPBCS. **2016**, 7, 1009.

[14] V.K. Gaikwad, M.Y. Urmila. Metal complexes of Schiff bases. SRJIS. **2016,** 3, 2225-2234.

[15] M.A. Najat. Doctoral dissertation, Elecrochemical behavior and antioxidant activity of tetradentate Schiff bases and their Copper (II) complexes. University of Belgrade, **2014**.

[16] K. Anu, S.B., K. Sunil, N.S., and S. Vipin. Schiff Bases: A Versatile Pharmacophore. Journal of catalysts. **2013**.

[17] Al-Zaidi B.H., Mujbel Hasson M, Ismail A.H .New complexes of chelating Schiff base: Synthesis, spectral investigation, antimicrobial and thermal behavior studies. Journal of Applied Pharmaceutical Science. **2019**, 9, 045-057.

[18] J.D. Kamini. Synthesis and characterization of transition metal complexes of 2-(salicylimino)-3-hydroxypyridine. Journal of Chemical and Pharmaceutical Research. **2015**, 7, 798-803.

[19] D.O. Pius, M. Matsumoto. Metal Extraction with Ionic Liquids-Based Aqueous Two-Phase System. Recent Advances in Ionic Liquids , **2018**.

[20] L. Zheng , Z. Zidan, S. Simon, L.X., R. Stijin, N. Erik, E.D.V. Dirk , B. Koen. Enhancing Metal Separations by Liquid-Liquid Extraction Using Polar Solvents. Chem. Eur. J. **2019**, 25, 9197-9201.

[21] G. Amel, B. Djamal. Influence of the solvent on the extraction of copper(II) from nitrate medium using salicylideneaniline. Journal of dispersion science and technology. **2017**, 38, 930-934.

[22] D.C. Seidel. Laboratory procedures for hydrometallurgical-processing and waste-management experiments. United States, **1995**.

[23] A. Amel, B. Djamel. Extraction liquide–liquide du Ni(II) et Co(II) par une base de Schiff type salicylidèneaniline [N-(2-hydroxybenzylidene) aniline. Editions universitaires européennes, **2018**.

[24] C.V. Henry, C. L. Todaro. Fermentation and biochemical engineering handbook Principal, process design, and equipment, 2nd ed .Noyes, Westwood, New Jersey, U.S.A, **1997**, 354-355.

[25] S. Moldoveanu, D. Victor. Chapter 6. Solvent extraction. Modern Sample Preparation for Chromatography. Elsevier B.V, **2015**.

[26] I. Bouraqadi, Azeddine. These de doctorat, Extraction par solvant : Etude et modelisation du système tributylphosphate-acides monocarboxyliques. University de Tolouse, France, **2006**.

[27] S. Touati, B. Epouse. Thèse doctorat, Etude Expérimentale et Modélisation de la Purification de l'acide sulfurique. Chimie industrielle de la faculté des sciences de l'Ingénieur Université Mentouri, Constantine, **2012**.

[28] Singh, P. Yadav, Shalini, Yadava, N. Ram. Water Quality management Select proceedings of ICWEES-2016, Springer nature Singapore, **2018**.

[29] M.M. Rahman. Recent advances in ionic liquids. London, United Kingdom, IntechOpen, **2018**.

[30] C. M. Subhash C. Mandal, M. Vivekananda, K.D. Anup. Extraction of botanicals, in essentials of botanical extraction. Principals and applications. San Diego, United States, Elsevier, **2015**.

[31] B. Pourya, A.M. Amir. Microextraction techniques as a sample preparation step for metal analysis. Culture & research (ACECR), Urmia Iran, **2012**.

Chapter III

Study on the reactivity of Salicylideneaniline ligands

1.   Introduction

All compounds that contain an imine function (-C=N-) are appointed Schiff bases, and these compounds represented as a significant class due to their diversity of properties and applications. The studies of the Schiff bases fastly developed because they have excellent characteristics such as structural similarities with natural biological substances.

Schiff bases may contain various substituents with various electron-donating or electron-withdrawing groups and may have interesting chemical structural properties. They cause a specific interest in their biological activities **[1]**.

Among molecules that belong to the Schiff base family, N-Salicylideneaniline (HSA) is a model compound that has been studied with different solvents in solutions and solid-state, because of its photochromic, thermochromic, and solvatochromic properties. This molecule has great importance for potential applications in many fields, from optical devices and molecular switches to medicine [**2**].

So in this chapter we will study the Schiff bases of type (Salicylideneaniline HSA) and its ligands in 3 different positions (Ortho-Meta-Para): Salicylidene-2-fluoroaniline (2F-SA), salicylidene-3-fluoroaniline (3F-SA), salicylidene-4- fluoroaniline (4F-SA), salicylidene-2-chloroaniline (2Cl-SA), salicylidene-3-chloroaniline (3Cl-SA), salicylidene-4-chloroaniline (4Cl-SA), salicylidene-2-bromoaniline (2Br-SA), salicylidene-3-bromoaniline (3Br-SA), salicylidene-4-bromoaniline (4Br-SA), salicylidene-2-iodoaniline(2I-SA), salicylidene-3-iodoaniline (3I-SA) salicylidene-4-iodoaniline(4I-SA),salicylidene-2-methylaniline(2Me-SA), salicylidene-3-methylaniline (3Me-SA), salicylidene-4- methylaniline (4Me-SA), salicylidene-2-ethylaniline(2Et-SA), salicylidene-3-ethylaniline (3Et-SA), salicylidene-4-ethylaniline(4Et-SA), salicylidene-2-propylaniline (2Pr-SA), salicylidene-3-propylaniline (3Pr-SA), salicylidene-4-propylaniline (4Pr-SA), salicylidene-2-isopropylaniline (2iPr-SA), salicylidene-3-isopropylaniline (3iPr-SA), salicylidene-4-isopropylaniline (4iPr-SA).Whose occupied a lot of interest because of their interesting properties in behaving with transition metals.

2.   Study of the reactivity of substituted Salicylideneaniline

$[C_6H_4OCHNC_6H_4X]^-$, $[C_6H_4OCHNC_6H_4R]^-$
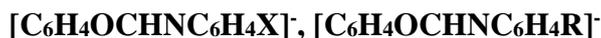
(**X**= H, F, Cl, Br, I), (**R**= Me, Et, Pr, iPr)

The presence of substituents (X, R) on the phenyl ring has a decisive influence on the reactivity of this type of compounds (ligands).

2.1.   Geometry optimization

2.1.1. Amsterdam density functional theory (ADF)

ADF is a quantum chemistry Fortran code based on the DFT. It got developed since the early 1970s and got named that time as HFS then as AMOL, principally by theoretical chemistry groups at Vrije University in Amsterdam, University of Calgary, and Canada. More developments are being led by the theoretical chemistry group at the University of Groningen, the Netherlands. Maintenance and distribution of the commercial (export) version of the program are done by Scientific Computing & Modelling NV (SCM), a company based in Amsterdam.

ADF can be useful in multiple fields, e.g. in Molecular Spectroscopy, Organic and Inorganic chemistry, Crystallography, and Pharmacochemistry as well **[3]**.

2.1.2. Characterization of ADF

A.   Functionality

- ✓ Single Point calculation.
- ✓ Geometry Optimization.
- ✓ Transition States.
- ✓ Frequencies and thermodynamic properties.
- ✓ Tracing a Reaction Path.
- ✓ Computation of any electronic configuration.
- ✓ Excitation energies, oscillator strengths, transition dipole moments, (hyper) polarizabilities, Van der Waals dispersion coefficients, CD spectra, ORD, using Time-Dependent Density Functional Theory (TDDFT).
- ✓ ESR (EPR) g-tensors, A-tensors, NQCCs.
- ✓ NMR chemical shifts and spin-spin coupling constants.
- ✓ Various other molecular properties.

✓ Treatment of large systems and environment by the QM/MM (Quantum Mechanics / Molecular Mechanics) hybrid approach **[4]**.

B.   **Applicability**

✓ All elements of the periodic table can be used (Z = 1-118). For each of the elements, the database contains basis sets of different sizes, ranging from minimal to high quality. Special basis sets are provided for relativistic calculations within the ZORA approach and for response calculations that require additional diffuse basis functions **[4]**.

C.   **Exchange – correlation functional**

Some of the exchange-correlation functionals available in the ADF program can be summarized in the following table **[5]**:

Approximations	Functionals
LDA	VWN
GGA	BP, BLYP, PW91, mPw, PBE, RPBE, revPBE, mPBE, PBEsol, OLYP, OPBE
GGA-D	BP86-D, BLYP-D, PBE-D, PBEsol-D
Meta-GGA	M06-L, TPSS
Model	SAOP, LB94
Hybrid	B3LYP, B3LYP*, KMLYP, O3LYP, BH and HLYP, B1PW91, mPW1PW, mPW1K, PBEO, OPBEO
Meta-Hybrid	M06, M06-2X, M06-HF, TPSSH

Table III.5: Available exchange-correlation functionals in ADF software.

D.   **STO basis sets**

The basis functions used in ADF are generally known as Slater Type Orbitals [**6**].

$$\chi^{STO}(r, \theta, \varphi) = NY_{l,m}(\theta, \varphi)r^{r-1}e^{-\varepsilon r}$$

A basis set can roughly be characterized by two things, firstly by its size (single-, double-, triple-zeta; with or without polarization), secondly by the level of frozen core approximation.

The standard basis sets available in ADF are **[7]**:

SZ: simple zeta or « single zeta ».

DZ: double zeta.

DZP: double zeta + one function of polarization.

TZP: triple zeta + one function of polarization.

TZ2P: triple zeta + two functions of polarization.

QZ2P: quadruple zeta + two functions of polarization.

E.   ADF applications

✓ It treats solvation problems and conduct transition state searches.

✓ It permits calculation of ground and excited-state energies, just as harmonic vibrational frequencies, optimized structures, and even molecular properties like NMR spin coupling or NMR spin-spin coupling.

✓ It allows using QM/MM methods for treating larger systems.

✓ With ADF program, Both of Sybil and Amber force fields are provided, and it can be modified easily by the user.

✓ Another available model of ADF called Band permits studying of polymers and bulk crystals. It is a helpful tool for studying the chemisorptions phenomena or reactions on surfaces.

✓ For larger calculations, ADF input files can be made from a Protein Data Bank record by utilizing contributing software, pdb2adf, that is accessible on the SCM site, with ADF we can easily run calculations on bigger and organically significant particles.

✓ ADF can perform IR simulations, Raman, and electronic spectra also it visualizes the density of states. So this feature makes the software package attractive and interesting for both computational and experimental groups searching for easiness and rapidity but approximate simulation of molecular spectra.

✓ ADF is used for treating multiple chemical problems that are necessary for academia and industry fields.

✓ ADF affords a great flexibility and it can be utilized for a wide range of chemical applications from inorganic chemistry to biology and surface science **[8]**.

F.   Calculation method

The structural determination was supplemented by a theoretical study in order to determine the geometric structure & the electronic structure. The calculations were carried out within the framework of the DFT.

The calculation method is based on the TZP (Triple Zeta polarized) base and GGA: BLYP functional using the ADF code 2012.01 with a frozen core at "medium" and integration accuracy "6.0".

2.2. Presentation of the studied geometries

The reactivity of the Salicylideneaniline ligands is linked generally to its structure and its electronic properties, and specifically in our study we highlighting two influencers on its reactivity:

✓ The influence of substituent position (Ortho, Meta, Para).**(Fig III.1)**

✓ The influence of substituent nature (X, R).**(Fig III.2)**

For starting our study, we chose 8 Salicylideneaniline ligands with different substituents on the aniline part, which are X= F, Cl, Br, I, and R= Me, Et, Pr, iPr, comparing with HSA (Reference). We will study each of the previous substituents separately in three different positions (Ortho, Meta, Para) to analyze and compare the influence of each one of them on the Salicylideneaniline reactivity.

X:F,Cl,Br,I / R:CH$_3$,C$_2$H$_5$, Pr, iPr
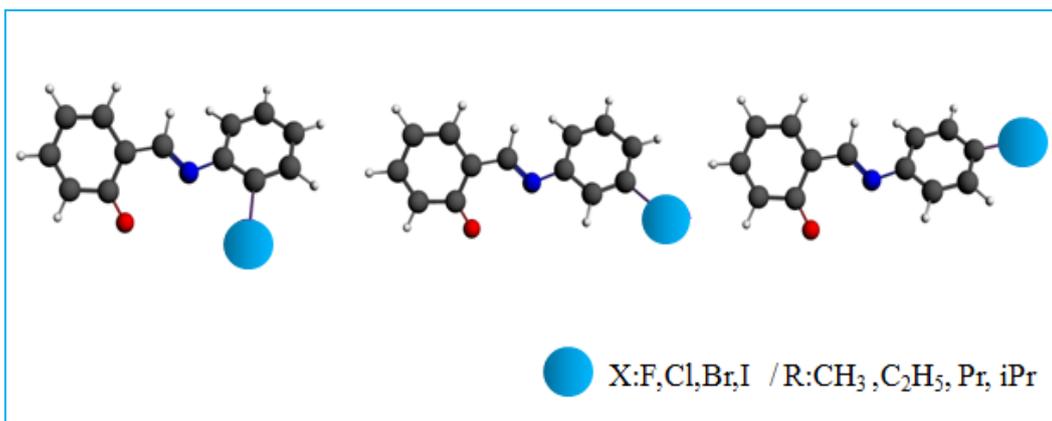
Figure III.1: The influence of substituent position.

F: ⬤   Cl : ⬤   Br : ⬤   I : ⬤

Methyl :   Ethyl :   Propyl :   Isopropyl :

⬤ **Carbon**   ⬤ **Oxygen**   ⬤ **Nitrogen**
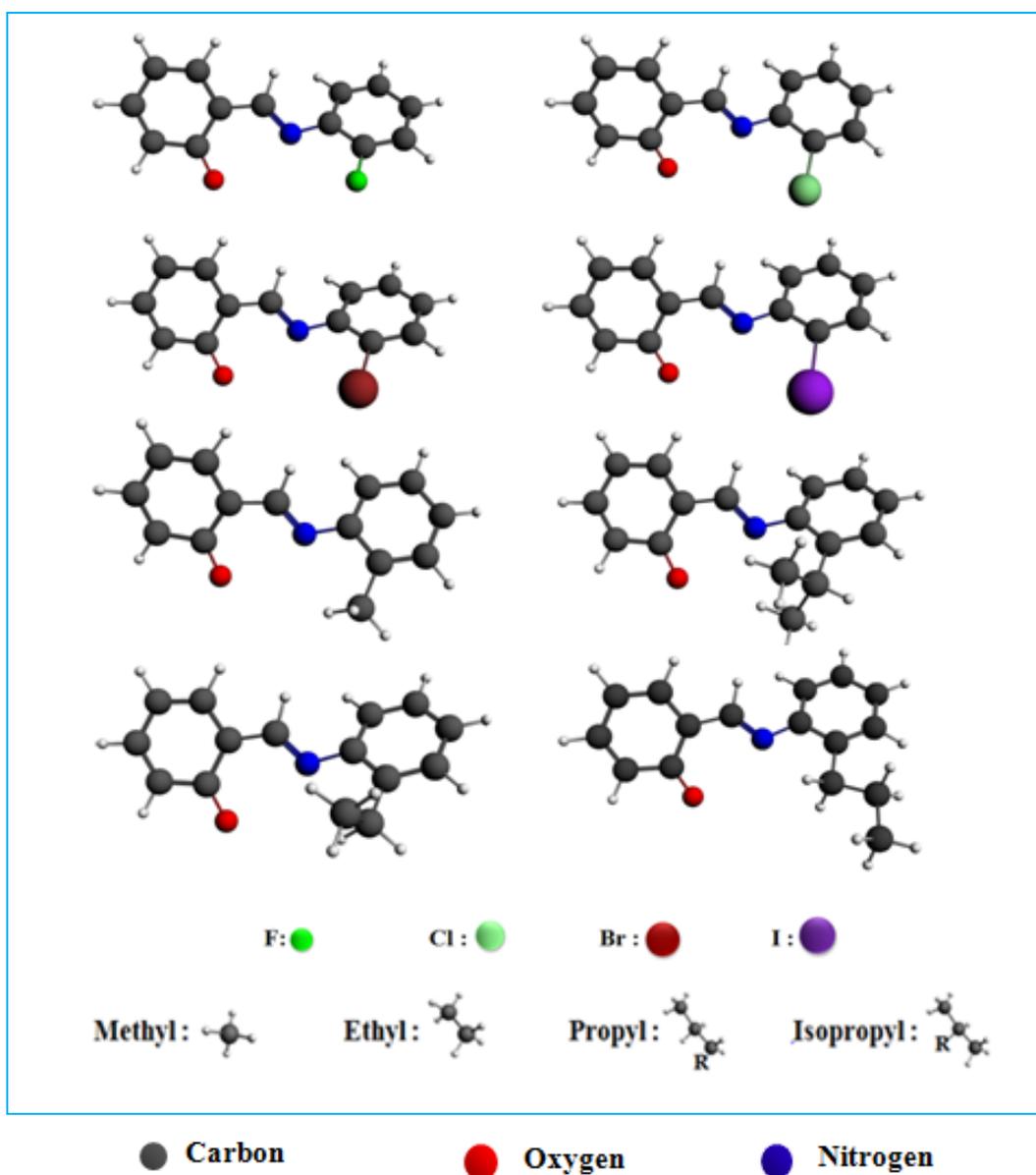
Figure III.2: The influence of substituent nature (X, R).

3.   Results and discussion

3.1.   Structure of Salicylideneaniline and its ligands

Salicylidenanilines compounds are whose main active site consists of an imine function R-CH=N-R 'can be substituted by R and R' aliphatic radicals aromatic **[9]**.

The optimized structure of the HSA molecule is shown in the **Fig III.3**

The atomes of the studied system are numbered as shown in the figures below:
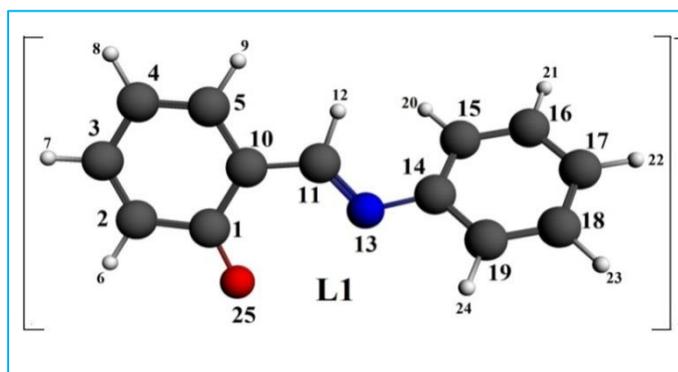
Figure III.3: HSA 3D conformation (according to input numbering).
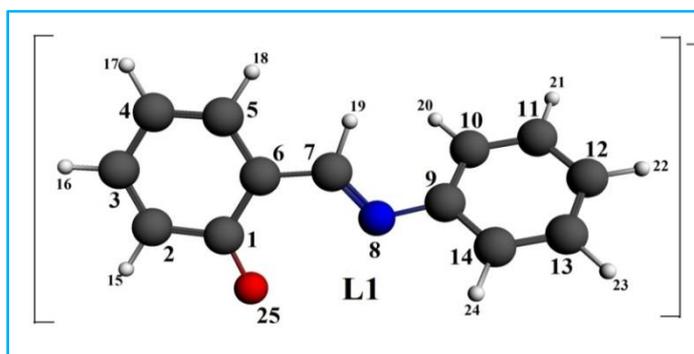
Figure III.4: HSA 3D conformation (according to our numbering)

Although the studied system is the same, the numbering of the atoms that make up it differs in the input window from the output window of some descriptors. So to avoid making mistakes, we again numbered the atoms to unite it when collecting the necessary data that we will summarize in all tables.

Fig III.5 and **Fig III.6** represent the structures of different Salicylideneaniline ligands.
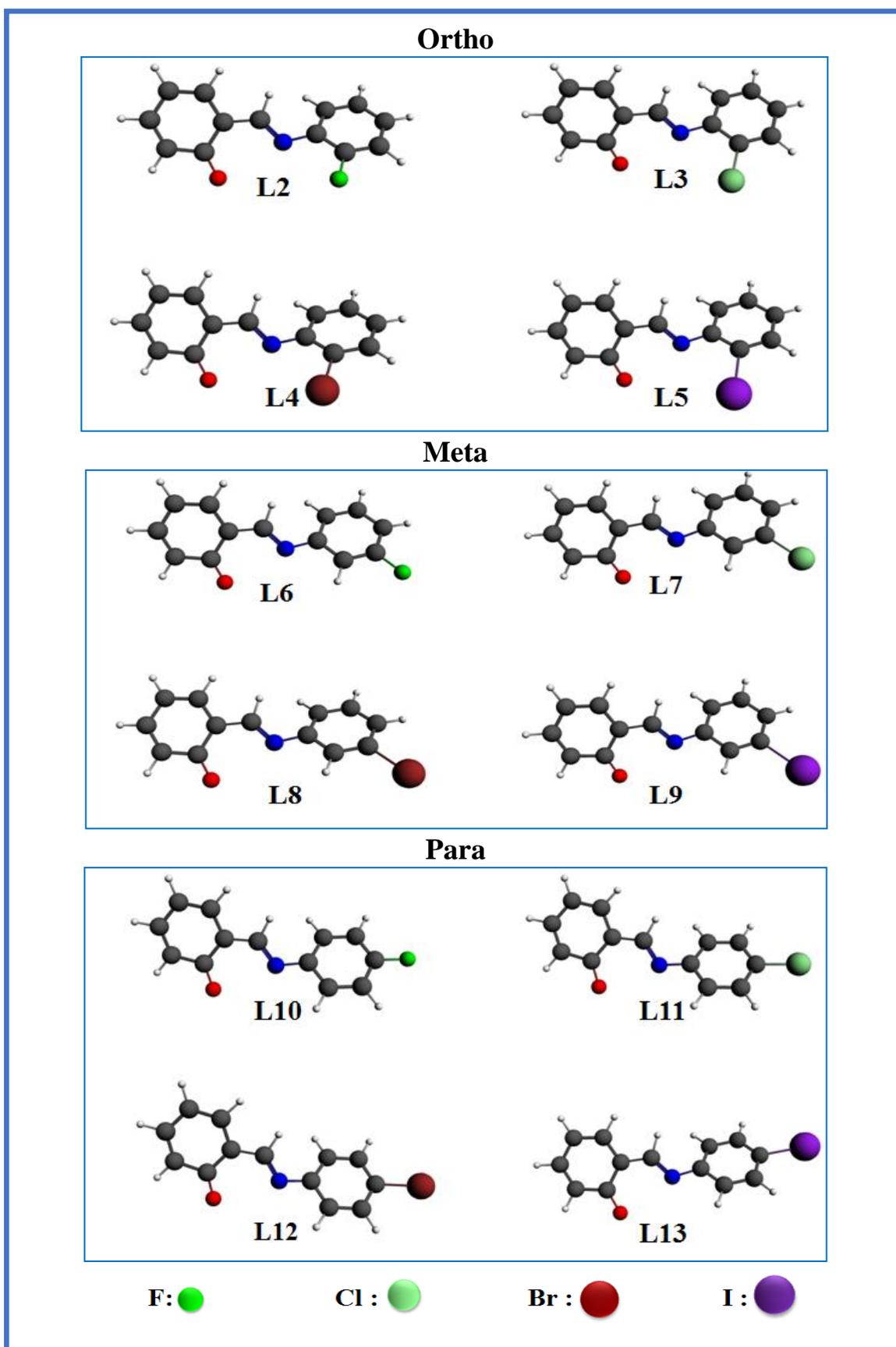
Figure III.5: Salicylideneaniline ligands structures (F,Cl,Br,I substituents in different positions Ortho, Meta, Para).

Ortho

L14

L15

L16

L17

Meta

L18

L19

L20

L21

Para

L22

L23

L24

L25

Methyl :   **Ethyl :**   **Propyl :**   **Isopropyl :**
                                              R   R
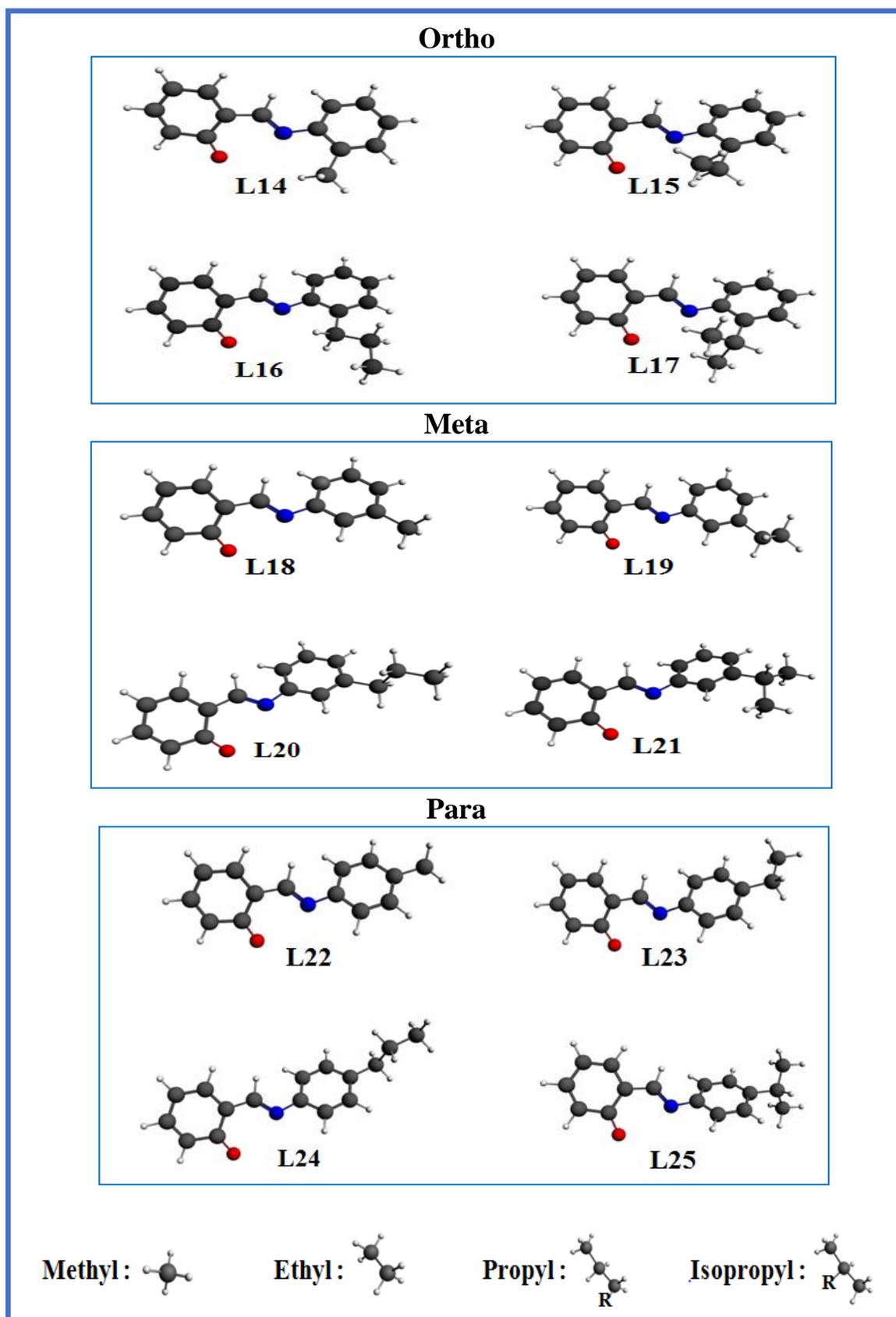
Figure III.6: Salicylideneaniline ligands structures (Me, Et, Pr, iPr substituents in different positions Ortho, Meta, Para).

3.2. The influence of substituent position (Ortho, Meta, Para)

3.2.1. Study of geometric structure

Table III.2: presents the main geometric parameters of the substituted Salicylideneaniline in the (Ortho, Meta, Para) positions:

X Nature			F			Cl			Br			I			HAS (Reference)
Ligands			2F-SA	3F-SA	4F-SA	2Cl-SA	3Cl-SA	4Cl-SA	2Br-SA	3Br-SA	4Br-SA	2I-SA	3I-SA	4I-SA	
Distances (pm)	Ring 1	C_1-C_2	146.9	146.8	147.9	146.9	146.8	146.7	146.9	146.9	146.8	147.0	146.8	146.9	146.8
		C_2-C_3	137.9	137.9	134.4	137.9	137.9	137.9	137.9	137.8	137.9	137.8	137.9	137.9	138.0
		C_3-C_4	142.6	142.6	140.4	142.6	142.6	142.5	142.6	142.7	142.6	142.7	142.7	142.6	142.5
		C_4-C_5	138.5	138.6	140.0	138.5	138.5	138.6	138.5	138.5	138.5	138.5	138.5	138.6	138.7
		C_5-C_6	142.8	142.7	140.1	142.8	142.8	142.7	142.8	142.9	142.8	142.9	142.8	142.8	142.6
		C_6-C_1	149.1	148.9	148.8	148.9	149.0	148.9	148.9	149.0	149.0	149.0	149.0	149.0	148.9
	(Ring 1 avg)		142.96	142.92	141.93	142.93	142.92	142.93	142.96	142.93	142.98	142.95	142.97		142.62
	Ring 2	C_9-C_{10}	142.6	142.7	141.4	142.8	142.6	142.4	143.0	142.4	142.5	143.2	142.5	142.6	142.4
		C_{10}-C_{11}	140.0	139.8	139.9	139.7	139.8	140.0	139.6	139.7	140.2	139.6	139.7	140.2	140.0
		C_{11}-C_{12}	140.2	140.6	139.7	140.3	140.3	139.8	140.3	140.5	139.5	140.3	140.7	139.6	140.4
		C_{12}-C_{13}	140.9	139.6	139.6	140.5	140.2	140.1	140.6	140.0	140.0	140.6	140.0	140.0	140.8
		C_{13}-C_{14}	138.9	138.4	139.8	139.5	138.8	139.5	139.3	138.5	139.6	139.4	138.5	139.7	139.6
		C_{14}-C_9	142.2	142.4	140.3	142.7	142.6	142.1	142.3	142.8	142.3	142.1	143.0	142.3	142.2
	(Ring 2 avg)		140.8	140.58	140.12	140.92	140.72	140.65	140.85	140.65	140.68	140.86	140.73	140.73	140.9
		C_6-C_7	143.4	143.5	148.2	143.4	143.3	143.5	143.3	143.4	143.4	143.3	143.3	143.3	143.8
		C_7=N_8	131.2	131.1	130.4	131.2	131.2	131.1	131.3	131.3	131.2	131.3	131.3	131.2	130.9
		N_8-C_9	138.4	138.6	136.2	138.0	138.6	138.8	137.9	138.7	138.7	138.0	138.3	138.6	139.1
Valence angle (°)		C_6-C_7=N_8	129.1	128.8	120.8	129.1	128.9	128.8	129.1	128.7	128.8	129.5	128.8	128.6	128.9
		C_7=N_8-C_9	118.7	119.4	127.4	119.4	119.3	119.2	119.2	119.3	119.4	119.2	119.4	119.7	119.4
Dihedral angle (°)		C_6-C_7=N_8-C_9	171.0	172.7	178.0	171.2	171.4	175.1	170.5	173.1	173.9	170.2	174.1	172.0	174.0

Table III.3: presents the main geometric parameters of the substituted Salicylideneanilines in the (Ortho, Meta, Para) positions:

Alkyl Nature		Me			Et			Pr			iPr			HSA (Reference)
Ligands		2Me-SA	3Me-SA	4Me-SA	2Et-SA	3Et-SA	4Et-SA	2Pr-SA	3Pr-SA	4Pr-SA	2iPr-SA	3iPr-SA	4iPr-SA	
Ring 1	C_1-C_2	145.8	146.8	145.8	146.8	146.8	146.8	146.7	146.8	146.8	146.5	146.9	146.8	146.8
	C_2-C_3	136.7	138.4	136.7	138.0	138.0	138.1	138.1	138.0	138.0	138.0	138.0	138.0	138.0
	C_3-C_4	141.4	143.1	141.4	142.4	142.5	142.5	142.4	142.5	142.4	142.4	142.5	142.4	142.5
	C_4-C_5	137.2	139.2	137.2	138.8	138.8	138.8	138.8	138.8	138.7	138.7	138.8	138.8	138.7
	C_5-C_6	141.3	143.1	141.3	142.6	142.6	142.6	142.6	142.6	142.6	142.5	142.6	142.6	142.6
	C_6-C_1	147.3	148.5	147.3	148.9	148.9	148.9	148.8	148.9	148.9	149.0	148.9	148.8	148.9
Ring 1 avg		141.62	143.18	141.62	142.92	142.93	142.95	142.90	142.92	142.90	142.85	142.95	0142.9	142.62
Ring 2	C_9-C_{10}	141.0	142.4	141.0	142.2	142.3	142.0	142.0	142.3	142.2	142.3	142.5	142.1	142.4
	C_{10}-C_{11}	139.0	140.6	139.0	139.9	140.0	140.3	140.0	140.0	140.0	139.9	139.6	140.1	140.0
	C_{11}-C_{12}	139.2	140.7	139.2	140.2	140.2	140.7	140.0	140.2	140.7	140.0	140.6	140.8	140.4
	C_{12}-C_{13}	139.6	141.8	139.6	140.6	141.3	141.3	140.8	141.2	141.3	140.5	141.4	141.2	140.8
	C_{13}-C_{14}	138.5	140.2	138.5	140.2	140.0	139.4	140.1	139.9	139.5	140.5	140.4	139.5	139.6
	C_{14}-C_9	140.9	142.4	140.9	143.3	142.1	142.2	143.4	142.1	142.1	143.5	141.8	142.0	142.2
Ring 2 avg		139.7	141.35	139.7	141.07	140.98	140.98	141.05	140.95	140.97	141.12	141.05	140.62	140.9
Distances (pm)	C_6-C_7	143.1	143.9	143.1	143.9	143.8	143.9	143.9	143.8	143.8	143.8	143.9	143.9	143.8
	C_7=N_8	129.3	130.7	129.3	130.8	130.9	130.9	130.8	130.9	130.9	130.6	130.8	130.9	130.9
	N_8-C_9	138.1	139.1	138.1	139.4	139.2	139.4	139.3	139.2	139.2	139.3	139.1	139.2	139.1
Valence angles (°)	C_6-C_7=N_8	128.8	128.8	128.8	128.6	128.8	129.1	128.8	128.8	128.9	128.1	128.5	128.9	128.9
	C_7=N_8-C_9	119.4	119.5	119.4	120.1	119.5	119.2	119.8	119.5	119.1	120.5	120.0	119.2	119.4
Dihedral angle (°)	C_6-C_7=N_8-C_9	174.4	173.1	174.4	174.8	173.7	173.9	174.5	174.1	174.3	174.2	171.8	174.8	174.0

Table III.7: Geometric descriptors, distances (pm) & angles (°) of HSA & its ligands.

Table III.2 and Table III.3 Analysis

We note from obtained results in these tables that:

- ✓ The median values of distances between carbons of Ring(1) for both of X and R substituents are all somehow equal to each other in whatever position but, the median values of the Ring (2) for unsubstituted HSA for first table, is the highest value comparing with the rest median values of the other mentioned subs.

- ➢ The joining of either X or R subs to the SA molecule rings leads to decreasing of distances between carbons that form that rings, so we result that the median values of distances between carbons of the Ring (1) are bigger than of the Ring(2)**[10].**

- ➢ The sub presence in a molecule leads to the contraction of rings bonds, and as well influence on interatomic distances that are out of the rings **[10]**.

- ✓ The $(C_6\text{-}C_7)$ distances of all ligands didn't get affected much. And that is due to the difference in position between the mentioned carbons and subs which that ligands have. So its values almost came (less or equal to 143.8 pm). Except for sub F in Para position: it's (around 148,2pm) means longer than of unsubstituted HSA.

- ✓ For ligands that contain (X subs) : $(C_7\text{=}N_8)$ distances in all positions increases (around 131pm) comparing to that of HSA (reference), except for F sub in the Para position it decreases to 130.4pm.

  While for ligands that contain (R subs): $(C_7\text{=}N_8)$ distances in all positions are almost equal to the HSA (reference), except for Me sub in Ortho and Para, it decreased to (129.3pm).

- ✓ For ligands of (X subs) in all positions: $(N_8\text{-}C_9)$ distances is lesser than of HSA (reference). And almost are equaled to HSA (139.1pm) for the case of ligands of (R subs), except for Me it is lesser in Ortho and Para (around 138.1pm).

- ✓ Due to the position and electronegativity of X subs, valence angels of $(C_6\text{-}C_7\text{=}N_8)$ decrease. For example: for F sub in the Ortho position, the angle is about (129.1°) but, once it is farther in position (Para position) the valence angle becomes(120.8°). But for R subs, it is the reverse thing, that the valence angels increase a little bit , e.g. for the iPr sub, the valence angels are (128.1°-128.5°-128.9°) for o-m-p respectively, except for Me it stays equaled.

✓ For (X) subs, the valence angles of (C$_7$=N$_8$-C$_9$) are somehow equal to that of HSA, but for the case of F sub, the affection on that angle noted, so that when F is in Ortho position angle be (118.7 °), and in Para (127.4°).

While for R subs that angles decreases from Ortho to Para positions.

✓ The Dihedral angles for (X subs) ligands increase progressively from Ortho to Para, according to the position of sub. But, for R subs, the dihedral angles in Ortho and Para positions are remarkable big than of HSA dihedral angle comparing to subs in Meta position which is less values.

3.2.2. Study of chemical descriptors

A. Global chemical quantities

Density functional theory (DFT) has been found to be successful in providing theoretical insights into the chemical reactivity and selectivity, in terms of qualitative chemical concepts like electronegativity (χ), hardness (η), softness (S), electrophilicity index (ω) **[12]**:

B. Ionization potential (I) is defined as the amount of energy required to remove an electron from a molecule. It is related to the energy of the E$_{HOMO}$ through the equation:

$$I = -E_{HOMO}$$

C. Electron affinity (A) is defined as the energy released when a proton is added to a system. It is related to E$_{LUMO}$ through the equation:

$$A = -E_{LUMO}$$

Note that: the MOs are energy levels which are the outcome of electrostatic interaction of atomic orbitals of atoms constituting the molecule. The electrons with unique quantum numbers reside in these MOs. The highest energy level which has electrons is called the Highest Occupied Molecular Orbital (HOMO) and the lowest energy level of the empty MOs is called Lowest Unoccupied Molecular Orbital (LUMO).The HOMO is the outermost filled orbital of the molecule. It can be semilarised to the valence shell. Surrounding the molecules are probabilistic empty energy levels in which electrons can be added from outside or might jump from HOMO due to energy absorption. The LUMO is like the conduction shell. As the size of molecules is very small the charging energy for electrons is very large **[12]**.

When the values of I and A are known, one can determine the electronegativity χ and the chemical potential (μ).

D. The electronegativity (χ) is defined as the measure of the power of an atom or group of atoms to attract electrons towards itself, it can be estimated by using this equation:

$$\chi = \frac{I + A}{2}$$

The basic relationship of the DFT is precisely, the one established by Parr et al. that links the chemical potential of DFT with the first derivative of the energy with respect to the n number of electrons, and therefore with the negative of the electronegativity χ.

$$\mu = \left(\frac{\partial E}{\partial N}\right)_{v(r)} = -\chi$$

Where μ is the chemical potential, E is the total energy, N is the number of electrons, and $v(r)$ is the external potential of the system.

E. Chemical hardness (η) measures the resistance of an atom to a charge transfer, it is estimated by using the equation:

$$\eta = \frac{I - A}{2}$$

F. Chemical softness (S) is the measure of the capacity of an atom or group of atoms to receive electrons, it is estimated by using the equation:

$$S = \frac{1}{\eta}$$

G. The electrophilicity index ($\boldsymbol{\omega}$) is a descriptor of reactivity that allows a quantitative classification of the global electrophilic nature of a molecule within a relative scale.
Parr et al have proposed electrophilicity index as a measure of energy lowering due to maximal electron flow between donor and acceptor. They defined electrophilicity index (ω) as follows.

$$\omega = \frac{\mu^2}{2\eta}$$

According to the definition, this index measures the propensity of chemical species to accept electrons. A good, more reactive, nucleophile is characterized by lower value of μ, ω; and conversely a good electrophile is characterized by a high value of μ, ω **[11]**. All the global quantities of were calculated in **Table III.4**.

After optimizing the studied programmed systems, we collected the calculation results from the obtained output files and put them together in the following table:

Substituent (Sub)		E HOMO (ev)	E LUMO (ev)	(ΔE)	I	A	χ	μ	Iɳ	S	ω
H		-0.372	1.640	2.012	0.372	-1.640	-0.634	0.634	1.006	0.994	0.199
F	2F-SA	-0.484	1.486	1.970	0.484	-1.486	-0.501	0.501	0.985	1.015	0.127
	3F-SA	-0.545	1.427	1.972	0.545	-1.427	-0.441	0.441	0.986	1.014	0.099
	4F-SA	-0.478	1.528	2.006	0.478	-1.528	-0.525	0.525	1.003	0.997	0.137
Cl	2Cl-SA	-0.519	1.449	1.968	0.519	-1.449	-0.465	0.465	0.984	1.016	0.110
	3Cl-SA	-0.616	1.324	1.940	0.616	-1.324	-0.354	0.354	0.970	0.103	0.065
	4Cl-SA	-0.581	1.354	1.935	0.581	-1.354	-0.387	0.387	0.968	1.033	0.077
Br	2Br-SA	-0.560	1.391	1.951	0.560	-1.391	-0.416	0.416	0.976	1.025	0.088
	3Br-SA	-0.660	1.235	1.895	0.660	-1.235	-0.288	0.288	0.948	1.055	0.044
	4Br-SA	-0.625	1.175	1.800	0.625	-1.175	-0.275	0.275	0.900	1.111	0.042
I	2I-SA	-0.607	1.227	1.834	0.607	-1.227	-0.310	0.310	0.917	1.091	0.052
	3I-SA	-0.687	0.623	1.310	0.687	-0.623	0.032	-0.032	0.655	1.527	0.001
	4I-SA	-0.675	0.577	1.252	0.675	-0.577	0.049	-0.049	0.626	1.597	0.002
Me	2Me-SA	-0.365	1.647	2.012	0.365	-1.647	-0.641	0.641	1.006	0.994	0.204
	3Me-SA	-0.351	1.648	1.999	0.351	-1.648	-0.649	0.649	1.000	1.001	0.210
	4Me-SA	-0.322	1.686	2.008	0.322	-1.686	-0.682	0.682	1.004	0.996	0.232
Et	2Et-SA	-0.388	1.619	2.007	0.388	-1.619	-0.616	0.616	1.004	0.997	0.189
	3Et-SA	-0.369	1.625	1.994	0.369	-1.625	-0.628	0.628	0.997	1.003	0.198
	4Et-SA	-0.344	1.653	1.997	0.344	-1.653	-0.655	0.655	0.999	1.002	0.215
Pr	2Pr-SA	-0.387	1.645	2.032	0.387	-1.645	-0.629	0.629	1.016	0.984	0.195
	3Pr-SA	-0.375	1.623	1.998	0.375	-1.623	-0.624	0.624	0.999	1.001	0.195
	4Pr-SA	-0.366	1.623	1.989	0.366	-1.623	-0.629	0.629	0.995	1.005	0.199
iPr	2iPr-SA	-0.425	1.600	2.025	0.425	-1.600	-0.588	0.588	1.013	0.988	0.170
	3iPr-SA	-0.358	1.664	2.022	0.358	-1.664	-0.643	0.643	1.011	0.989	0.204
	4iPr-SA	-0.355	1.656	2.011	0.355	-1.656	-0.651	0.651	1.006	0.995	0.210

Table III.8: The Principal chemical descriptors of optimized SA ligands.

Table III.4 analysis

We note in this table that:

> ➢ The position of the substituent has an influence on the stability and reactivity of the studied ligands **[10]**.
>
> ✓ The stabilization of the system decreases when moving the (R/X) subs from ortho to para position, except for F-SA its stability increases when moving sub from ortho to para.
>
> ➢ The position of the substituent influences on the electronegativity of the ligands.
>
> ✓ When X subs be in ortho position the χ increases, except for F sub,   and decreases in meta and para. But for R Ligands the reverse thing happens.
>
> ✓ Me-SA ligand in the para position shows a high value of the chemical potential (μ) as well as its electrophilicity index ω compared with the other positions of all the other subs; that implies its ability of electronic transferring (most electrophilic).
>
> ✓ I-SA ligand in meta position shows a low value of the chemical potential(μ) as well as its electrophilicity index ω compared to other positions of all the other subs; that implies its nucleophilicity (most nucleophilic).

3.2.3. Study of electronic structure

a) Population analysis

Population analysis is used mainly for deriving the atomic charge, which is almost the simplest model that describes charge distribution. Experimentally Atomic charges can't be observable, so it does not have a rigorous physical basis. However, the concept of atomic charge is so useful because it helps to understand the basic properties of molecules. As well it has significant applications in various fields such as in QM, MM, and chemical informatics **[13]**.

The types of electronic analyses which we used by the ADF program are the atomic charges of Hirshfeld, and the analysis of population of Mulliken.

b) Mulliken population analysis

It's one of the original and still most widely used population analysis schemes. The fundamental assumption used by the Mulliken scheme for partitioning the wave function is that the overlap between two orbitals is shared equally.

This does not completely affect the electronegativity of the individual elements. However, it does give one a means for partitioning a wave function and has been found to be very effective for small basis sets. For large basis sets, results can be very unreasonable. This is due to diffuse functions describing adjacent atoms more than they describe the atom on which they are centered. In some cases, Mulliken analysis can assign an electron population to an orbital that is negative or more than two electrons. It also tends to underestimate the charge separation in ionic bonded systems.

Although of its disadvantages, this Mulliken population scheme is so popular because it's very easy to implement, so it is available in many software packages. And maybe the main reason for its popularity is the fact that the method is easy to understand, and this is a great advantage because population analysis is often used for understanding chemistry instead of quantitatively predicting experimental results **[14]**.

c) Hirshfeld population

In the Hirshfeld model the partial charge of each atom is calculated by assuming that the electron density at each point is shared between the surrounding atoms in direct proportion to their free-atom electron densities at the corresponding distances from the nuclei.

The original partial atomic charges obtained from the Hirshfeld population analysis can be improved through parameterization to reproduce accurately a particular molecular property **[15]**.

3.2.3.1. Mulliken and Hirschfeld population charges analysis

For better understanding of the electronic structure of each system, we carried out a Mulliken and Hirshfeld charges analysis. We report in Tables (III.5 and III.6) the results of the calculations obtained for the different systems studied.

Table III.5: represents the main results of the Mulliken charge calculation for substituted SA.

Mulliken charge	H	F			Cl			Br			I		
		Ortho	Meta	Para	Ortho	Meta	Para	Ortho	Meta	Para	Ortho	Meta	Para
O_{25}	-0.642	-0.635	-0.638	-0.641	-0.633	-0.635	-0.639	-0.632	-0.634	-0.638	-0.629	-0.635	-0.636
N_8	-0.273	-0.267	-0.273	-0.274	-0.268	-0.272	-0.274	-0.267	-0.270	-0.273	-0.292	-0.272	-0.273
C_9	0.172	0.120	0.173	0.160	0.197	0.173	0.175	0.212	0.172	0.178	0.334	0.189	0.195
C_{10}	0.137	0.141	0.127	0.139	0.139	0.134	0.135	0.144	0.136	0.138	0.146	0.145	0.150
C_{11}	0.184	0.169	0.188	0.130	0.183	0.186	0.196	0.184	0.188	0.212	0.201	0.195	0.327
C_{12}	0.151	0.155	0.100	0.395	0.152	0.166	-0.017	0.153	0.186	-0.024	0.166	0.288	-0.567
C_{13}	0.180	0.136	0.411	0.125	0.196	0.001	0.191	0.217	-0.012	0.208	0.335	-0.539	0.319
C_{14}	0.192	0.429	0.136	0.198	0.004	0.205	0.197	-0.015	0.230	0.198	-0.572	0.344	0.206

Mulliken charge	H	Me			Et			Pr			iPr		
		Ortho	Meta	Para	Ortho	Meta	Para	Ortho	Meta	Para	Ortho	Meta	Para
O_{25}	-0.642	-0.649	-0.644	-0.644	-0.649	-0.642	-0.644	-0.649	-0.642	-0.643	-0.658	-0.643	-0.644
N_8	-0.273	-0.279	-0.274	-0.273	-0.286	-0.274	-0.276	-0.287	-0.274	-0.275	-0.297	-0.274	-0.276
C_9	0.172	0.198	0.164	0.172	0.201	0.164	0.169	0.203	0.164	0.169	0.216	0.166	0.170
C_{10}	0.137	0.139	0.132	0.135	0.141	0.131	0.128	0.140	0.129	0.126	0.150	0.132	0.136
C_{11}	0.184	0.179	0.181	0.210	0.176	0.176	0.198	0.174	0.176	0.209	0.175	0.173	0.220
C_{12}	0.151	0.148	0.182	0.112	0.147	0.184	0.124	0.150	0.186	0.107	0.143	0.182	0.132
C_{13}	0.180	0.207	0.127	0.192	0.214	0.133	0.205	0.214	0.119	0.208	0.219	0.145	0.203
C_{14}	0.192	0.123	0.209	0.181	0.122	0.221	0.186	0.113	0.224	0.186	0.124	0.231	0.180

Table III.9: The main calculation results of the Mulliken charge for substituted SA.

Table III.6 represents the main results of the Hirshfeld charge calculation for substituted SA.

Hirshfeld charge	H	F			Cl			Br			I		
		Ortho	Meta	Para	Ortho	Meta	Para	Ortho	Meta	Para	Ortho	Meta	Para
O_{25}	-0.361	-0.353	-0.357	-0.359	-0.352	-0.353	-0.357	-0.350	-0.352	-0.356	-0.347	-0.353	-0.354
N_8	-0.174	-0.175	-0.173	-0.176	-0.171	-0.174	-0.175	-0.171	-0.175	-0.175	-0.175	-0.172	-0.175
C_7	0.015	0.017	0.017	0.014	0.019	0.016	0.015	0.019	0.016	0.015	0.020	0.016	0.014
C_9	0.040	0.028	(0.045)	0.036	0.033	(0.043)	0.039	0.034	(0.044)	0.040	0.033	(0.047)	0.043
X_{24}	-	-0.117	-0.140	-0.147	-0.076	-0.105	-0.112	-0.080	-0.111	-0.116	-0.052	-0.082	-0.085
	H	Me			Et			Pr			iPr		
		Ortho	Meta	Para	Ortho	Meta	Para	Ortho	Meta	Para	Ortho	Meta	Para
O_{25}	-0.361	-0.359	-0.361	-0.362	-0.360	-0.361	-0.363	-0.361	-0.361	-0.361	-0.347	-0.361	-0.362
N_8	-0.174	-0.155	-0.173	-0.174	-0.155	-0.174	-0.176	-0.157	-0.174	-0.175	-0.141	-0.173	-0.175
C_7	0.015	0.017	0.014	0.014	0.017	0.014	0.014	0.016	0.014	0.014	0.019	0.014	0.014
C_9	0.040	0.041	0.038	0.036	0.042	0.038	0.036	0.038	0.038	0.037	0.046	0.037	0.037

Table III.10: The main calculation results of the Hirshfeld charge for substituted SA.

A. Mulliken analysis (Table III.5)

We focused on writing down charges atoms (Oxygen and Nitrogen) because of their importance during complexation, and charges of (Ring 2) carbons because they get affected by substituent during complexation as well.

We note in this table that:

- ✓ For the all ligands that contain (X subs), the electronic density charge of their two atoms (O_{25} and N_8) increases from Ortho to Para position while passing through the Meta position , while all they are less than HSA reference because of their electro-attracting effects. On the other hand, the presence of (R subs) in ligands makes difference due to their effects of electron-donating.

- ➢ So we can result that: the position of a sub influences on the density charge of the two atoms (O and N).

- ✓ The electron-withdrawing effects of these X decreases with the increasing of the distance between the sub and the O or N atom, so that last atoms are retaining a high density charge when the sub be in Para position, while for those ligands of (R subs) which results an electon-donating effects, the electronic density charge of their (O and N atoms) increases whenever the subs are closer in position to that atoms (The density charge be higher in Ortho position).

- ✓ For halogens substituents, the positive charge of the carbon atoms (C12-C13-C14) of the phenyl (ring 2) increases corresponding to the position (para-meta-ortho) respectively , and that reflects the negative charge transfer between substituents and these atoms and arounded field**,** while for R substituents, the influence on that carbons is remarkable mostly in meta position according to the difference of electro-donating effect of each substituent.

B. Hirshfeld analysis(Table III.6)

- ✓ For all ligands that contain (X and R subs), the Hirshfeld charges of their two atoms (O_{25} and N_8) increases from Ortho to Para position while passing through the Meta position proportionally with density charge increment of X_{24} for the case of (X ligands).

- ➢ So that means the position of the substituent effects on the Hirshfeld charges of those atoms.

✓ As well for all ligands; Hirshfeld charges of C_7 increase whenever the sub be closer in position, and same with C_9 Charges of (R subs) ligands, but for (X subs) ligands their C_9 charges are in high value in Meta position only, comparing to the other positions.

3.2.3.2. Study of orbital diagrams

For best knowledge about the influence of the substituent nature and its positions on the studied compounds we offer a study of orbital diagrams to know the existent differences between the different geometries on stability situation and the frontier orbitals.

First of all we start with optimized HSA basic frontier orbitals diagram which is presented in the figure bellow:
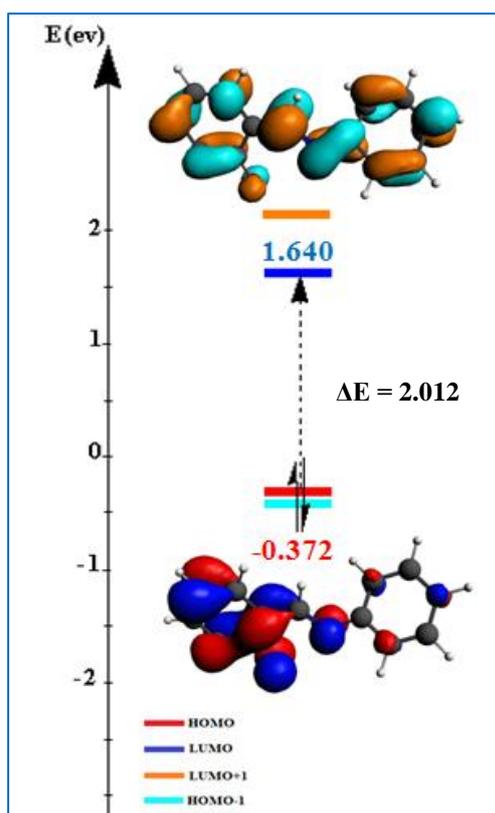
Figure III.7: Frontiers orbitals diagram of HSA.

In **figs III. (8, 9, 10, 11, 12, 13, 14, 15)**, the values of the HOMO-LUMO energy gap of the various studied ligands are given, expressed in electron volts.

- ✓ First, it is observed that the smallest values of the energy gap are marked for the ligands (Cl-SA, Br-SA, and I-SA, Pr-SA, iPr-SA), which are equal to 1.935 ev, 1.800 ev, 1.252 ev, 1.989ev, 2.011 ev) respectively in the Para position. In the other hand, the smallest energy gap value of the (F-SA) system is 1.970 ev in the Ortho position.

- ✓ For (Me-SA, Et-SA) ligands, their smallest values of energy are marked (1.999ev, 1.994ev) respectively in Meta position.

- ➤ This implies that the position of the studied substituents has an effect on the energy gap which is related to the stability of the systems.
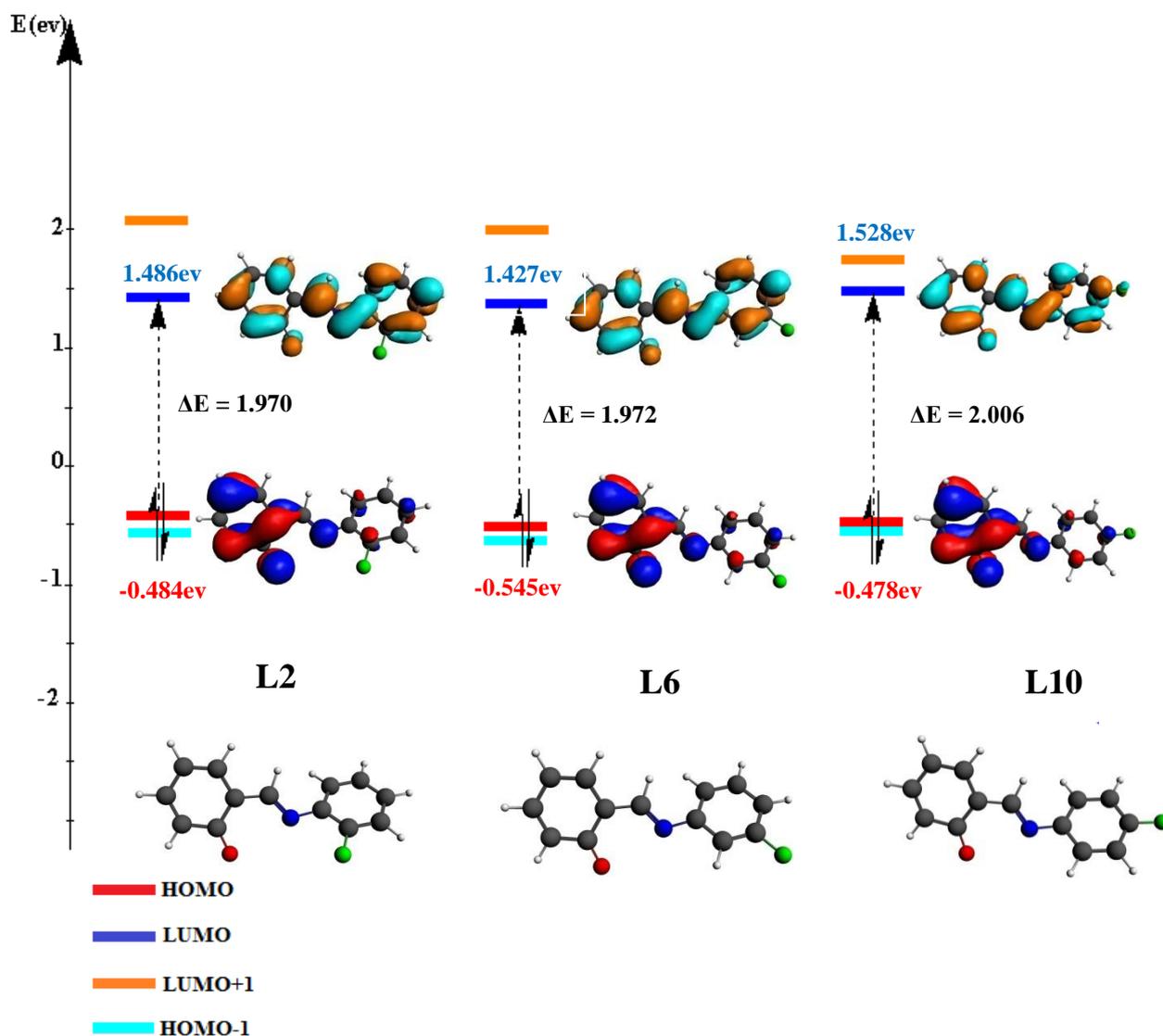
Figure III.8: Frontier orbitals (FO) energetic diagram of (F-SA).

(L2 -L6- L10).

We can observe in this diagram that the energy gap HOMO-LUMO (around 2.006ev) of L10 is the biggest one among the other compounds L2 and L6, that means L10 is the most stable compound among them .
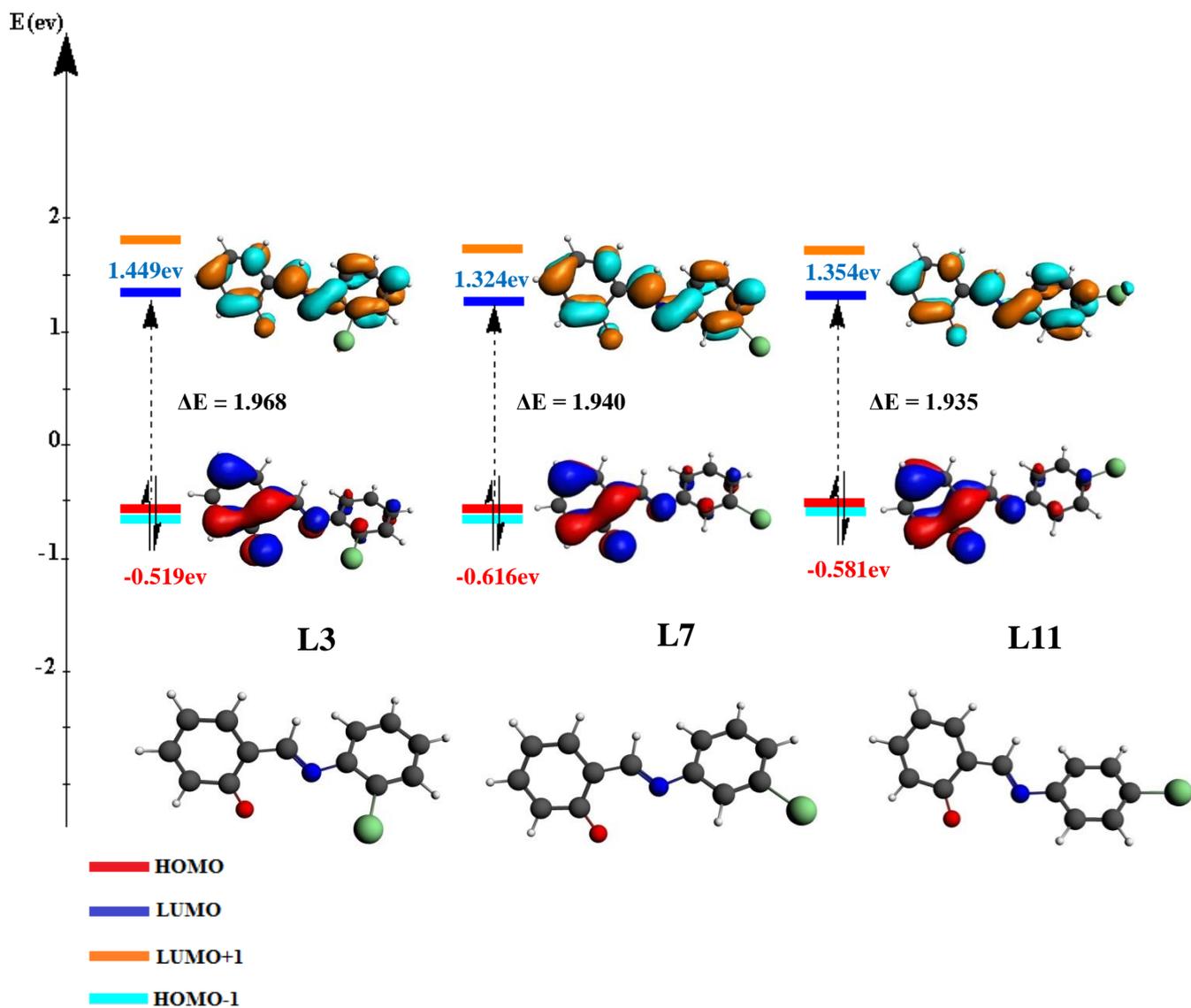
Figure III.9: Frontier orbitals (FO) energetic diagram of (Cl-SA)

(L3 -L7-L11).

We can observe in this diagram that the energy gap HOMO-LUMO (around 1.968 ev) of L3 is the biggest one among the other compounds L7 and L11, that means L3 is the most stable compound among them .
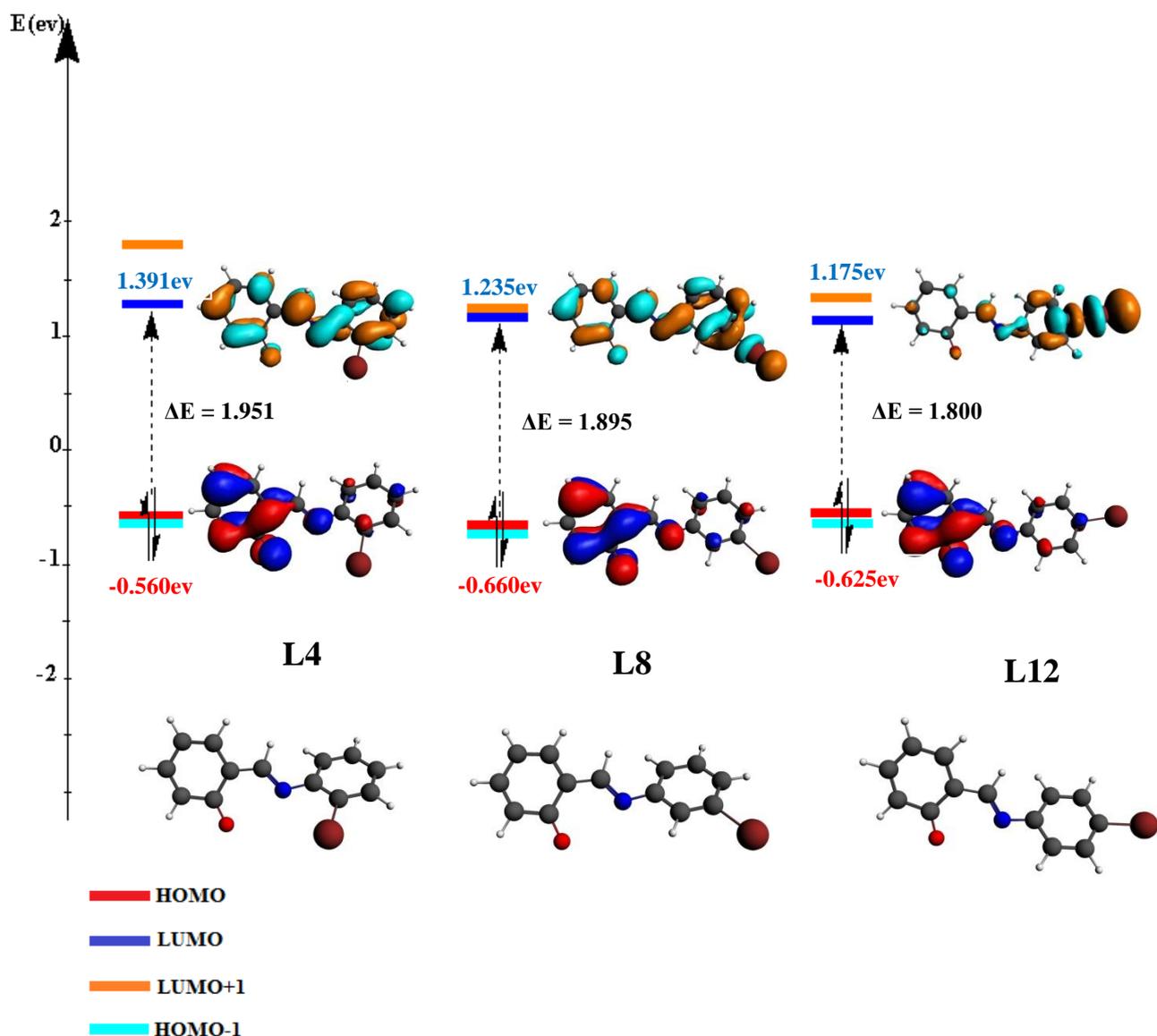
Figure III.10: Frontier orbitals (FO) energetic diagram of (Br-SA)

(L4 -L8-L12).

We can observe in this diagram that the energy gap HOMO-LUMO (around 1.951 ev) of L4 is the biggest one among the other compounds L8 and L12 , that means L4 is the most stable compound among them .
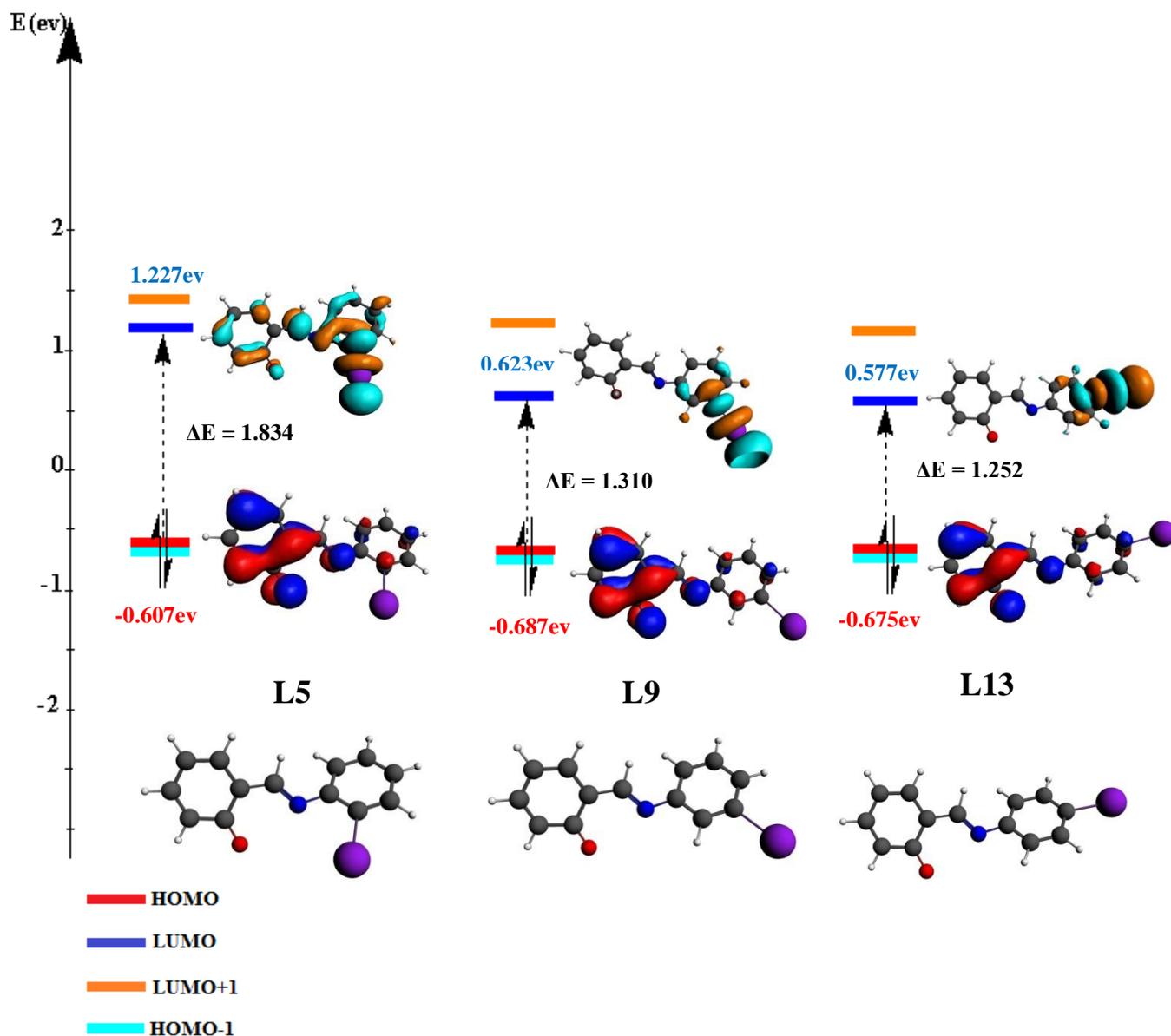
Figure III.11: Frontier orbitals (FO) energetic diagram of (I-SA)

(L5 -L9-L13).

    We can observe in this diagram that the energy gap HOMO-LUMO (around 1.834 ev) of L5 is the biggest one among the other compounds L9 and L13, that means L5 is the most stable compound among them.
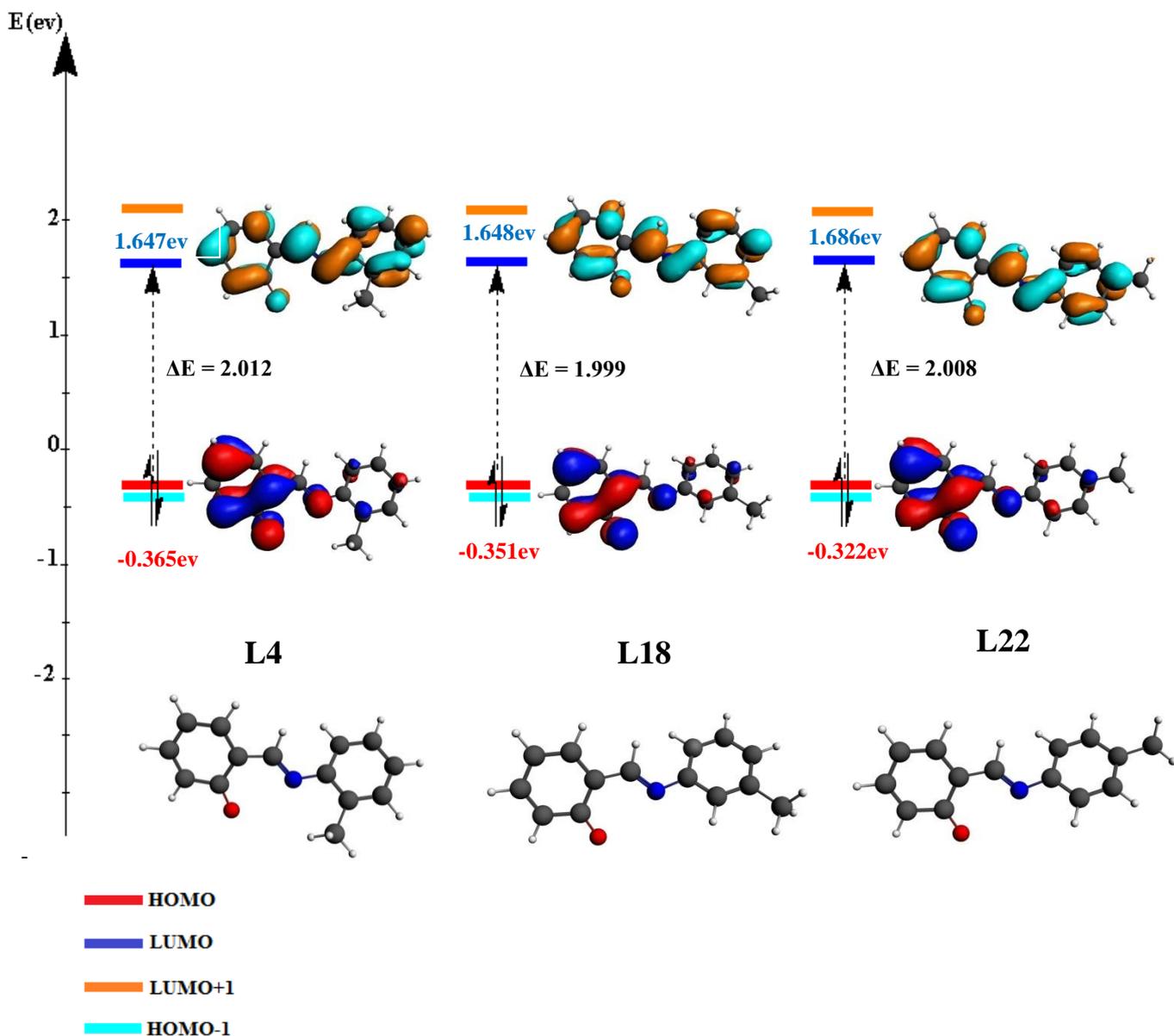
Figure III.12: Frontier orbitals (FO) energetic diagram of (Me-SA)

(L14-L18-L22).

We can observe in this diagram that the energy gap HOMO-LUMO (around 2.012 ev) of L4 is the biggest one among the other compounds L18 and L22, that means L4 is the most stable compound among them.
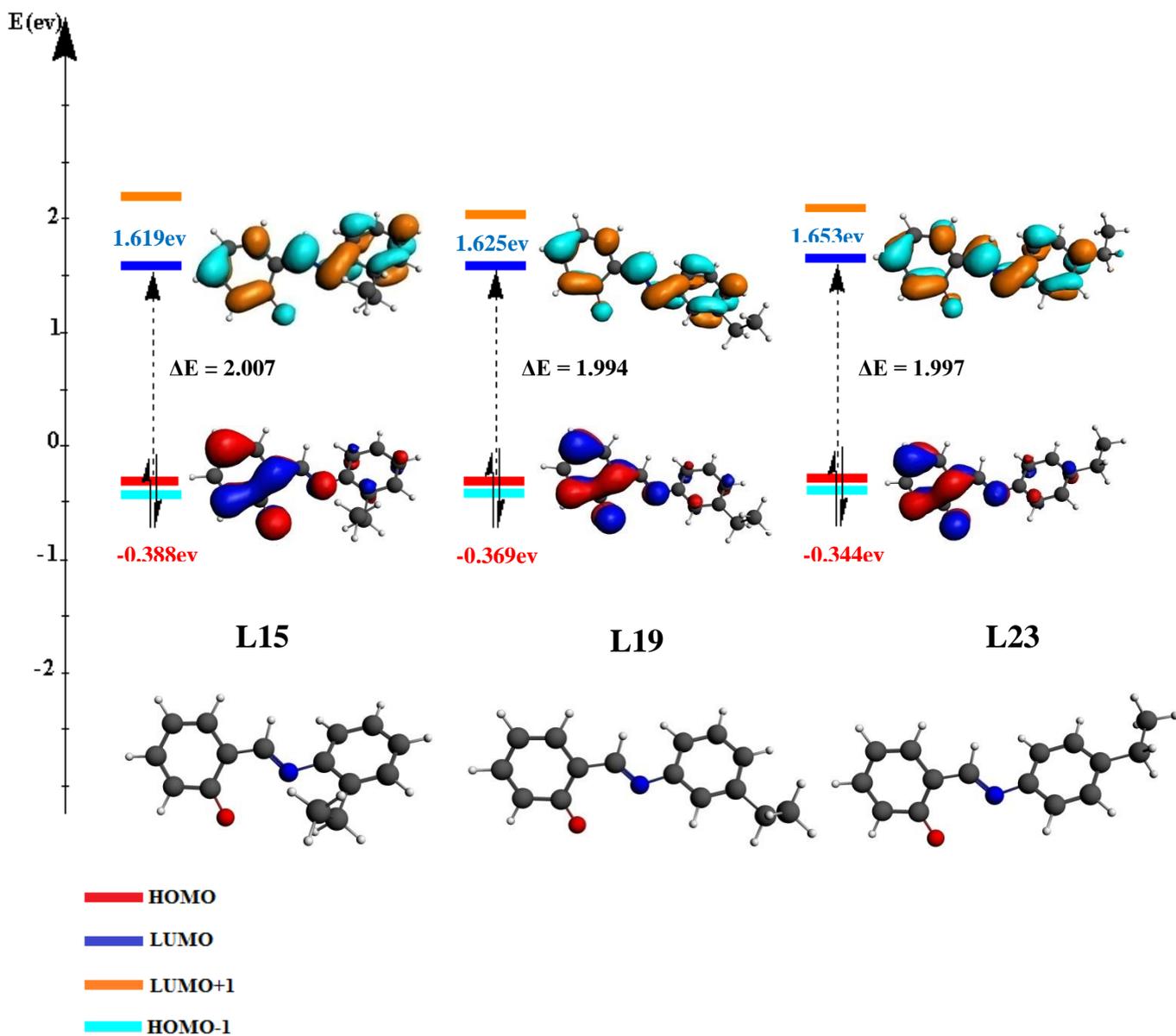
Figure III.13: Frontier orbitals (FO) energetic diagram of (Et-SA)

(L15-L19-L23).

We can observe in this diagram that the energy gap HOMO-LUMO (around 2.007 ev) of L15 is the biggest one among the other compounds L19 and L23, that means L15 is the most stable compound among them .
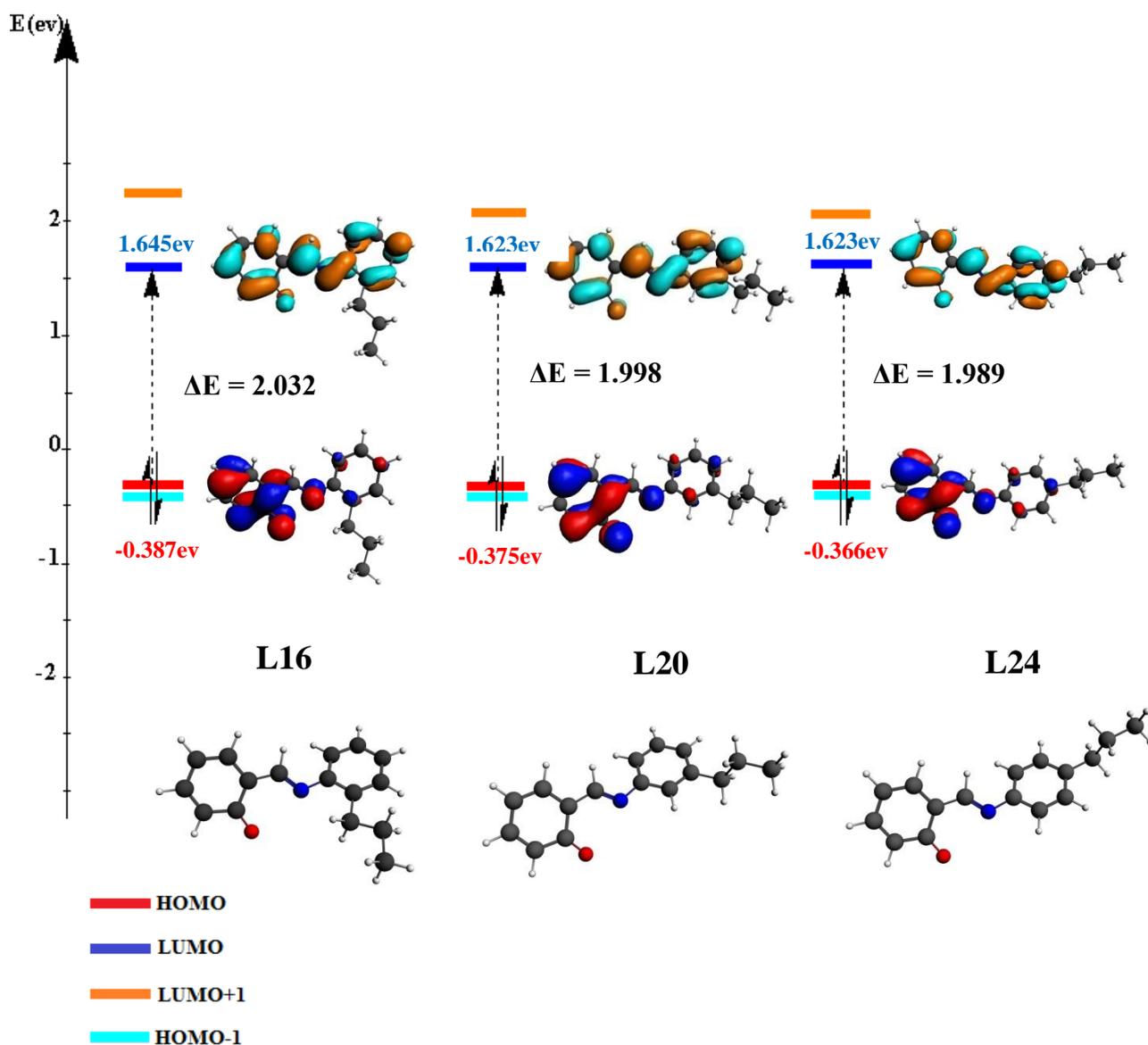
Figure III.14: Frontier orbitals (FO) energetic diagram of (Pr-SA)

(L16-L20-L24).

We can observe in this diagram that the energy gap HOMO-LUMO (around 2.032 ev) of L16 is the biggest one among the other compounds L20 and L24, that means L16 is the most stable compound among them.
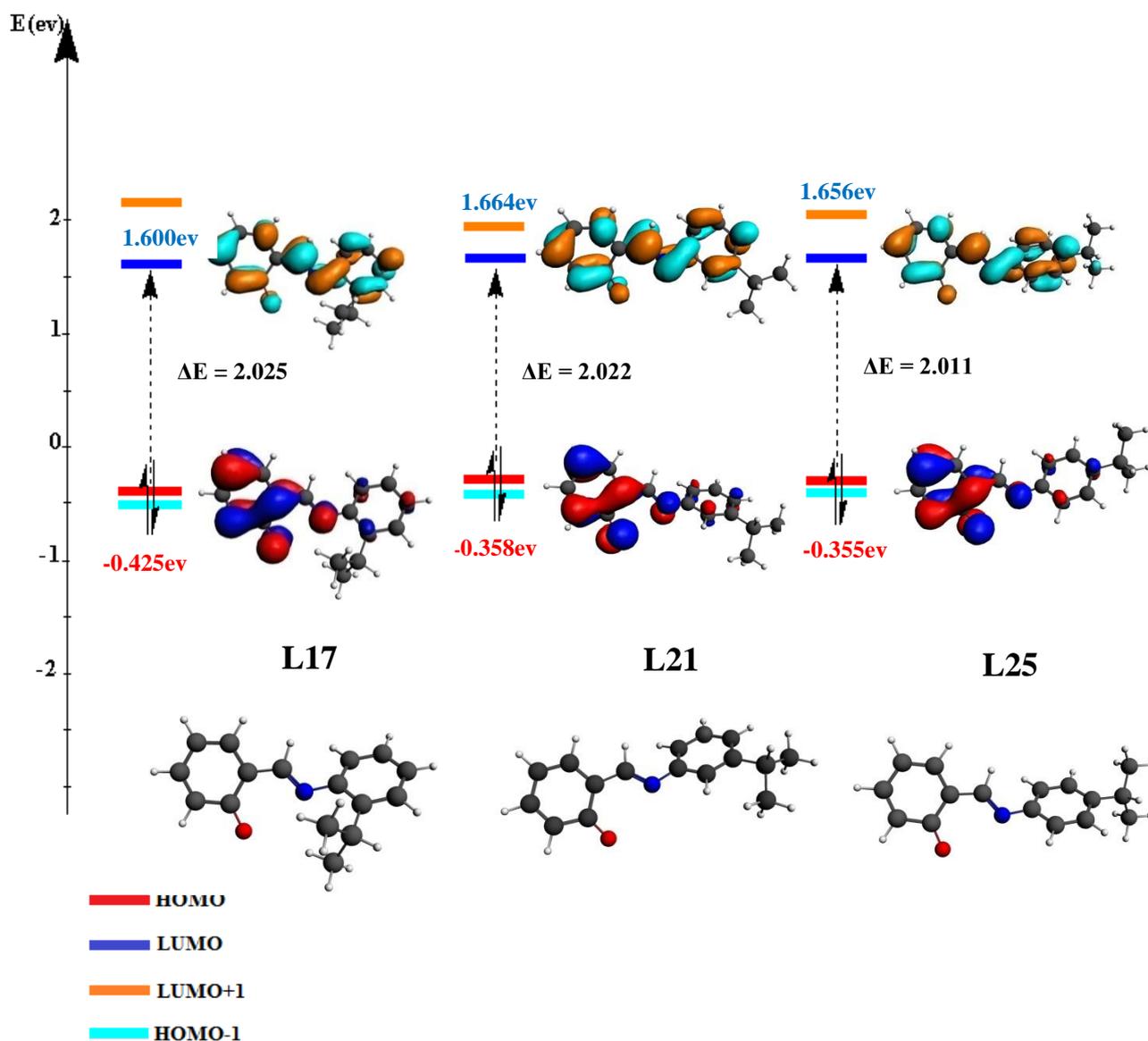
Figure III.15: Frontier orbitals (FO) energetic diagram of (iPr-SA)

(L17-L21-L25)

We can observe in this diagram that the energy gap HOMO-LUMO (around 2.025 ev) of L17 is the biggest one among the other compounds L21 and L25, that means L17 is the most stable compound among them.

3.2.3.3. Analysis of atomic orbitals contribution in molecular orbitals

In **Tables. (7, 8, 9),** we present the contributions values of the atomic orbitals of SA ligands in the frontier orbitals HOMO and LUMO:

Percentage (%) — Ortho position

H

	HOMO									LUMO												
	C_1	C_2	C_4	C_6	C_9	C_{11}	C_{13}	N_8	O_{25}	C_1	C_2	C_3	C_5	C_7	C_8	C_9	C_{10}	C_{11}	C_{12}	C_{13}	N_8	O_{25}
H	1.36	14.12	18.01	16.53	1.73	1.61	1.42	9.28	25.56	3.37	6.41	8.61	8.91	18.65	9.45	5.03	1.18	11.61	3.15	2.23	7.99	4.94

Ortho position — F

	HOMO									LUMO												
	C_1	C_2	C_4	C_6	C_9	C_{11}	C_{13}	N_8	O_{25}	C_1	C_2	C_3	C_4	C_5	C_7	C_8	C_9	C_{11}	C_{12}	C_{13}	N_8	O_{25}
F	1.29	13.81	18.16	16.13	1.74	1.51	1.35	9.14	27.39	3.38	6.16	8.18	1.04	8.51	18.30	9.51	6.52	12.38	5.05	1.24	6.72	5.20

Ortho position — Cl

	HOMO									LUMO													
	C_1	C_2	C_4	C_6	C_9	C_{11}	C_{13}	N_8	O_{25}	C_1	C_2	C_3	C_4	C_5	C_7	C_8	C_9	C_{10}	C_{11}	C_{12}	C_{13}	N_8	O_{25}
Cl	1.26	13.75	16.89	15.69	1.63	1.42	1.41	7.95	28.00	3.44	6.30	8.34	1.09	8.66	19.78	10.11	4.28	1.40	11.94	1.65	3.20	6.71	5.37

Ortho position — Br

	HOMO									LUMO													
	C_1	C_2	C_4	C_6	C_9	C_{11}	C_{13}	N_8	O_{25}	C_1	C_2	C_3	C_4	C_5	C_7	C_8	C_9	C_{10}	C_{11}	C_{12}	C_{13}	N_8	O_{25}
Br	1.23	13.3	17.24	15.45	1.74	1.61	1.49	8.7	30.39	3.39	6.09	8.07	1.11	8.41	19.61	9.73	4.36	1.32	11.59	1.77	3.16	6.65	5.32

Ortho position — I

	HOMO									LUMO										
	C_1	C_2	C_4	C_6	C_9	C_{11}	C_{13}	N_8	O_{25}	C_1	C_2	C_3	C_5	C_7	C_8	C_{11}	C_{13}	I_{24}	N_8	O_{25}
I	1.24	13.96	18.23	15.75	1.49	2.41	1.00	8.39	27.83	1.69	2.86	3.88	4.03	11.28	4.80	5.46	21.39	28.05	2.59	2.87

Ortho position — Me

	HOMO									LUMO												
	C_1	C_2	C_4	C_6	C_9	C_{11}	C_{13}	N_8	O_{25}	C_1	C_2	C_3	C_5	C_7	C_8	C_9	C_{11}	C_{12}	C_{13}	N_8	O_{25}
Me	1.43	14.59	19.55	16.82	1.61	2.4	1.42	8.83	24.56	3.39	6.32	8.63	8.83	19.12	8.47	6.86	11.04	3.94	1.57	8.03	4.87

Ortho position — Et

	HOMO									LUMO												
	C_1	C_2	C_4	C_6	C_9	C_{11}	C_{13}	N_8	O_{25}	C_1	C_2	C_3	C_5	C_7	C_8	C_9	C_{11}	C_{12}	C_{13}	N_8	O_{25}
Et	1.43	13.54	18.24	16.54	1.61	2.34	1.45	8.64	25.72	3.38	6.26	8.59	8.78	20.03	7.55	5.50	10.99	3.58	1.90	7.96	4.87

Ortho position — Pr

	HOMO									LUMO												
	C_1	C_2	C_4	C_6	C_9	C_{11}	C_{13}	N_8	O_{25}	C_1	C_2	C_3	C_5	C_7	C_8	C_9	C_{11}	C_{12}	C_{13}	N_8	O_{25}
Pr	1.41	13.15	19.02	16.43	1.82	1.59	1.62	9.26	26.52	3.38	6.44	8.78	9.00	18.73	8.36	5.46	10.73	2.09	2.31	8.58	4.79

Ortho position — iPr

	HOMO									LUMO												
	C_1	C_2	C_4	C_6	C_9	C_{11}	C_{13}	N_8	O_{25}	C_1	C_2	C_3	C_5	C_7	C_8	C_9	C_{11}	C_{12}	C_{13}	N_8	O_{25}
iPr	1.55	14.9	19.9	17.08	1.46	2.24	1.21	8.79	25.93	3.44	6.29	8.78	8.87	21.32	8.31	4.60	10.63	2.82	1.90	8.79	4.88

Table III.11: The percentages of the contribution of AO in MO when the substituents are in the Ortho position.

Percentage (%) — Meta position

H

HOMO

C_1	C_2	C_4	C_6	C_9	C_{11}	C_{13}	N_8	O_{25}
1.36	14.12	18.01	16.53	1.73	1.61	1.42	9.28	25.56

LUMO

C_1	C_2	C_3	C_5	C_7	C_8	C_9	C_{10}	C_{11}	C_{12}	C_{13}	N_8	O_{25}
3.37	6.41	8.61	8.91	18.65	9.45	5.03	1.18	11.61	3.15	2.23	7.99	4.94

F

HOMO

C_1	C_2	C_4	C_6	C_9	C_{11}	C_{13}	N_8	O_{25}
1.34	14.27	17.87	16.41	1.60	1.49	1.36	8.23	26.93

LUMO

C_1	C_2	C_3	C_4	C_5	C_7	C_8	C_9	C_{10}	C_{11}	C_{13}	N_8	O_{25}
3.43	6.20	8.29	1.05	8.63	18.81	10.51	2.61	3.95	11.74	5.80	6.87	5.24

Cl

HOMO

C_1	C_2	C_4	C_6	C_9	C_{11}	C_{13}	N_8	O_{25}
1.33	14.44	19.13	16.58	1.58	2.62	1.23	8.69	26.29

LUMO

C_1	C_2	C_3	C_4	C_5	C_7	C_8	C_9	C_{10}	C_{11}	C_{12}	C_{13}	N_8	O_{25}
3.47	6.00	8.02	1.13	8.36	18.89	10.76	4.06	1.38	12.85	3.03	3.32	6.21	5.37

Br

HOMO

C_1	C_2	C_4	C_5	C_6	C_7	C_9	C_{11}	N_8	O_{25}
1.32	14.16	19.83	1.02	15.86	1.03	1.33	2.57	9.19	25.29

LUMO

C_1	C_2	C_3	C_4	C_5	C_7	C_8	C_9	C_{11}	C_{12}	C_{13}	Br_{24}	N_8	O_{25}
2.89	4.81	6.37	1.03	6.71	16.16	7.42	4.15	9.72	11.62	2.5	9.05	4.10	4.55

I

HOMO

C_1	C_2	C_4	C_5	C_6	C_9	C_{11}	C_{13}	N_8	O_{25}
1.24	13.45	18.57	1.03	15.63	1.95	2.04	1.59	9.12	27.80

LUMO

C_{11}	C_{12}	C_{13}	H_{20}	I_{24}
2.32	38.31	1.00	1.13	51.52

Me

HOMO

C_1	C_2	C_4	C_6	C_9	C_{11}	C_{13}	N_8	O_{25}
1.39	14.43	18.28	16.73	1.63	1.47	1.25	8.27	26.91

LUMO

C_1	C_2	C_3	C_5	C_7	C_8	C_9	C_{10}	C_{11}	C_{12}	C_{13}	H_{23}	N_8	O_{25}
3.28	6.31	8.44	8.72	18.36	9.77	4.58	1.31	12.16	2.96	1.91	1.12	7.33	4.92

Et

HOMO

C_1	C_2	C_4	C_6	C_9	C_{11}	C_{13}	N_8	O_{25}
1.38	14.36	18.21	16.74	1.63	2.48	1.29	8.40	26.11

LUMO

C_1	C_2	C_3	C_5	C_7	C_8	C_9	C_{11}	C_{12}	C_{13}	N_8	O_{25}
3.30	6.25	8.36	8.65	18.38	9.45	4.99	11.87	3.41	1.63	7.44	4.91

Pr

HOMO

C_1	C_2	C_4	C_6	C_9	C_{11}	C_{13}	N_8	O_{25}
1.38	14.08	18.03	16.54	1.70	1.60	1.36	9.29	27.30

LUMO

C_1	C_2	C_3	C_5	C_7	C_8	C_9	C_{10}	C_{11}	C_{12}	C_{13}	N_8	O_{25}
3.36	6.35	8.51	8.82	18.45	9.55	4.85	1.18	11.80	2.19	1.94	7.64	4.97

iPr

HOMO

C_1	C_2	C_4	C_6	C_9	C_{11}	C_{13}	N_8	O_{25}
1.37	13.54	16.87	15.89	1.58	1.55	1.55	9.13	28.33

LUMO

C_1	C_2	C_3	C_5	C_7	C_8	C_9	C_{10}	C_{11}	C_{12}	N_8	O_{25}
3.40	6.58	8.94	9.23	18.95	8.59	3.94	1.35	10.66	1.40	3.5	4.99

Table III.12: The percentages of the contribution of AO to MO when the substituents are in the Meta position.

Percentage (%)

H

	HOMO									LUMO											
	C_1	C_2	C_4	C_6	C_9	C_{11}	C_{13}	N_8	O_{25}	C_1	C_2	C_3	C_5	C_7	C_8	C_9	C_{10}	C_{11}	C_{12}	C_{13}	N_8
	1.36	14.12	18.01	16.53	1.73	1.61	1.42	9.28	25.56	3.37	6.41	8.61	8.91	18.65	9.45	5.03	1.18	11.61	3.15	2.23	7.99

(last HOMO/LUMO value O_{25} = 4.94)

Para position — F

C_1	C_2	C_4	C_6	C_9	C_{11}	C_{13}	N_8	O_{25}	C_1	C_2	C_3	C_5	C_7	C_8	C_9	C_{11}	C_{12}	C_{13}	N_8	O_{25}
1.38	14.50	19.20	16.21	1.64	1.24	1.27	8.46	26.33	3.43	6.45	8.69	8.99	19.23	8.73	8.08	10.08	3.82	1.21	8.02	5.05

(Columns C_1–O_{25} are HOMO; C_1–O_{25} are LUMO)

Cl

C_1	C_2	C_4	C_6	C_9	C_{11}	C_{13}	N_8	O_{25}	C_1	C_2	C_3	C_4	C_5	C_7	C_8	C_9	C_{10}	C_{11}	C_{12}	C_{13}	N_8	O_{25}
1.37	14.47	18.45	16.59	1.60	1.34	1.22	8.46	26.22	3.33	5.78	7.78	1.08	8.10	18.27	10.47	5.38	1.04	10.87	4.76	1.37	6.08

(final LUMO O_{25} = 5.19)

Br

C_1	C_2	C_4	C_6	C_9	C_{11}	C_{13}	N_8	O_{25}	C_2	C_3	C_5	C_7	C_8	C_9	C_{11}	H_{19}	H_{20}	H_{21}	Br_{24}	N_8	O_{25}
1.36	14.48	18.23	16.59	1.60	2.29	1.21	8.55	26.43	1.22	1.68	1.72	5.24	2.74	1.62	33.36	1.12	1.63	1.04	34.92	1.29	1.36

I

C_1	C_2	C_4	C_6	C_9	C_{11}	C_{13}	N_8	O_{25}	C_9	C_{10}	C_{11}	C_{12}	I_{24}
1.32	13.73	17.51	16.07	1.78	2.70	1.43	9.30	26.89	1.01	1.47	38.36	2.28	52.60

Me

C_1	C_2	C_4	C_6	C_9	C_{11}	C_{13}	N_8	O_{25}	C_1	C_2	C_3	C_5	C_7	C_8	C_9	C_{10}	C_{11}	C_{12}	C_{13}	H_{22}	H_{26}	N_8	O_{25}
1.40	14.35	18.24	16.71	1.51	1.39	1.35	8.29	26.91	3.32	6.48	8.69	8.95	18.56	9.11	3.39	1.66	9.36	1.34	4.40	1.29	1.79	7.79

(final LUMO O_{25} = 4.90)

Et

C_1	C_2	C_4	C_6	C_9	C_{11}	C_{13}	N_8	O_{25}	C_1	C_2	C_3	C_5	C_7	C_8	C_9	C_{11}	C_{12}	H_{26}	H_{27}	N_8	O_{25}
1.40	14.48	18.34	16.79	1.69	1.36	1.20	8.48	26.30	3.25	6.18	8.32	8.60	17.76	8.98	7.63	9.92	4.74	1.43	2.38	7.45	4.80

Pr

C_1	C_2	C_4	C_6	C_9	C_{11}	C_{13}	N_8	O_{25}	C_1	C_2	C_3	C_5	C_7	C_8	C_9	C_{11}	C_{12}	C_{13}	H_{27}	N_8	O_{25}
1.40	14.33	18.06	16.63	1.61	2.38	1.22	8.36	26.97	3.22	6.07	8.18	8.45	17.99	9.25	5.19	11.01	3.94	1.31	1.43	6.91	4.84

iPr

C_1	C_2	C_4	C_6	C_9	C_{11}	C_{13}	N_8	O_{25}	C_1	C_2	C_3	C_5	C_7	C_8	C_9	C_{10}	C_{11}	C_{12}	C_{13}	H_{27}	H_{29}	N_8	O_{25}
1.34	13.52	17.37	16.12	1.82	1.75	1.52	9.15	28.85	3.28	6.30	8.41	8.75	18.72	9.20	5.00	1.40	10.13	2.42	2.23	1.12	1.02	7.96

(final LUMO O_{25} = 4.79)

Table III.13: The percentages of the contribution of AO in MO when the substituents are in Para position.

Table III. (7, 8, 9) Analysis

The most contribution percentage of AO in MO is by Oxygen atom which is around (25.29**%** and 30.39**%**) in HOMO, As well for the carbons atoms (C_2, C_4, C_6) of the system Ring 1 that contains the oxygen atom, their contribution is (more or less than 49 %) in HOMO. On the other hand, the most contribution in LUMO is by C_7 (around 11.28% and 21.32%), and C_{11} around (9.36% and 38.36%).

3.3. The influence of substituent nature (X, R)

The purpose from the variation of these substituents is the study of their influence on the extractive properties of the previous ligands.

3.3.1. Study of geometric structure

We have summarized in **Table III.10** the main geometric parameters of the nine substituted Salicylideneanilines in three different positions.

From Table III.10 we can note that:

➢ The affection of the substituent nature on the molecule distances is almost negligible comparing to the HSA reference molecule.

➢ The affection of substituent nature on the molecule valence angles is also negligible except for the F sub; it makes a difference when it is in position Para by making the (C_6-C_7=N_8) the smallest angle (120, 8°), and (C_7=N_8-C_9) the biggest angle (127, 4°) comparing with the other substituents.

➢ Unlike the other angles, the dihedral angle (C_6-C_7=N_8-C_9) is affected depending on the substitutent nature.

		Distances(pm)				Valence angles (°)		Dihedral angle(°)
		Ring 1	Ring 2	C$_6$-C$_7$	C$_7$=N$_8$	N$_8$-C$_9$	C$_6$-C$_7$=N$_8$	C$_7$=N$_8$-C$_9$	C$_6$-C$_7$=N$_8$-C$_9$
HSA(Reference)		142.62	140.9	143.8	130.9	139.1	128.9	119.4	174.0
Ortho	2F-SA	142.96	140.80	143.4	131.2	138.4	129.1	118.7	171.0
	2Cl-SA	142.93	140.92	143.4	131.2	138.0	129.1	119.4	171.2
	2Br-SA	142.93	140.85	143.3	131.3	137.9	129.1	119.2	170.5
	2I-SA	142.98	140.86	143.3	131.3	138.0	129.5	119.2	170.2
	2Me-SA	141.62	139.70	143.1	129.3	138.1	128.8	119.4	174.4
	2Et-SA	142.92	141.07	143.9	130.8	139.4	128.6	120.1	174.8
	2Pr-SA	142.90	141.05	143.9	130.8	139.3	128.8	119.8	174.5
	2iPr-SA	142.85	141.12	143.8	130.6	139.6	128.1	120.5	174.2
Meta	3F-SA	142.92	140.12	143.5	131.1	138.6	128.8	119.4	172.7
	3Cl-SA	142.93	140.72	143.3	131.2	138.6	128.9	119.3	171.4
	3Br-SA	142.96	140.65	143.4	131.3	138.7	128.7	119.3	173.1
	3I-SA	142.95	140.73	143.3	131.3	138.3	128.8	119.4	174.1
	3Me-SA	143.18	141.35	143.9	130.7	139.1	128.8	120.6	173.1
	3Et-SA	142.93	140.98	143.8	130.9	139.2	128.8	119.5	173.7
	3Pr-SA	142.92	140.95	143.8	130.9	139.2	128.8	119.5	174.1
	3iPr-SA	142.95	141.05	143.9	130.8	139.1	128.5	120.0	171.8
Para	4F-SA	141.93	140.12	148.2	130.4	136.2	120.8	127.4	178.0
	4Cl-SA	142.92	140.65	143.5	131.3	138.8	128.8	119.2	175.1
	4Br-SA	142.93	140.68	143.4	131.2	138.7	128.8	119.4	173.9
	4I-SA	142.97	140.73	143.3	131.2	138.6	128.6	119.7	172.0
	4Me-SA	141.62	139.70	143.1	129.3	138.1	128.8	119.4	174.4
	4Et-SA	142.95	140.98	143.9	130.9	139.4	129.1	119.2	173.9
	4Pr-SA	142.90	140.97	143.8	130.9	139.2	128.9	119.1	174.3
	4iPr-SA	142.90	140.62	143.9	130.9	139.2	128.9	119.2	174.8

Table III.14: Geometric descriptors, distances (pm) & angles (°) of HSA & its ligand.

3.3.2. Study of chemical descriptors

		E_{HOMO} (ev)	E_{LUMO} (ev)	(ΔE)	I	A	X	μ	Ƞ	S	ω
	HSA (Refrence)	-0.372	1.640	2.012	0.372	-1.640	-0.634	0.634	1.006	0.994	0.199
Ortho	2F-SA	-0.484	1.486	1.970	0.484	-1.486	-0.501	0.501	0.985	1.015	0.127
	2Cl-SA	-0.519	1.449	1.968	0.519	-1.449	-0.465	0.465	0.984	1.016	0.110
	2Br-SA	-0.560	1.391	1.951	0.560	-1.391	-0.416	0.416	0.976	1.025	0.088
	2I-SA	-0.607	1.227	1.834	0.607	-1.227	-0.310	0.310	0.917	1.091	0.052
	2Me-SA	-0.365	1.647	2.012	0.365	-1.647	-0.641	0.641	1.006	0.994	0.204
	2Et-SA	-0.388	1.619	2.007	0.388	-1.619	-0.616	0.616	1.004	0.997	0.189
	2Pr-SA	-0.387	1.645	2.032	0.387	-1.645	-0.629	0.629	1.016	0.984	0.195
	2iPr-SA	-0.425	1.600	2.025	0.425	-1.600	-0.588	0.588	1.013	0.988	0.170
Meta	3F-SA	-0.545	1.427	1.972	0.545	-1.427	-0.441	0.441	0.986	1.014	0.099
	3Cl-SA	-0.616	1.324	1.940	0.616	-1.324	-0.354	0.354	0.970	0.103	0.065
	3Br-SA	-0.660	1.235	1.895	0.660	-1.235	-0.288	0.288	0.948	1.055	0.044
	3I-SA	-0.687	0.623	1.310	0.687	-0.623	0.032	-0.032	0.655	1.527	0.001
	3Me-SA	-0.351	1.648	1.999	0.351	-1.648	-0.649	0.649	1.000	1.001	0.210
	3Et-SA	-0.369	1.625	1.994	0.369	-1.625	-0.628	0.628	0.997	1.003	0.198
	3Pr-SA	-0.375	1.623	1.998	0.375	-1.623	-0.624	0.624	0.999	1.001	0.195
	3iPr-SA	-0.358	1.664	2.022	0.358	-1.664	-0.643	0.643	1.011	0.989	0.204
Para	4F-SA	-0.478	1.528	2.006	0.478	-1.528	-0.525	0.525	1.003	0.997	0.137
	4Cl-SA	-0.581	1.354	1.935	0.581	-1.354	-0.387	0.387	0.968	1.033	0.077
	4Br-SA	-0.581	1.354	1.935	0.581	-1.354	-0.387	0.387	0.968	1.033	0.077
	4I-SA	-0.675	0.577	1.252	0.675	-0.577	0.049	-0.049	0.626	1.597	0.002
	4Me-SA	-0.322	1.686	2.008	0.322	-1.686	-0.682	0.682	1.004	0.996	0.232
	4Et-SA	-0.344	1.653	1.997	0.344	-1.653	-0.655	0.655	0.999	1.002	0.215
	4Pr-SA	-0.366	1.623	1.989	0.366	-1.623	-0.629	0.629	0.995	1.006	0.199
	4iPr-SA	-0.355	1.656	2.011	0.355	-1.656	-0.651	0.651	1.006	0.995	0.210

Table III.15: The principal chemical descriptors of optimized SA ligands.

From the observed results in **Table III.11** of the main chemical descriptors correspond to the studied ligands it is noted that:

✓ The HOMO and LUMO energies of (F, Cl, Br, I) ligands are inferior comparing with HSA, this implies that the substitution by halogens has a destabilizing effect on the ligand because they are an electron-withdrawing group that removes electrons thus decreases the HOMO and LUMO energies so that the energy gap decreases according to the following order : F>Cl>Br>I

Unlike the subs (Me, Et, Pr, iPr) which stabilize the ligands because they are an electron-donating group that adds more electrons to the system, as a consequence the HOMO and LUMO energies increase.

- ✓ The energy levels associated with the HOMO and LUMO orbitals are lower in the case where the substituent is Iodine (I), on the other hand, methyl (Me) corresponds to the highest values whatever the position is.

- ➢ iPr-SA ligand marks the greatest energy gap in all sub positions, which gives it a significant stability compared with the other ligands, because it's the most encumbered sterically than the other substituents so its electro-donating effect is the least.

- ➢ The R subs which have a positive inductive effect lead to a greater energy gap.

3.3.3. Study of electronic structure

3.3.3.1. Mulliken analysis

We performed Mulliken analysis for substituted HSAs in the Ortho, Meta and Para positions. The results are reported in **Table III.12**

- ✓ The most important remark that can be made from the different results shown in Table III.12 is the distribution of the electronic cloud on the nitrogen and oxygen atoms, this prepares these atoms for nucleophilic attacks during the coordination of the ligand with metals.

- ✓ The greatest density charge of Oxygen atom is marked for Isopropyl (iPr) in the Ortho position which is (-0.658)

- ✓ As well for the nitrogen atom, the iPr sub in the Ortho position associated with this atom has the biggest negative value (-0.297).

- ➢ For X substituents, the density charge of atoms of O increases according to the increasing of their electronegativity as following order:

$$I < Br < Cl < F$$

So that whenever the substituent has more electro-withdrawing effect, the charge transferring with the environment will be more than the charge transfering with the O atom, so its density charge doesn't get affected much.

		Mulliken charges							
		O_{25}	N_8	C_9	C_{10}	C_{11}	C_{12}	C_{13}	C_{14}
	HSA	-0.642	-0.273	0.172	0.137	0.184	0.151	0.180	0.192
Ortho	2F-SA	-0.635	-0.267	0.120	0.141	0.169	0.155	0.136	0.429
	2Cl-SA	-0.633	-0.268	0.197	0.139	0.183	0.152	0.196	0.004
	2Br-SA	-0.632	-0.267	0.212	0.144	0.184	0.153	0.217	-0.015
	2I-SA	-0.629	-0.292	0.334	0.146	0.201	0.166	0.335	-0.572
	2Me-SA	-0.649	-0.279	0.198	0.139	0.179	0.148	0.207	0.123
	2Et-SA	-0.649	-0.286	0.201	0.141	0.176	0.147	0.214	0.122
	2Pr-SA	-0.649	-0.287	0.203	0.140	0.174	0.150	0.214	0.113
	2iPr-SA	-0.658	-0.297	0.216	0.150	0.175	0.143	0.219	0.124
Meta	3F-SA	-0.638	-0.273	0.173	0.127	0.188	0.100	0.411	0.136
	3Cl-SA	-0.635	-0.272	0.173	0.134	0.186	0.166	0.001	0.205
	3Br-SA	-0.634	-0.270	0.172	0.136	0.188	0.186	-0.012	0.230
	3I-SA	-0.635	-0.272	0.189	0.145	0.195	0.288	-0.539	0.344
	3Me-SA	-0.644	-0.274	0.164	0.132	0.181	0.182	0.127	0.209
	3Et-SA	-0.642	-0.274	0.164	0.131	0.176	0.184	0.133	0.221
	3Pr-SA	-0.642	-0.274	0.164	0.129	0.176	0.186	0.119	0.224
	3iPr-SA	-0.643	-0.274	0.166	0.132	0.173	0.182	0.145	0.231
Para	4F-SA	-0.641	-0.274	0.160	0.139	0.130	0.395	0.125	0.198
	4Cl-SA	-0.639	-0.274	0.175	0.135	0.195	-0.017	0.191	0.197
	4Br-SA	-0.638	-0.273	0.178	0.138	0.212	-0.024	0.208	0.198
	4I-SA	-0.636	-0.273	0.195	0.150	0.327	-0.567	0.319	0.206
	4Me-SA	-0.644	-0.273	0.172	0.135	0.210	0.112	0.192	0.181
	4Et-SA	-0.644	-0.276	0.169	0.128	0.198	0.124	0.205	0.186
	4Pr-SA	-0.643	-0.275	0.169	0.126	0.209	0.107	0.208	0.186
	4iPr-SA	-0.644	-0.276	0.170	0.136	0.220	0.132	0.203	0.180

Table III.16: The main calculation results of the Mulliken charge for substituted SA.

3.3.3.2. Study of Orbital diagrams

Figures III. (16, 17, 18) present the molecular orbital diagrams of the different studied ligands in the ortho, meta and para positions successively.

We note that:

➢ The X-SA ligands, keep the smallest values of the energy gap for X = I comparing with R-SA ligands in all studied positions. On the other hand, the iPr-SA ligand always presents the highest energy gap in all positions.

➢ When the HOMO-LUMO energy gap is large, the flow of electrons at the higher energy state is difficult, making the ligand iPr-SA the most hard ligand among the other ligands.

➢ On the other hand, the lower HOMO-LUMO energy gap leads to an easy flow of electrons, which makes the ligand I-SA the most soft ligand among the other ligands.
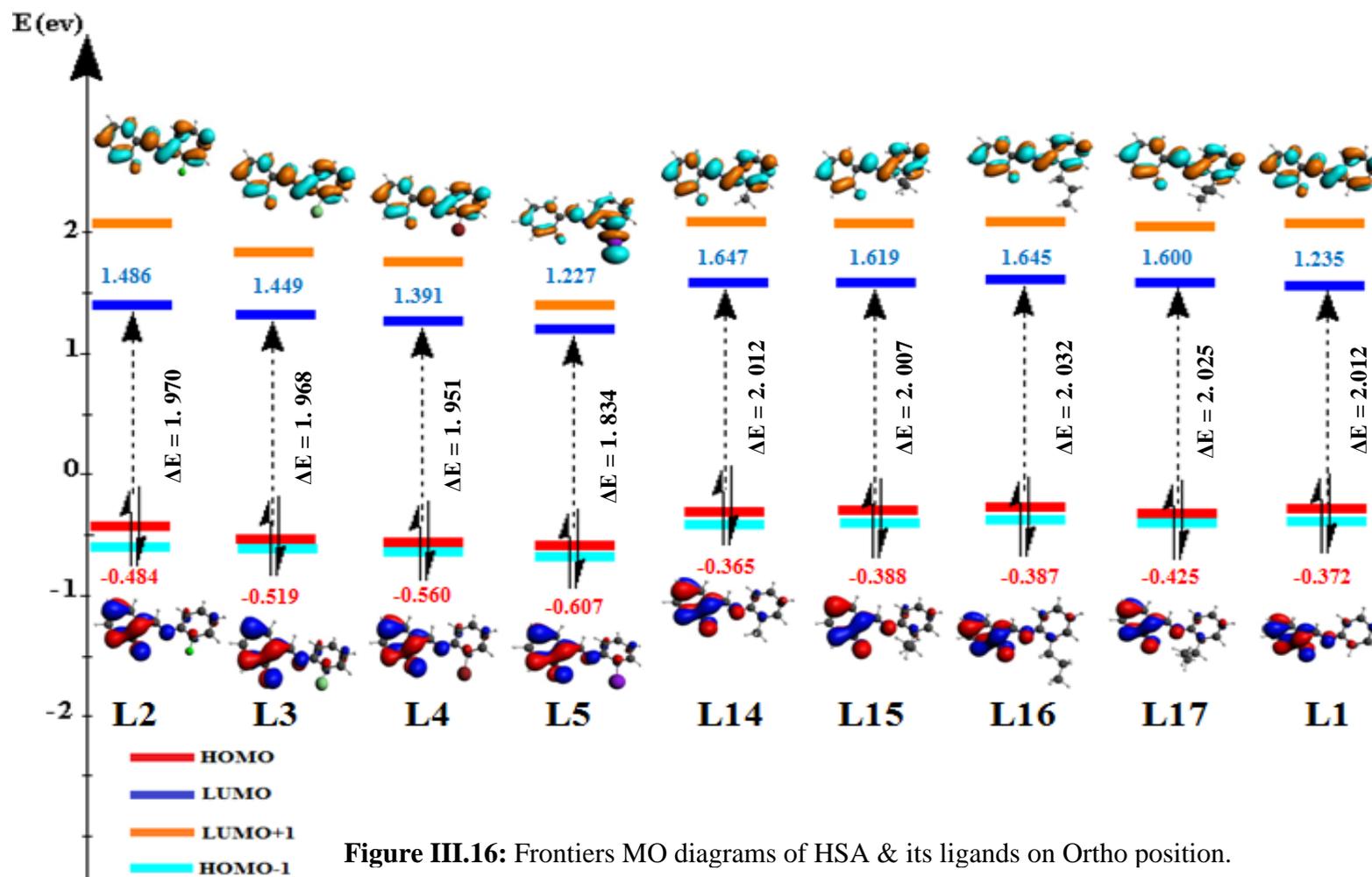

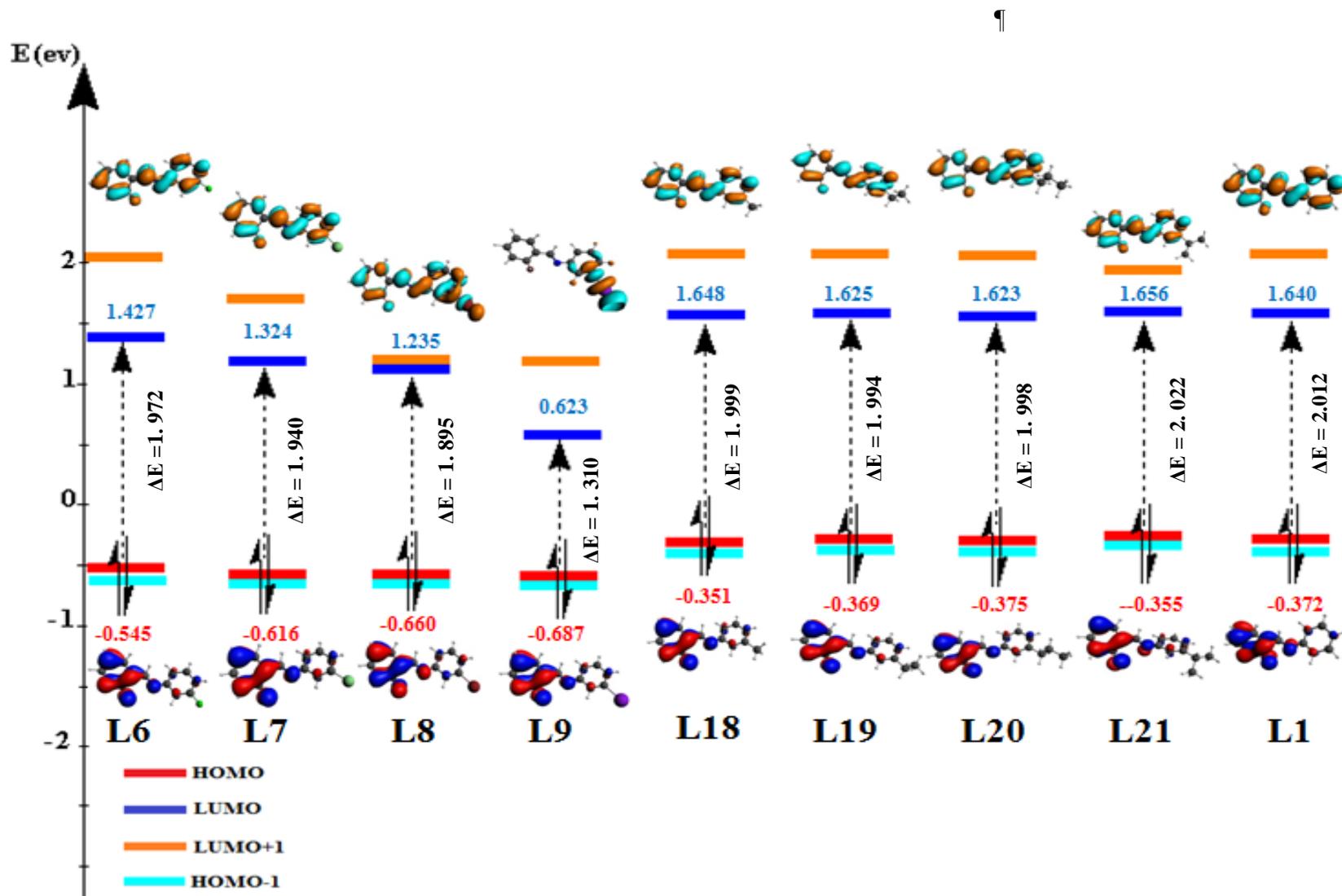**Figure III.16:** Frontiers MO diagrams of HSA & its ligands on Ortho position.

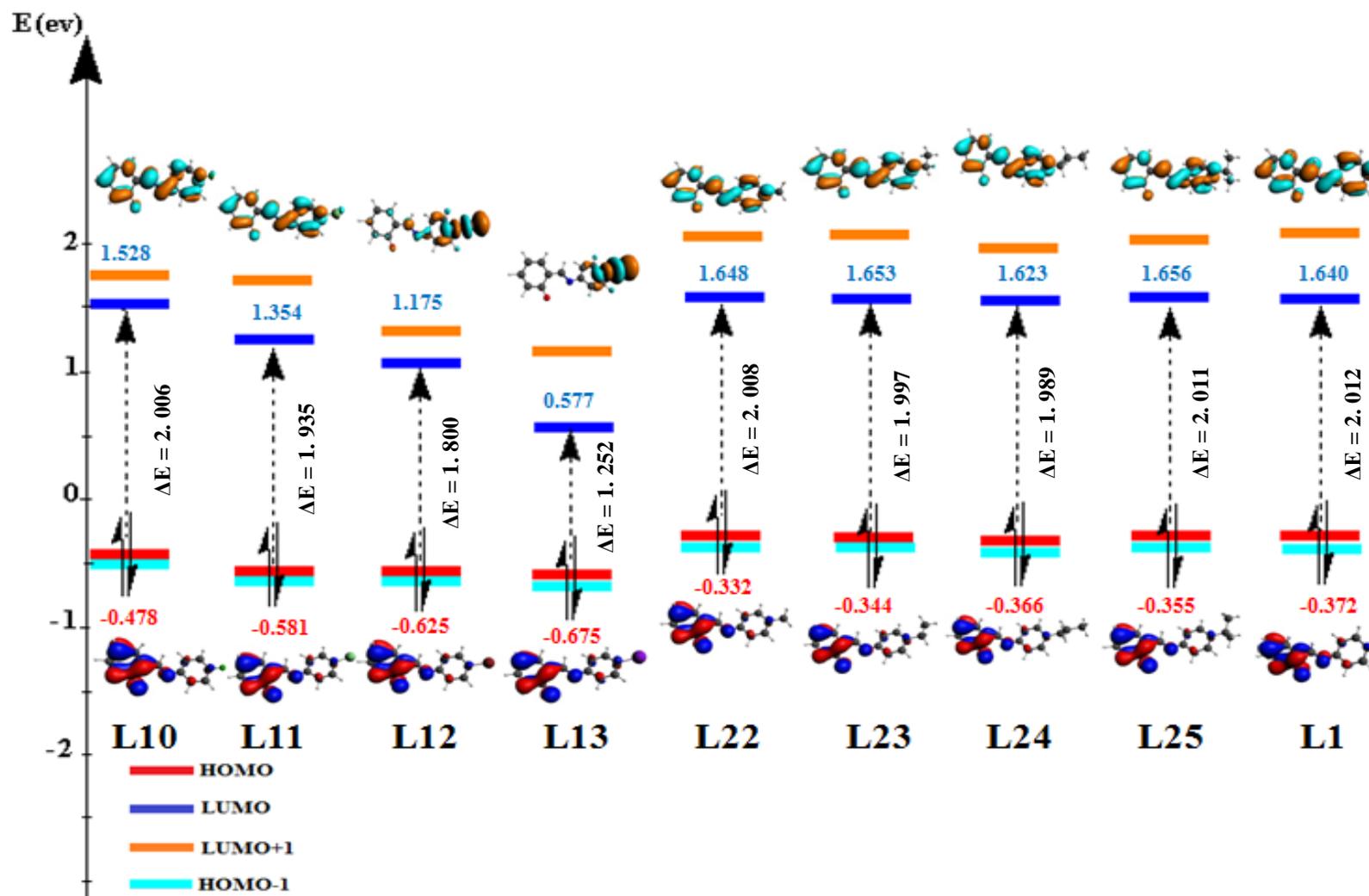**Figure III.17:** Frontiers MO diagrams of HSA & its ligands on Meta position.

Figure III.18: Frontiers MO diagrams of HSA & its ligands on Para position.

4.   Conclusion

The complete geometric optimization of the organic compound Salicylideneaniline of HSA formula and its ligands with X =H, F, Cl, Br, I and R= Me, Et, Pr, iPr by GGA-BLYP functional and TZP base with medium frozen core has carried out in this part .

The geometric parameters and the reactivity of the compounds are calculated by DFT / BLYP / TZP.

These parameters were calculated to study the reactivity of the ligands that are treated in this chapter.

The substitution of the deprotonated Salicylidenaniline ligands by halogen and alkyl substitutents influences on the geometric and electronic parameters of the studied systems and hence on their reactivity during their coordination with metals to form complexes will become an object of study.

The performed calculations that have been done allowed us to conclude the following:

- ✓ The insertion of substituents X or R on the phenyl rings of the ligands decreases the distances between the carbon atoms that form that rings, as well it does the same with the interatomic distances.

- ✓ For Halogen substituents: the valence angle (C6-C7=N8) decreases whenever the halogen elements are farther in position, unlike with the Alkyl group it increases whenever their position be near, except with Me it didn't change.

- ✓ While for valence angle (C7=N8-C9) didn't get affected much comparing with HSA, except with F it makes difference so that whenever the position is farther that angle increases.

- ✓ For halogen substituents, the dihedral angle increases according to the position. While for R substituents it marks a difference in Meta position only. As a result, the sub position and nature influence the bonding rotation.

- ✓ The substituents position and nature influences on the electronegativity, electrophilicity index, and on chemical potential μ, this influence is remarkable for Methyl(most electrophilic) and Iodine (most nucleophilic),

- ✓ The density charge of O and N atoms increases by the alkyl group which has an electro-donation effect, and it decreases by the halogen elements which has an electro-attraction effect.

- ✓ The stability of ligands gets affected by the nature and position of the substituents; Halogens destabilize the system while the alkyl group stabilizes it.

References

[1] M.B. Yazid, A. Moussi, D. Barkat. In vitro antifungal activity of some Schiff bases derived from ortho-hydroxybenzaldehyde against fusarium, Journal of Engineering Science and Technology. **2017**, 12, 1710.

[2] M. Hureau, A. Moissette, S. K, A. Smirnov. Spectroscopic study of tautomeric equilibrium of Salicylideneaniline in ZSM-5 Zeolites. Molecules **2019**, 24, 795.

[3] J. Qiyou. Amsterdam Density Functional (ADF) Benchmarking on IBM Platforms.IBM Corp, **2006**.

[4] https://www.scm.com/doc/ADF/General/Introduction.html

[5] https://www.scm.com/doc/ADF/Input/Density_Functional.html

[6] Kharouba Abdelmadjid, thése de Magistére, université Mentouri de Constantine.

[7] https://www.scm.com/doc/ADF/Input/Basis_sets_and_atomic_fragments.html

[8] J.B. Yannick. Amsterdam Density Functional. Scientific Computing and Modelling NV. J.Am. Chem. Soc. **2006**, 128, 3103.

[9] Yamina Boukraa. Thèse de doctorat, synthese, caracterisation et étude en solution d'une serie d'Anilinesalicylidenes différemment substituées.Application dans l'extraction liquide-liquide du Cuivre (II), Cobalt(II) et Nickel(II). **2013**

[10] H. Hanaa, C. Samiha, Mémoire de master, Etude théorique du procédé d'extraction des métaux de transition, université Mohammed Khider de Biskra. **2019**

[11] P. Udhayakalaa, T. V. Rajendiranb, and S. Gunasekaran. A theoretical study of some barbiturates as corrosion inhibitors for mild steel. J. Chem. Pharm. Res., **2014**, 6, 1030-1031.

[12] Information resources management association. Biomedical engineering: concepts, methodologies, Tools and Applications. USA, IGI Global, **2018**.

[13] T. Lu and F. Chen. Multiwfn: A Multifunctional Wavefunction Analyzer. Journal of Computational Chemistry. **2012**, 33, 580–592.

[14] D.C. Young. Computational Chemistry: A Practical Guide for Applying Techniques to Real World Problems. John Wiley & Sons, New York, NY, **2001**.

[15] M. Piotr. A Test of Various Partial Atomic Charge Models for Computations on Diheteroaryl Ketones and Thioketones. Computation. **2016**, 4, 3.

Chapter IV

Study of substituted SA complexes of   Platinum
& Copper divalents

1.   Introduction

Coordination chemistry deals with metals and ligands. Metal coordination happens when lone pair of electrons from a ligand are donated to an empty orbital in a metal ion. There are many broad classes of ligands for example classical, organo-metallic, cluster, and bioinorganic. A classical ligand is a ligand that binds through the lone pairs of its main atom group. **[1]**

In the development of coordination chemistry, metal complexes of Schiff bases have played a central role because Schiff bases offer a versatile and flexible series of ligands that are capable of binding with various metal ions to give complexes with suitable properties for theoretical or practical applications **[2]**, in analytical chemistry, organic synthesis, metallurgy, refining of metals …etc **[3]**.

During the past two decades, considerable attention has been paid to the chemistry of the metal complexes of Schiff bases containing N and O donor atoms due to their structural lability, unusual configuration, and sensitivity to molecular environments, ease of preparation and stabilization of both oxidation states of the metal usual in biological systems **[4, 5]**.

The use of organic-based ligands such as Schiff bases that form stable coordination compounds have been suggested as a suitable procedure for the extraction and removal of dissolved heavy metals from contaminated water as example **[6]**.

In this chapter, we use Salicylideneaniline and its substituted ligands, and we study its complexation with platinum and copper metals. The position and nature of the substituent on the atoms and the carbon atoms of the phenyl ring of ligands have a significant influence on geometric and electronic properties, therefore on the stability of the studied complexes.

2.   Introduction to the chemistry of platinum and copper

2.1   Platinum Metal

Platinum with the symbol (Pt) and an atomic number of 78 in the periodic table is considered as "rich man's gold." It was discovered in 1735 by the Spanish explorer Antonio de Ulloa. The name "platinum" is derived from the Spanish word "*Platina*" which literally means a tiny form of "*Plata*" or "little silver" **[7]**.

Platinum's unique physical and chemical properties make it irreplaceable in an uncountable of industrial applications such as **[8]**:

- ✓ In medical industry, it is used in devices such as catheters, pacemakers and stents. As well it's used in neuromodulation devices, cardiac implants, and anti-cancer drugs …etc **[9]**.
- ✓ In the chemical industry, it's used in catalysis in the production of a variety of products e.g. nitric acid, silicon, oleum, and hydrocyanic acid, etc.
- ✓ In the environmental industry, it's used as catalysts for the purification of gases.
- ✓ In the steel industry, it's used as a component of thermocouples for temperature measurements.
- ✓ In the electronics industry, it's used for the fabrication of semiconductors, flat-panel televisions, digital cameras, and plasma display panels, etc.
- ✓ In the glass industry, it's used for the production of high-quality optical glass, liquid crystal displays, and cathode-ray tubes for televisions and computer monitors, in tanks, dies, and valves for fiberglass production, in crucibles for melting optical salt crystals, and in heater winding for glass, etc.
- ✓ In Jewelry Industry, it's used in producing medals and commemorative coins **[8]**.

2.2   Copper Metal

The copper metal (Cu) was discovered in -9000 BC **[10]**, and it is a naturally-occurring metallic element that occurs in soil at an average concentration of about 50 parts per million (ppm). It is present in all animals and plants and is an essential nutrient for humans and animals in small amounts.

Copper is used currently for production of bactericides and fungicides, oral hygiene products, in the pharmaceutical industry, and also for applications in the HVAC systems (heating, ventilation, and air conditioning systems), and also in water distribution(water pipes) and production of the medical instruments**,** and medical environments(doors, knobs, piping material. As well copper has many biological activities such as: antibacterial, antiviral etc **[11, 12, 13]**.

2.3   Physical and chemical properties of Pt and Cu

Platinum	Copper
✓ High melting point: 2042 K. ✓ Good ductility. ✓ Resistance to the alternating effect of heating and cooling. ✓ Physical and chemical stability at extreme temperatures. ✓ Resistance to oxidation in air at any temperature. ✓ Resistance to chemical corrosion and molten materials. ✓ Resistance to nitric and sulfuric acids at high temperatures. ✓ Corrosion limited to the action of halogens, cyanides, sulfur and caustic alkalis. ✓ Excellent catalytic activity. ✓ Constant electrical resistance over a wide range of operating conditions, and in particular of temperature, as well as in cases requiring intermittent use. ✓ Dimensional stability of platinum alloys under normal conditions. .	✓ It's a reddish-brown metallic element. ✓ High ductility and malleability that is an excellent conductor of heat and electricity. ✓ Atomic weight 63.54 ✓ Density 8.94g/ cm^3. ✓ Melting point 1083°C. ✓ Boiling point 2595°C. ✓ Has two stable isotopes, 63Cu and 65Cu ✓ The water solubility of copper(II) sulfate is 143g/L at 0°C, whereas cuprous(I) oxide and metallic copper are practically insoluble. ✓ Copper can assume oxidation states 0, +1, +2, and +3. ✓ Cu(0) is very stable, but can dissolve in acids such as sulfuric and nitric acids. ✓ The cuprous ion [Cu(I)] is unstable in oxidizing environments. ✓ Cu(II) is the most abundant oxidation state in hydrophilic and oxidizing environments, and the ion is stable in most environments. ✓ Cu(III) is very unstable, and of negligible biological significance.

Table IV.1: Physical and chemical properties of Pt and Cu [14, 15].

3. Comparative study of platinum and copper complexes based on Salicylideneaniline ligands substituted in the ortho position.

The study will be with [M = Pt, Cu; X = H, F, Me, Br, Cl]. In order to highlight the importance of substitution on the stability of the studied compounds, we conducted   a geometrical and electronic study on the different complexes for highlighting these characteristics.

3.1   Calculation method and geometry optimization

The studied complexes within the framework of our thesis comprise more than fifty atoms, so the chosen method must be able to treat large systems with precision. In addition, it will be necessary not only to access the energy of the complex but also it should be able to optimize its geometry, for that we have chosen the DFT as the best method for studying our transition metals complexes.

All the calculations presented in the context of this chapter were carried out within the framework of the density functional theory (DFT) and, performed with the ADF code 2010. As well are made with the weak TZP base and, GGA: BLYP functional with a frozen core at "medium"   and integration accuracy "6.0".

The Fig IV.1 presents the different optimized structures of Pt and Cu metals coordination with deprotonated Schiff bases ligands by using the recent calculation parameters.

1) Pt (HSA) $_2$ **6)** Cu (HSA) $_2$

2) Pt (2F-SA) $_2$ **7)** Cu (2F-SA) $_2$

3) Pt (2Cl-SA) $_2$ **8)** Cu (2Cl-SA) $_2$

4) Pt (2Br-SA) $_2$ **9)** Cu (2Br-SA) $_2$

5) Pt (2Me-SA) $_2$ **10)** Cu (2Me-SA) $_2$

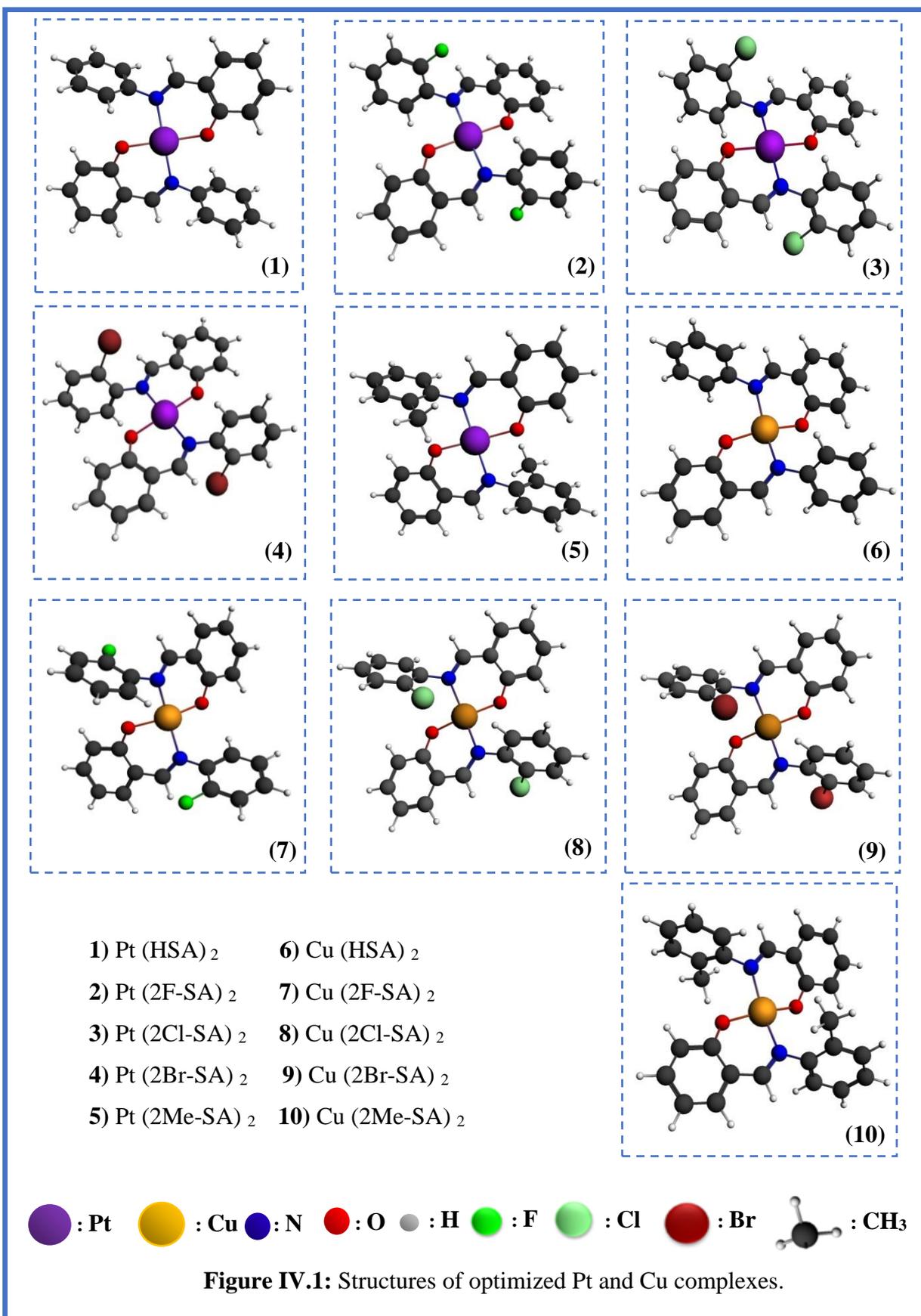**Figure IV.1:** Structures of optimized Pt and Cu complexes.

Fig IV.2 shows the main structural parameters calculated in the study of this chapter.
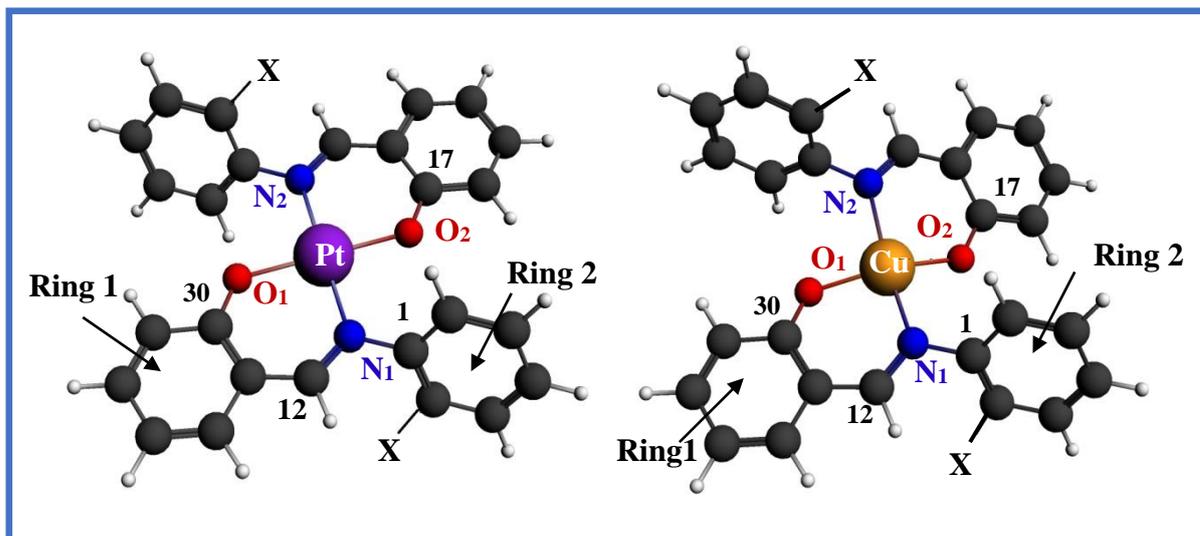

Figure IV.2: Calculated geometric parameters of Pt and Cu metals complexes.

3.2   Results and discussion

3.2.1 Geometric analysis

We present in Table IV.2 the calculated geometric parameters: the bond length expressed in (pm) and the valence, and dihedral angles expressed in degrees (°).

- ✓ For the $Pt-O_1$ and $Pt-O_2$ distances are almost equal to 212pm for all complexes but, for distances of $Cu-O_1$ and $Cu-O_2$ change according to the change of the substituents nature.

- ✓ The atoms N_1, N_2, O_1, and O_2 of Pt complexes are almost located on the same plane regardless of the substituent on the phenyl ring.

- ✓ For the Pt complexes, the valence angles have values close to 90° for (N_1-Pt-O_1 and N_2-Pt-O_2), and 180 ° for (N_1-Pt-N_2 and O_1-Pt-O_2), this implies that the N_1, Pt, O_1 and N_2, Pt, O_2 are collinear whatever the substituent is. While they are not for the case of Cu complexes.

- ➤ So we can result, that the geometric shape adopted by the Oxygen and Nitrogen atoms of Pt complexes is a pyramid with a distorted rectangle base.

- ➤ The electronegativity of the substituents has an influence on the geometric shape adopted by the complex.

Complexes	Bond length (pm)						Valence and dihedral angles (°)					
	Ring 1	Ring 2	$Pt\text{-}N_1$	$Pt\text{-}N_2$	$Pt\text{-}O_1$	$Pt\text{-}O_2$	$N_1\text{-}Pt\text{-}O_1$	$N_2\text{-}Pt\text{-}O_2$	$N_1\text{-}Pt\text{-}N_2$	$O_1\text{-}Pt\text{-}O_2$	$N_1\text{-}Pt\text{-}O_2\text{-}C_{17}$	$N_2\text{-}Pt\text{-}O_1\text{-}C_{30}$
$Pt(HSA)_2$	141.5	140.2	216.3	216.3	212.1	212.0	90.2	90.1	179.4	179.7	178.2	180.8
$Pt(2F\text{-}SA)_2$	141.6	140.1	216.2	216.7	212.4	212.1	89.9	89.4	179.1	178.0	161.5	167.9
$Pt(2Cl\text{-}SA)_2$	141.6	140.2	215.6	215.5	212.2	212.2	90.3	90.2	179.9	179.9	177.5	181.4
$Pt(2Br\text{-}SA)_2$	141.6	140.2	215.6	215.6	212.1	212.1	90.1	90.1	179.9	180.0	176.8	183.0
$Pt(2Me\text{-}SA)_2$	141.6	140.5	215.0	215.1	212.5	212.5	89.9	89.7	177.9	177.0	174.8	178.7

	Bond length (pm)						Valence and dihedral angles (°)					
	Ring 1	Ring 2	$Cu\text{-}N_1$	$Cu\text{-}N_2$	$Cu\text{-}O_1$	$Cu\text{-}O_2$	$N_1\text{-}Cu\text{-}O_1$	$N_2\text{-}Cu\text{-}O_2$	$N_1\text{-}Cu\text{-}N_2$	$O_1\text{-}Cu\text{-}O_2$	$N_1\text{-}Cu\text{-}O_2\text{-}C_{1}$	$N_2\text{-}Cu\text{-}O_1\text{-}C_{30}$
$Cu(HSA)_2$	141.5	140.2	210.2	209.3	198.2	197.8	91.5	91.6	160.8	156.3	199.1	204.1
$Cu(2F\text{-}SA)_2$	141.6	140.1	206.9	211.1	200.3	198.1	91.6	90.7	155.8	150.6	171.8	192.7
$Cu(2Cl\text{-}SA)_2$	141.6	140.3	206.9	207.6	198.8	199.1	92.5	92.2	150.5	147.0	210.2	216.1
$Cu(2Br\text{-}SA)_2$	141.6	140.3	207.0	207.7	198.7	199.0	92.2	92.1	152.8	148.9	206.6	216.0
$Cu(2Me\text{-}SA)_2$	141.6	140.4	209.1	209.9	198.2	198.1	91.1	91.1	163.9	161.7	200.6	207.5

Table IV.2: Geometric descriptors, Bond length (pm) & valence angles (°) of Pt (X- SA)$_2$ and Cu (X- SA)$_2$ complexes.

3.2.2 Analysis of the electronic structure

To arrive at a complete description of the studied systems, we conducted in addition to the previous geometric study, a study of the electronic structure.

3.2.2.1 Analysis of the Mulliken charge

The results of the Mulliken charges are shown in the table IV.3**:**

	Mulliken charge									
	Pt (HSA)$_2$	Pt (2F-SA)$_2$	Pt (2Cl-SA)$_2$	Pt (2Br-SA)$_2$	Pt (2Me-SA)$_2$	Cu(HSA)$_2$	Cu (2F-SA)$_2$	Cu (2Cl-SA)$_2$	Cu(2Br-SA)$_2$	Cu(2Me-SA)$_2$
M	0.993	0.993	1.022	1.019	0.986	0.577	0.573	0.582	0.583	0.568
O$_1$	-0.683	-0.687	-0.683	-0.684	-0.681	-0.653	-0.673	-0.641	-0.643	-0.647
O$_2$	-0.683	-0.684	-0.683	-0.684	-0.685	-0.646	-0.642	-0.636	-0.637	-0.660
N$_1$	-0.503	-0.500	-0.517	-0.518	-0.539	-0.402	-0.404	-0.412	-0.415	-0.442
N$_2$	-0.504	-0.507	-0.518	-0.518	-0.535	-0.419	-0.403	-0.416	-0.418	-0.431
C$_1$	0.175	0.116	0.186	0.199	0.183	0.211	0.139	0.223	0.233	0.224
C$_{12}$	0.408	0.430	0.421	0.423	0.415	0.430	0.454	0.438	0.441	0.430
C$_{30}$	0.448	0.450	0.450	0.451	0.441	0.497	0.503	0.489	0.491	0.480

Table IV.3: Mulliken charge Analysis.

From Table IV.3 we can note that:

✓ The charges of the Pt and Cu atoms are lower than the formal charges (+2) for all substituents, and that explains their phenomenon of ligand-metal donation.

This donation is notable in the case of Methyl for both of metals, and low in the case of Cl for the Pt, which is proved by the metals charges: for Pt, the highest charge is in the case of Cl substituent, and the lowest one is in the case of Me substituent, and for Cu, the highest charge is in the case of Br substituent, and the lowest one is in the case of Me substituent.

➢ The electron-donor and electro-withdrawing of substituents influence on the ligand → metal donation **[16]**.

➢ An electron-donor substituent leads to good ligand-metal donation. On the other hand, an electro-withdrawing substituent leads to a bad ligand-meta donation **[16].**

3.2.2.2 Orbital analysis

The output result file of the calculations allowed us to draw up the following table:

		$(HSA)_2$	$(2F\text{-}SA)_2$	$(2Cl\text{-}SA)_2$	$(2Br\text{-}SA)_2$	$(2Me\text{-}SA)_2$
E_{HOMO} (ev)	Pt	-4.384	-4.490	-4.436	-4.452	-4.349
	Cu	-4.555	-4.621	-4.595	-4.615	-4.543
E_{LUMO} (ev)	Pt	-2.549	-2.676	-2.620	-2.645	-2.488
	Cu	-2.258	-2.444	-2.355	-2.360	-2.183
(ΔE)	Pt	1.835	1.814	1.816	1.807	1.861
	Cu	2.297	2.177	2.240	2.255	2.360

Table IV.4: Principal chemical descriptors of optimized Pt (X-SA) $_2$ and Cu (X-SA) $_2$ complexes.
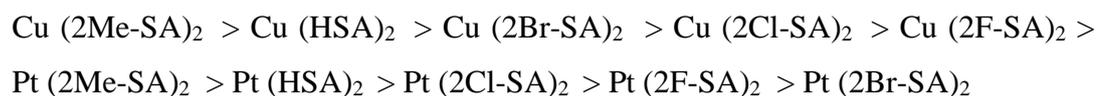
It is noted from Table IV.4 that:

➢ The stability of the Pt-SA and Cu-SA complexes is influenced by the nature of the substituents.

➢ An electro-donor substituent (Me) stabilizes the Pt and Cu complexes more than the unsubstituted states.
  On the other hand, the least electron-withdrawing substituents effect destabilizes the complexes.

➢ The increasing of electronegativity destabilizes more the Cu complexes.
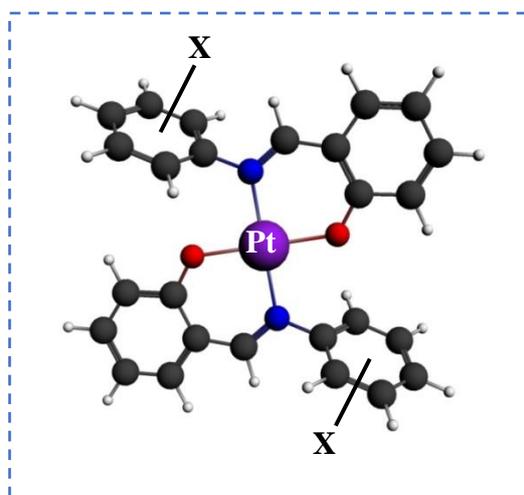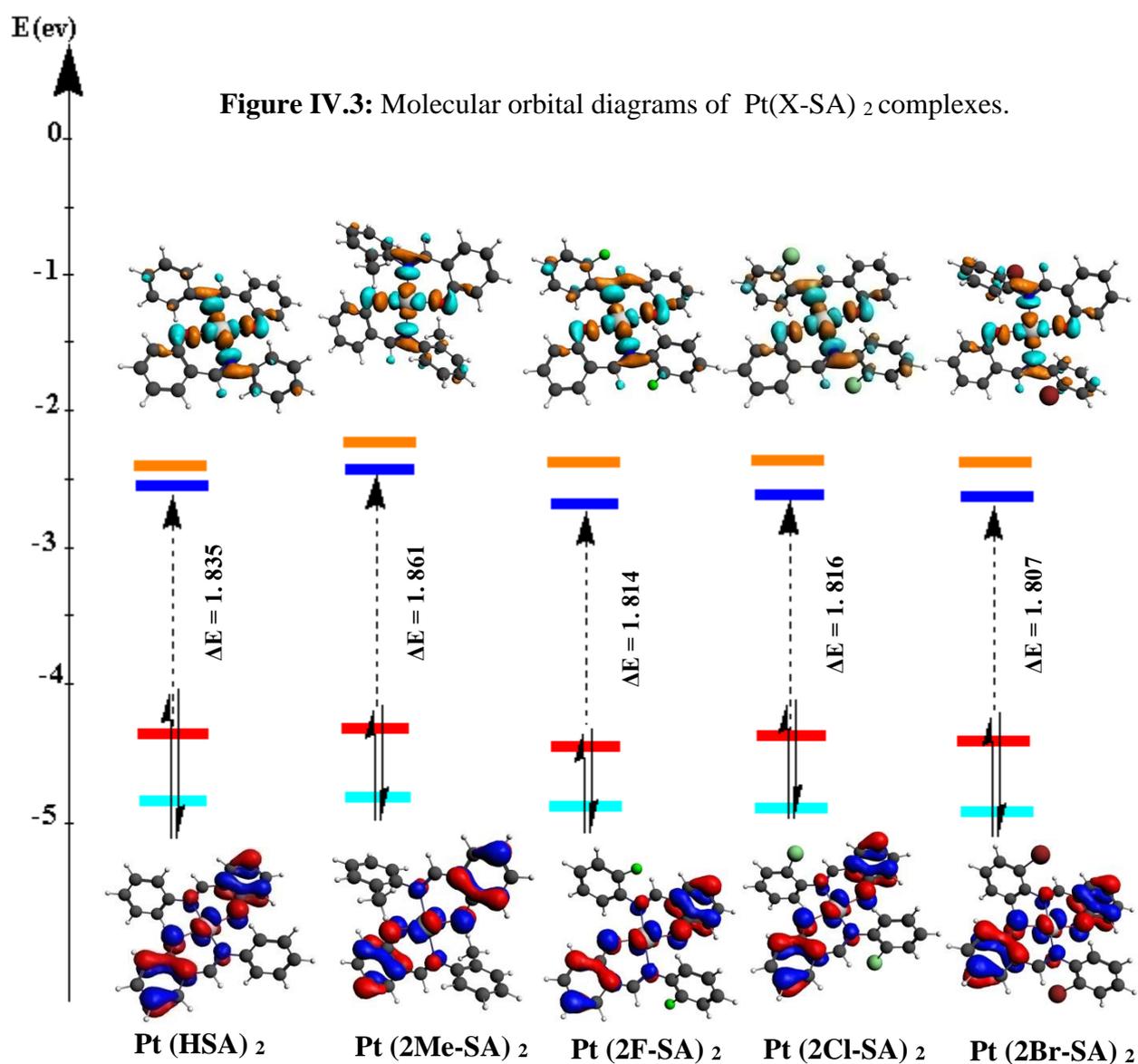
We figured out the MO diagrams of the optimized Pt and Cu complexes that are obtained by the DFT method in Fig IV.3 and Fig IV.4.
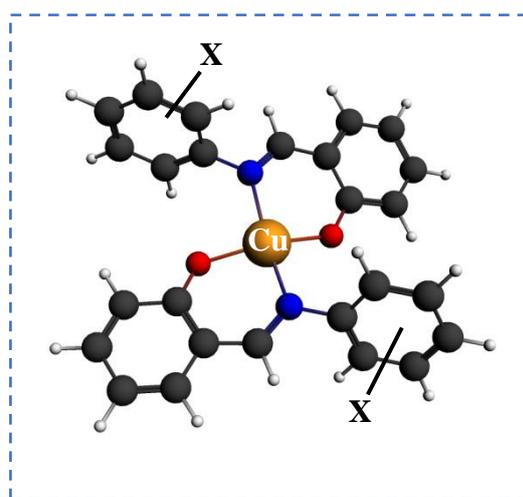
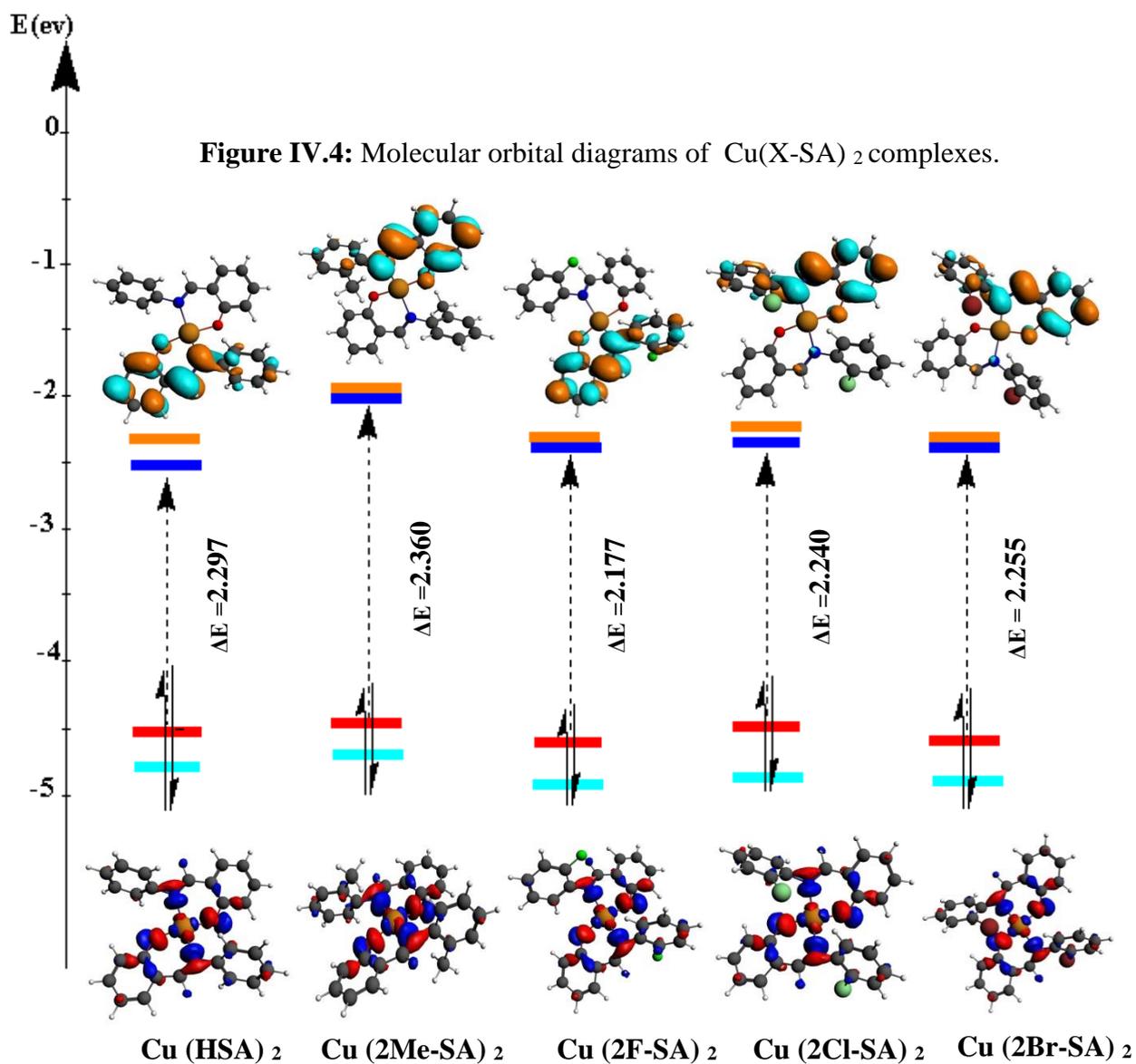From that figures we can note that:

✓ The lowest values of energy gap correspond to the Pt $(2Br\text{-}SA)_2$ and Cu $(2F\text{-}SA)_2$, which correspond to an energy gaps of 1.807ev and 2.117ev respectively, comparing with the other energy gaps of the studied complexes.

✓ While the highest values of the ΔE, are of Pt $(2Me\text{-}SA)_2$ and Cu $(2Me\text{-}SA)_2$ complexes that correspond to an energy gap of 1.861ev and 2.360ev respectively comparing with the other energy gaps of the studied complexes.

➢ So we can result that Pt$(2Me\text{-}SA)_2$ and Cu$(2Me\text{-}SA)_2$ are the most stable complexes, while Pt$(2Br\text{-}SA)_2$ and Cu $(2F\text{-}SA)_2$ complexes are the most unstable complexes among the other complexes.

✓ In another perspective, when we compare Pt complexes with Cu complexes we can find that Cu complexes are more stable than Pt complexes.

➢ As a result, we can order complexes according to their stability according to the following order :

Cu (2Me-SA)$_2$ > Cu (HSA)$_2$ > Cu (2Br-SA)$_2$ > Cu (2Cl-SA)$_2$ > Cu (2F-SA)$_2$ > Pt (2Me-SA)$_2$ > Pt (HSA)$_2$ > Pt (2Cl-SA)$_2$ > Pt (2F-SA)$_2$ > Pt (2Br-SA)$_2$

Figure IV.3: Molecular orbital diagrams of Pt(X-SA) $_2$ complexes.

Pt (HSA) $_2$ Pt (2Me-SA) $_2$ Pt (2F-SA) $_2$ Pt (2Cl-SA) $_2$ Pt (2Br-SA) $_2$

$\Delta E = 1.835$ $\Delta E = 1.861$ $\Delta E = 1.814$ $\Delta E = 1.816$ $\Delta E = 1.807$

Pt (HSA) $_2$

Figure IV.4: Molecular orbital diagrams of Cu(X-SA) $_2$ complexes.

Cu (HSA) $_2$ Cu (2Me-SA) $_2$ Cu (2F-SA) $_2$ Cu (2Cl-SA) $_2$ Cu (2Br-SA) $_2$

ΔE =2.297   ΔE =2.360   ΔE =2.177   ΔE = 2.240   ΔE = 2.255

Cu (HSA) $_2$

4. Conclusion

In the course of this chapter, we got interested in the complexes that are formed by the coordination of Salicylideneaniline ligands with copper (+2) and Platinum (+2) divalent by using DFT / BLYP / TZP.

From the obtained results we can conclude the following:

- ✓ The electro-donor group stabilizes the complexes however the metal nature be platinum or copper, while the electro-attractor elements have a destabilizing influence.
- ✓ The copper complexes are more stable than platinum complexes.
- ✓ The stability of copper complexes increasing according to the decreasing of the electro-attracting effect.

References

[1] V. K. Gaikwad1, M. Y. Urmila. Metal complexes of Schiff bases. Scholarly research journal for interdisciplinary studies .**2016**, 3/24, 2225-2226.

[2] S. Archana. Synthesis and characterization of schiff base salicylaldehyde and thiohydrazones and its metal complexes. **2013**, 4, 152-154.

[3] W.A. Mahmoud, A.A.S Al-Hamdani, B.A. Jasim. 2017.Synthesis and characterization of some new metal complexes with 2-(2-(2- hydroxylbenzylidene amino) ethyl] isoindoline-1,3-dione. RJPBCS. **2017**, 8, 305.

[4] T. Xishi , Y. Xianhong ,C.Q ,T. Minyu. .Synthesis of Some Transition Metal Complexes of a Novel Schiff Base Ligand Derived from 2,2'-bis(*p*-Methoxyphenylamine) and Salicylicaldehyde. **2003**, 8, 439–443.

[5] Timur, Mahir.2017. Synthesis and Metal Ion Uptake Studies of Silica Gel-Immobilized Schiff Base Derivatives and Catalytic Behaviors of their Cu(II) Complexes . Iran. J. Chem. Chem. Eng. **2017**, 36, 112.

[6] S.S. Muhammad, M.Y. Muhammadu, U.S. Usman. Synthesis and evaluation of the efficacies of some Schiff bases for the removal of heavy metals from wastewater. Science World Journal. **2018**, 13, 109.

[7] S.K. Haldar. Platinum-Nickel-Chromium Deposits. Geology, Exploration and Reserve Base. **2017**, 1-35.

[8] O. A. Babakina, T. E. Graedel. The Industrial Platinum Cycle for Russia: A Case Study of Materials Accounting. Forestry & Environmental Studies Publications. **2005**. Series, 14.

[9] A. Cowley. A healthy future: platinum in medical applications. The 4th International Platinum Conference, Platinum in transition 'Boom or Bust', The Southern African Institute of Mining and Metallurgy, **2010**.

[10] A.K. Keith, O.P Ma Marjorette, and J.T. Dennis. Copper-binding motifs in catalysis, transport, detoxification and signaling. Chemistry & Biology. **1997**, 4, 549.

[11] 29 Hazen Drive. Copper: Health Information Summary. Concord, environmental fact sheet. **2013**, 603, 271-3503.

[12] J. Konieczny, Z. Rdzawski. Antibacterial properties of copper and its alloys.International scientific journal. **2012**, 56, 53-60.

[13] M. Vincent, R.E. Duval, P. Hartemann and M. Engels-Deutsch. Contact killing and antimicrobial properties of copper. Journal of Applied Microbiology. **2017**, 124, 1032—1046.

[14] P.P. Blazy, J. El-Aid .Propriétés physique et chimiques métallurgie des platinoïdes-Minerais et procédés. **2003**.

[15] G. F. Nordberg, B.A. Flower, M. Nordberg, L. T. Friberg. Handbook on the Toxicology of Metals Fourth Edition Volume I: General Considerations. Elsevier B.V. **1986**.

[16] H. Hanaa, C. Samiha, Mémoire de master, Etude théorique du procédé d'extraction des métaux de transition, université Mohammed Khider de Biskra. **2019**, 71.

General conclusion

General conclusion

The work that was performed during this research represents a theoretical contribution on the reactivity of substituted Salicylideneaniline ligands.

The constraints of transition metals toxicity, the high cost of the used products and the loss of time during the realization of the experiments at the laboratory instigate scientists to use the informative tool in molecular modeling especially with the development of the instruments power of calculation which increases day by day.

The study done during this thesis allowed us to study the reactivity of substituted Salicylideneaniline and their copper and platinum complexes at the DFT / BLYP / TZP level with ADF software.

From these calculations we can conclude that:

The position and nature of the substituent has a significant influence on the reactivity of ligands and on the stability of complexes, that influence changes according the effect of the substituent (electro-withdrawing or electo-donating).

The electro-donor substituent stabilizes the system while the electro-withdrawing substituent destabilizes it.

As well the metal nature has an influence on stability of system, we obtained that the coordination of the ligands with the copper metal results more stable complexes than that resulted by the coordination with platinum.

Abstract:

The research work carried out during this master's thesis is devoted on the one hand to the theoretical study of the geometrical and electronic properties of a series of organic compounds (ligands) through which we wanted to demonstrate the reactivity of these compounds to predict their coordination with the transition metals on the other hand.

During the course of this study the Schiff base of deprotonated Salicylidenaniline type substituted by a set of halogens and alkyl group elements was the main focus of our study.

The platinum and copper divalent were taken as transition metals in coordination with a few ligands from that mentioned above to form the complexes which interest has been given to geometric properties and stability.

Our calculations were performed with the ADF software using the updated quantitative computation DFT method, both of GGA-BLYP function and TZP base were proven reliable in studying such a compound and were some of the calculation settings that are chosen during this work.

Keywords: Salicylidenaniline, Transition metals, Schiff Base, ADF, DFT.

ملخص :

العمل البحثي الذي تم إجراؤه خلال أطروحة الماجستير هذه مكرس للدراسة النظرية للخصائص الهندسية والإلكترونية لسلسلة من المركبات العضوية (Ligands) التي أردنا من خلالها إثبات تفاعل هذه المركبات من ناحية و التنبؤ بتنسيقها مع المعادن الانتقالية من ناحية اخرى.

خلال هذه الدراسة، تم استبدال قاعدة شيف من نوع ساليسيليدان أنيلين منزوع البروتون بمجموعة من الهالوجينات والألكيلات وهذا هو المحور الرئيسي لدراستنا.

تم أخذ كل من البلاتين والنحاس ثنائيا التكافؤ كمعادن انتقالية بالتنسيق مع بعض المركبات المذكورة سابقا لتشكيل معقدات تهمنا خصائصها الهندسية واستقرارها.

تم إجراء حساباتنا باستخدام البرنامج الحاسوبي ADF باستخدام طريقة الحساب الكمي المحدثة DFT, و كل من الوظيفة GGA-BLYP والقاعدة TZP اللتان أثبتتا موثوقيتهما في دراسة مثل هذا المركب ويعدان من إعدادات الحساب المختارة أثناء هذا العمل.

الكلمات المفتاحية : ساليسيليدان أنيلين, المعادن الانتقالية, قاعدة شيف, ADF, DFT

Résumé :

Le travail de recherche mené au cour de ce mémoire de fin d'étude de master est consacré d'une part a l'étude théorique des propriétés géométrique et électronique d'une série de composés organique (Ligands) a travers laquelle on a voulu mettre en évidence la réactivité de ces composés pour prédire d'autre part leur coordination avec les métaux de transition.

Au cour de cette étude la base Schiff de type Salicylidenaniline deprotoné substitué par un ensemble d'éléments halogène et de groupe alkyl étaient l'objet principal de notre étude.

Le platine et le cuivre divalents étaient prit comme métaux de transition en coordination avec des quelque ligands qui en cité précédemment pour forme les complexes auxquels on s'est intéressé aux propriétés géométrique et a leurs stabilité.

Le logiciel ADF comme programme de calcule était l'outil informatique a travers l'quelle nos calcule ont été réalisé et avec l'utilisation de la méthode de calcule quantique actualisé DFT, la fonctionnelle GGA-BLYP et la base TZP qui a prouvé sa fiabilité a l'étude de telle composé étaient les paramètres de calcule choisit au cour de ce travail.

Mots clés : Salicylidenaniline, Métaux de transition, Base Schiff, ADF, DFT.